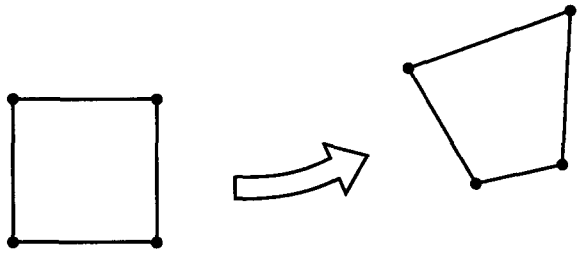

(d) Large displacements, large rotations, and large strains. Linear or nonlinear material bahavior

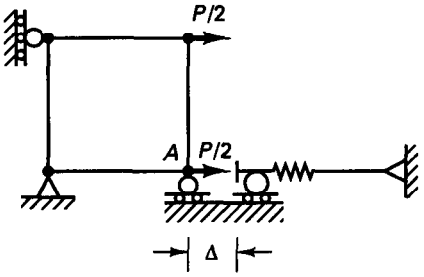

(e) Change in boundary condition at displacement Δ

Figure 6.1 *(continued)*

particular in the analysis of contact problems, of which a simple example is given in Fig. 6.1(e). In general, this change in boundary condition may be encountered in any one of the analyses summarized in Table 6.1.

In actual analysis, it is necessary to decide whether a problem falls into one or the other category of analysis, and this dictates which formulation will be used to describe the actual physical situation. Conversely, we may say that by the use of a specific formulation, a model of the actual physical situation is assumed, and the choice of formulation is part of the complete modeling process. Surely, the use of the most general large strain formulation "will always be correct"; however, the use of a more restrictive formulation may be computationally more effective and may also provide more insight into the response prediction.

Before we discuss the general formulations of nonlinear analyses, it would be instructive to consider first two simple examples that demonstrate some of the features listed in Table 6.1.

EXAMPLE 6.1: A bar rigidly supported at both ends is subjected to an axial load as shown in Fig. E6.1(a). The stress-strain relation and the load-versus-time curve relation are given in Figs. E6.1(b) and (c), respectively. Assuming that the displacements and strains are small and that the load is applied slowly, calculate the displacement at the point of load application.

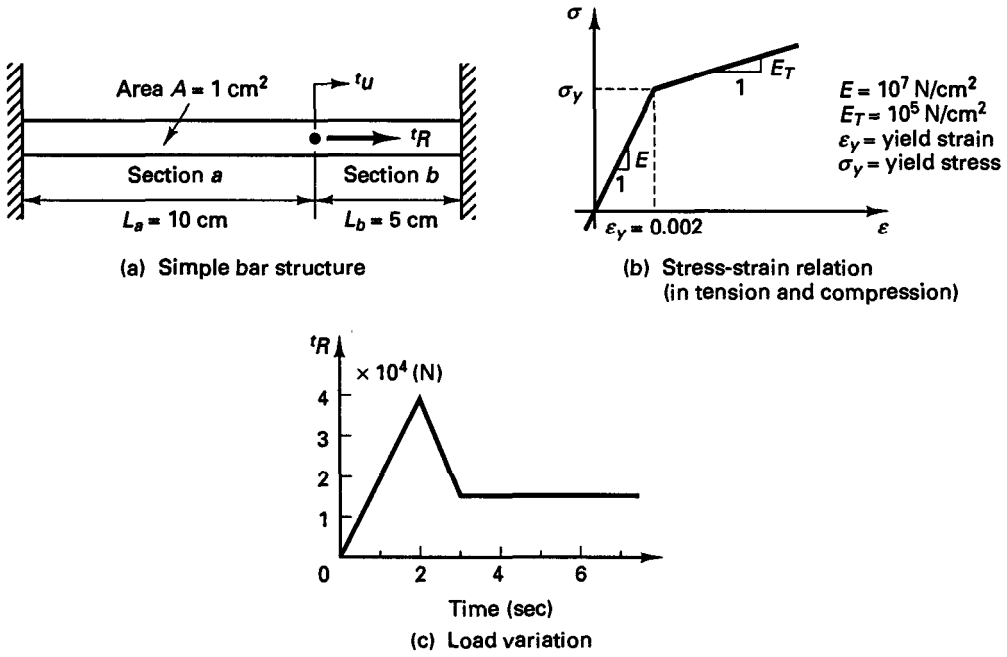

Figure E6.1 Analysis of simple bar structure

Since the load is applied slowly and the displacements and strains are small, we calculate the response of the bar using a static analysis with material nonlinearities only. Then we have for sections a and b, the strain relations

$$^t\epsilon_a = \frac{^tu}{L_a}; \qquad ^t\epsilon_b = -\frac{^tu}{L_b} \tag{a}$$

the equilibrium relations,

$$^tR + {}^t\sigma_b A = {}^t\sigma_a A \tag{b}$$

and the constitutive relations, under loading conditions,

$$^t\epsilon = \frac{^t\sigma}{E} \qquad \text{in the elastic region}$$

$$^t\epsilon = \epsilon_y + \frac{^t\sigma - \sigma_y}{E_T} \qquad \text{in the plastic region} \tag{c}$$

and in unloading,

$$\Delta\epsilon = \frac{\Delta\sigma}{E}$$

In these relations the superscript t denotes "at time t."

(i) *Both sections a and b are elastic*

During the initial phase of load application both sections a and b are elastic. Then we have, using (a) to (c),

$$^tR = EA^tu\left(\frac{1}{L_a} + \frac{1}{L_b}\right)$$

and substituting the values given in Fig. E6.1, we obtain

$$^{t}u = \frac{^{t}R}{3 \times 10^{6}}$$

with

$$^{t}\sigma_a = \frac{^{t}R}{3A}; \qquad ^{t}\sigma_b = -\frac{2}{3}\frac{^{t}R}{A} \tag{d}$$

(ii) *Section a is elastic while section b is plastic*

Section b will become plastic at time t^* when, using (d),

$$^{t^*}R = \tfrac{3}{2}\sigma_y A$$

Afterward we therefore have

$$^{t}\sigma_a = E\frac{^{t}u}{L_a}$$

$$^{t}\sigma_b = -E_T\left(\frac{^{t}u}{L_b} - \epsilon_y\right) - \sigma_y \tag{e}$$

Using (e), we therefore have for $t \geq t^*$,

$$^{t}R = \frac{EA\,^{t}u}{L_a} + \frac{E_T A\,^{t}u}{L_b} - E_T\epsilon_y A + \sigma_y A$$

and thus

$$^{t}u = \frac{^{t}R/A + E_T\epsilon_y - \sigma_y}{(E/L_a) + (E_T/L_b)}$$

$$= \frac{^{t}R}{1.02 \times 10^{6}} - 1.9412 \times 10^{-2}$$

We may note that section a would become plastic when $^{t}\sigma_a = \sigma_y$ or $^{t}R = 4.02 \times 10^{4}$ N. Since the load does not reach this value [see Fig. E6.1(c)], section a remains elastic throughout the response history.

(iii) *In unloading both sections act elastically*

we have

$$\Delta u = \frac{\Delta R}{EA[(1/L_a) + (1/L_b)]}$$

The calculated response is depicted in Fig. E6.1(d).

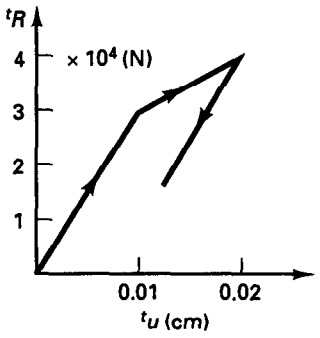

(d) Calculated response **Figure E6.1** (*continued*)

EXAMPLE 6.2: A pretensioned cable is subjected to a transverse load midway between the supports as shown in Fig. E6.2(a). A spring is placed below the load at a distance w_{gap}. Assume that the displacements are small so that the force in the cable remains constant, and that the load is applied slowly. Calculate the displacement under the load as a function of the load intensity.

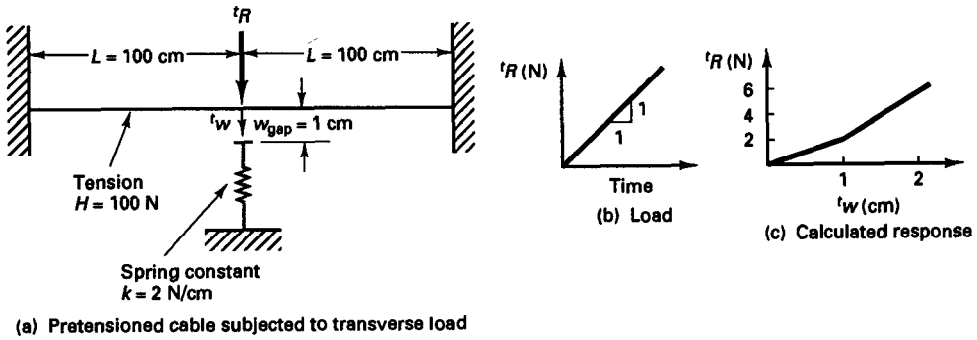

Figure E6.2 Analysis of pretensioned cable with a spring support

As in Example 6.1, we neglect inertia forces and assume small displacements. As long as the displacement ${}^tw$ under the load is smaller than w_{gap}, vertical equilibrium requires for small ${}^tw$,

$$ {}^tR = 2H\frac{{}^tw}{L} \tag{a}$$

Once the displacement is larger than w_{gap}, the following equilibrium equation holds:

$$ {}^tR = 2H\frac{{}^tw}{L} + k({}^tw - w_{gap}) \tag{b}$$

Figure E6.2(c) shows graphically the force displacement relations given in (a) and (b).

We should note that in this analysis we neglected the elasticity of the cable; therefore the response is calculated using only the equilibrium equations in (a) and (b), and the only nonlinearity is due to the contact condition established when ${}^tw \geq w_{gap}$.

Although these examples represent two very simple problems, the given solutions display some important general features. The basic problem in a general nonlinear analysis is to find the state of equilibrium of a body corresponding to the applied loads. Assuming that the externally applied loads are described as a function of time, as in Examples 6.1 and 6.2, the equilibrium conditions of a system of finite elements representing the body under consideration can be expressed as

$$ {}^t\mathbf{R} - {}^t\mathbf{F} = \mathbf{0} \tag{6.2}$$

where the vector ${}^t\mathbf{R}$ lists the externally applied nodal point forces in the configuration at time t and the vector ${}^t\mathbf{F}$ lists the nodal point forces that correspond to the element stresses in this configuration. Hence, using the notation in Chapter 4, relations (4.18) and (4.20) to (4.22), we have

$$ {}^t\mathbf{R} = {}^t\mathbf{R}_B + {}^t\mathbf{R}_S + {}^t\mathbf{R}_C \tag{6.3}$$

and, identifying the current stresses as initial stresses, $\mathbf{R}_I = {}^t\mathbf{F}$,

$$ {}^t\mathbf{F} = \sum_m \int_{{}^tV^{(m)}} {}^t\mathbf{B}^{(m)T}\, {}^t\boldsymbol{\tau}^{(m)}\, {}^tdV^{(m)} \tag{6.4} $$

where in a general large deformation analysis the stresses as well as the volume of the body at time t are unknown.

The relation in (6.2) must express the equilibrium of the system in the current deformed geometry taking due account of all nonlinearities. Also, in a dynamic analysis, the vector ${}^t\mathbf{R}$ would include the inertia and damping forces, as discussed in Section 4.2.1.

Considering the solution of the nonlinear response, we recognize that the equilibrium relation in (6.2) must be satisfied throughout the complete history of load application; i.e., the time variable t may take on any value from zero to the maximum time of interest (see Examples 6.1 and 6.2). In a static analysis without time effects other than the definition of the load level (e.g., without creep effects; see Section 6.6.3), time is only a convenient variable which denotes different intensities of load applications and correspondingly different configurations. However, in a dynamic analysis and in static analysis with material time effects, the time variable is an actual variable to be properly included in the modeling of the actual physical situation. Based on these considerations, we realize that the use of the time variable to describe the load application and history of solution represents a very general approach and corresponds to our earlier assertion that a "dynamic analysis is basically a static analysis including inertia effects."

As for the analysis results to be calculated, in many solutions only the stresses and displacements reached at specific load levels or at specific times are required. In some nonlinear static analyses the equilibrium configurations corresponding to these load levels can be calculated without also solving for other equilibrium configurations. However, when the analysis includes path-dependent nonlinear geometric or material conditions, or time-dependent phenomena, the equilibrium relations in (6.2) need to be solved for the complete time range of interest. This response calculation is effectively carried out using a step-by-step incremental solution, which reduces to a one-step analysis if in a static time-independent solution the total load is applied all together and only the configuration corresponding to that load is calculated. However, we shall see that for computational reasons, in practice, even the analysis of such a case frequently requires an incremental solution, performed automatically (see also Section 8.4), with a number of load steps to finally reach the total applied load.

The basic approach in an incremental step-by-step solution is to assume that the solution for the discrete time t is known and that the solution for the discrete time $t + \Delta t$ is required, where Δt is a suitably chosen time increment. Hence, considering (6.2) at time $t + \Delta t$ we have

$$ {}^{t+\Delta t}\mathbf{R} - {}^{t+\Delta t}\mathbf{F} = \mathbf{0} \tag{6.5} $$

where the left superscript denotes "at time $t + \Delta t$." Assume that ${}^{t+\Delta t}\mathbf{R}$ is independent of the deformations. Since the solution is known at time t, we can write

$$ {}^{t+\Delta t}\mathbf{F} = {}^t\mathbf{F} + \mathbf{F} \tag{6.6} $$

where $\mathbf{F}$ is the increment in nodal point forces corresponding to the increment in element displacements and stresses from time t to time $t + \Delta t$. This vector can be approximated

using a tangent stiffness matrix ${}^{t}\mathbf{K}$ which corresponds to the geometric and material conditions at time t,

$$\mathbf{F} \doteq {}^{t}\mathbf{K}\mathbf{U} \tag{6.7}$$

where $\mathbf{U}$ is a vector of incremental nodal point displacements and

$${}^{t}\mathbf{K} = \frac{\partial {}^{t}\mathbf{F}}{\partial {}^{t}\mathbf{U}} \tag{6.8}$$

Hence, the tangent stiffness matrix corresponds to the derivative of the internal element nodal point forces ${}^{t}\mathbf{F}$ with respect to the nodal point displacements ${}^{t}\mathbf{U}$.

Substituting (6.7) and (6.6) into (6.5), we obtain

$${}^{t}\mathbf{K}\mathbf{U} = {}^{t+\Delta t}\mathbf{R} - {}^{t}\mathbf{F} \tag{6.9}$$

and solving for $\mathbf{U}$, we can calculate an approximation to the displacements at time $t + \Delta t$,

$${}^{t+\Delta t}\mathbf{U} \doteq {}^{t}\mathbf{U} + \mathbf{U} \tag{6.10}$$

The exact displacements at time $t + \Delta t$ are those that correspond to the applied loads ${}^{t+\Delta t}\mathbf{R}$. We calculate in (6.10) only an approximation to these displacements because (6.7) was used.

Much of our discussion in this chapter will focus on the proper and effective evaluation of ${}^{t}\mathbf{F}$ and ${}^{t}\mathbf{K}$.

Having evaluated an approximation to the displacements corresponding to time $t + \Delta t$, we could now solve for an approximation to the stresses and corresponding nodal point forces at time $t + \Delta t$, and then proceed to the next time increment calculations. However, because of the assumption in (6.7), such a solution may be subject to very significant errors and, depending on the time or load step sizes used, may indeed be unstable. In practice, it is therefore necessary to iterate until the solution of (6.5) is obtained to sufficient accuracy.

The widely used iteration methods in finite element analysis are based on the classical Newton-Raphson technique (see, for example, E. Kreyszig [A] and see N. Bićanić and K. H. Johnson [A]), which we formally derive in Section 8.4. This method is an extension of the simple incremental technique given in (6.9) and (6.10). That is, having calculated an *increment* in the nodal point displacements, which defines a *new total* displacement vector, we can repeat the incremental solution presented above using the currently known total displacements instead of the displacements at time t.

The equations used in the Newton-Raphson iteration are, for $i = 1, 2, 3, \ldots,$

$$\boxed{\begin{aligned} {}^{t+\Delta t}\mathbf{K}^{(i-1)}\Delta\mathbf{U}^{(i)} &= {}^{t+\Delta t}\mathbf{R} - {}^{t+\Delta t}\mathbf{F}^{(i-1)} \\ {}^{t+\Delta t}\mathbf{U}^{(i)} &= {}^{t+\Delta t}\mathbf{U}^{(i-1)} + \Delta\mathbf{U}^{(i)} \end{aligned}} \tag{6.11}$$

with the initial conditions

$${}^{t+\Delta t}\mathbf{U}^{(0)} = {}^{t}\mathbf{U}; \qquad {}^{t+\Delta t}\mathbf{K}^{(0)} = {}^{t}\mathbf{K}; \qquad {}^{t+\Delta t}\mathbf{F}^{(0)} = {}^{t}\mathbf{F} \tag{6.12}$$

Note that in the first iteration, the relations in (6.11) reduce to the equations (6.9) and (6.10). Then, in subsequent iterations, the latest estimates for the nodal point displacements

are used to evaluate the corresponding element stresses and nodal point forces ${}^{t+\Delta t}\mathbf{F}^{(i-1)}$ and tangent stiffness matrix ${}^{t+\Delta t}\mathbf{K}^{(i-1)}$.

The out-of-balance load vector ${}^{t+\Delta t}\mathbf{R} - {}^{t+\Delta t}\mathbf{F}^{(i-1)}$ corresponds to a load vector that is not yet balanced by element stresses, and hence an increment in the nodal point displacements is required. This updating of the nodal point displacements in the iteration is continued until the out-of-balance loads and incremental displacements are small.

Let us summarize some important considerations regarding the Newton-Raphson iterative solution.

An important point is that the correct calculation of ${}^{t+\Delta t}\mathbf{F}^{(i-1)}$ from ${}^{t+\Delta t}\mathbf{U}^{(i-1)}$ is crucial. Any errors in this calculation will, in general, result in an incorrect response prediction.

The correct evaluation of the tangent stiffness matrix ${}^{t+\Delta t}\mathbf{K}^{(i-1)}$ is also important. The use of the proper tangent stiffness matrix may be necessary for convergence and, in general, will result in fewer iterations until convergence is reached.

However, because of the expense involved in evaluating and factoring a new tangent stiffness matrix, in practice, it can be more efficient, depending on the nonlinearities present in the analysis, to evaluate a new tangent stiffness matrix only at certain times. Specifically, in the modified Newton-Raphson method a new tangent stiffness matrix is established only at the beginning of each load step, and in quasi-Newton methods secant stiffness matrices are used instead of the tangent stiffness matrix (see Section 8.4). We note that, which scheme to use is only a matter of computational efficiency provided convergence is reached.

The use of the iterative solution requires appropriate convergence criteria. If inappropriate criteria are used, the iteration may be terminated before the necessary solution accuracy is reached or be continued after the required accuracy has been reached.

We discuss these numerical considerations in Section 8.4 but note here that whichever iterative technique is used, the basic requirements are (1) the evaluation of the (tangent) stiffness matrix corresponding to a given state and (2) the evaluation of the nodal force vector corresponding to the stresses in that state (the "state" being given by ${}^{t}\mathbf{U}$ or ${}^{t+\Delta t}\mathbf{U}^{(i-1)}$, $i = 1, 2, 3, \ldots$). Hence, our primary focus in this chapter is on explaining how, for a generic state, and we use the state at time t, the tangent stiffness matrices ${}^{t}\mathbf{K}$ and force vectors ${}^{t}\mathbf{F}$ for various elements and material stress-strain relations can be evaluated.

Let us now demonstrate these concepts in two examples.

EXAMPLE 6.3: Idealize the simple arch structure shown in Fig. E6.3(a) as an assemblage of two bar elements. Assume that the force in one bar element is given by ${}^{t}F_{\text{bar}} = k\,{}^{t}\delta$, where k is a constant and ${}^{t}\delta$ is the elongation of the bar at time t. (The assumption that k is constant is likely to be valid only for small deformations in the bar, but we use this assumption in order to simplify the analysis.) Establish the equilibrium relation (6.5) for this problem.

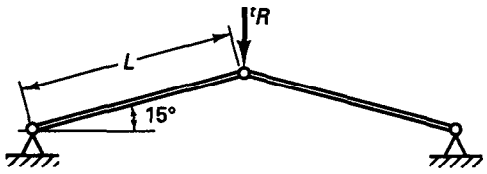

(a) Bar assemblage subjected to apex load

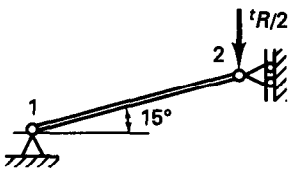

(b) Simple model using one bar (truss) element, nodes 1 and 2

Figure E6.3 A simple arch structure

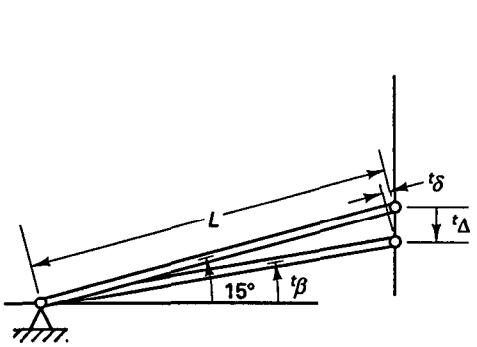

(c) Geometric variebles in typical configuretion

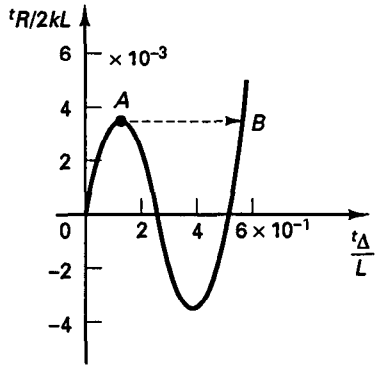

(d) Loed-displacement relation

Figure E6.3 *(continued)*

This is a large displacement problem, and the response is calculated by focusing attention on the equilibrium of the bar assemblage in the configuration corresponding to a typical time t. Using symmetry as shown in Figs. E6.3(b) and (c), we have

$$(L - {}^{t}\delta)\cos {}^{t}\beta = L\cos 15^\circ$$

$$(L - {}^{t}\delta)\sin {}^{t}\beta = L\sin 15^\circ - {}^{t}\Delta$$

hence,

$${}^{t}\delta = L - \sqrt{L^2 - 2L\,{}^{t}\Delta\sin 15^\circ + {}^{t}\Delta^2}$$

$$\sin {}^{t}\beta = \frac{L\sin 15^\circ - {}^{t}\Delta}{L - {}^{t}\delta}$$

Equilibrium at time t requires that

$$2\,{}^{t}F_{\text{bar}}\sin {}^{t}\beta = {}^{t}R$$

hence, the relation in (6.5) is

$$\frac{{}^{t}R}{2kL} = \left\{-1 + \frac{1}{\left[1 - 2\frac{{}^{t}\Delta}{L}\sin 15^\circ + \left(\frac{{}^{t}\Delta}{L}\right)^2\right]^{1/2}}\right\}\left(\sin 15^\circ - \frac{{}^{t}\Delta}{L}\right) \qquad \text{(a)}$$

Figure E6.3(d) shows the force-displacement relationship established in (a). It should be noted that between points A and B, for a given load level, we have two possible displacement configurations. If the structure is loaded with ${}^{t}R$ monotonically increasing, the displacement path with snap-through from A to B in Fig. E6.3(d) is likely to be followed in an actual physical situation.

EXAMPLE 6.4: Calculate the response of the bar assemblage considered in Example 6.1 using the modified Newton-Raphson iteration. Use two equal load steps to reach the maximum load application.

In the modified Newton-Raphson iteration, we use (6.11) and (6.12) but evaluate new tangent stiffness matrices only at the beginning of each step. Hence, the iterative equations are in this analysis

$$\begin{aligned}({}^{t}K_a + {}^{t}K_b)\,\Delta u^{(i)} &= {}^{t+\Delta t}R - {}^{t+\Delta t}F_a^{(i-1)} - {}^{t+\Delta t}F_b^{(i-1)} \\ {}^{t+\Delta t}u^{(i)} &= {}^{t+\Delta t}u^{(i-1)} + \Delta u^{(i)}\end{aligned} \qquad \text{(a)}$$

with

$$
\begin{aligned}
&{}^{t+\Delta t}u^{(0)} = {}^{t}u \\
&{}^{t+\Delta t}F_a^{(0)} = {}^{t}F_a; \qquad {}^{t+\Delta t}F_b^{(0)} = {}^{t}F_b \\
&{}^{t}K_a = \frac{{}^{t}CA}{L_a}; \qquad {}^{t}K_b = \frac{{}^{t}CA}{L_b}
\end{aligned}
\tag{b}
$$

where

$${}^{t}C \begin{cases} = E & \text{if section is elastic} \\ = E_T & \text{if section is plastic} \end{cases}$$

For an elastic section,

$${}^{t+\Delta t}F^{(i-1)} = EA\,{}^{t+\Delta t}\epsilon^{(i-1)} \tag{c}$$

for a plastic section,

$${}^{t+\Delta t}F^{(i-1)} = A[E_T({}^{t+\Delta t}\epsilon^{(i-1)} - \epsilon_y) + \sigma_y] \tag{d}$$

and the strains in the sections are

$$
\begin{aligned}
{}^{t+\Delta t}\epsilon_a^{(i-1)} &= \frac{{}^{t+\Delta t}u^{(i-1)}}{L_a} \\
{}^{t+\Delta t}\epsilon_b^{(i-1)} &= \frac{{}^{t+\Delta t}u^{(i-1)}}{L_b}
\end{aligned}
\tag{e}
$$

In the first load step, we have $t = 0$ and $\Delta t = 1$. Thus, the application of the relations in (a) to (e) gives

$t = 1$:

$$({}^{0}K_a + {}^{0}K_b)\,\Delta u^{(1)} = {}^{1}R - {}^{1}F_a^{(0)} - {}^{1}F_b^{(0)}$$

$$\Delta u^{(1)} = \frac{2 \times 10^4}{10^7(\frac{1}{10} + \frac{1}{5})} = 6.6667 \times 10^{-3} \text{ cm}$$

$(i = 1)$

$${}^{1}u^{(1)} = {}^{1}u^{(0)} + \Delta u^{(1)} = 6.6667 \times 10^{-3} \text{ cm}$$

$${}^{1}\epsilon_a^{(1)} = \frac{{}^{1}u^{(1)}}{L_a} = 6.6667 \times 10^{-4} < \epsilon_y \rightarrow \text{section } a \text{ is elastic}$$

$${}^{1}\epsilon_b^{(1)} = \frac{{}^{1}u^{(1)}}{L_b} = 1.3333 \times 10^{-3} < \epsilon_y \rightarrow \text{section } b \text{ is elastic}$$

$${}^{1}F_a^{(1)} = 6.6667 \times 10^3 \text{ N}$$

$${}^{1}F_b^{(1)} = 1.3333 \times 10^4 \text{ N}$$

$$({}^{0}K_a + {}^{0}K_b)\,\Delta u^{(2)} = {}^{1}R - {}^{1}F_a^{(1)} - {}^{1}F_b^{(1)}$$

$$= 0$$

$\therefore$ Convergence is achieved in one iteration

$${}^{1}u = 6.6667 \times 10^{-3} \text{ cm}$$

$t = 2$:

$${}^{1}K_a = \frac{EA}{L_a}; \qquad {}^{1}K_b = \frac{EA}{L_b}$$

$${}^{2}F_a^{(0)} = {}^{1}F_a; \qquad {}^{2}F_b^{(0)} = {}^{1}F_b$$

$$({}^1K_a + {}^1K_b)\,\Delta u^{(1)} = {}^2R - {}^2F_a^{(0)} - {}^2F_b^{(0)}$$

$$\Delta u^{(1)} = \frac{(4 \times 10^4) - (6.6667 \times 10^3) - (1.3333 \times 10^4)}{10^7(\frac{1}{10} + \frac{1}{5})}$$

$$= 6.6667 \times 10^{-3} \text{ cm}$$

$(i = 1)$

$${}^2u^{(1)} = {}^2u^{(0)} + \Delta u^{(1)} = 1.3333 \times 10^{-2} \text{ cm}$$

$${}^2\epsilon_a^{(1)} = 1.3333 \times 10^{-3} < \epsilon_y \rightarrow \text{section } a \text{ is elastic}$$

$${}^2\epsilon_b^{(1)} = 2.6667 \times 10^{-3} > \epsilon_y \rightarrow \text{section } b \text{ is plastic}$$

$${}^2F_a^{(1)} = 1.3333 \times 10^4 \text{ N}$$

$${}^2F_b^{(1)} = [E_T({}^2\epsilon_b^{(1)} - \epsilon_y) + \sigma_y]A = 2.0067 \times 10^4 \text{ N}$$

$$({}^1K_a + {}^1K_b)\,\Delta u^{(2)} = {}^2R - {}^2F_a^{(1)} - {}^2F_b^{(1)}$$

$$\Delta u^{(2)} = 2.2 \times 10^{-3} \text{ cm}$$

$(i = 2)$

$${}^2u^{(2)} = {}^2u^{(1)} + \Delta u^{(2)} = 1.5533 \times 10^{-2} \text{ cm}$$

$${}^2\epsilon_a^{(2)} = 1.5533 \times 10^{-3} < \epsilon_y$$

$${}^2\epsilon_b^{(2)} = 3.1066 \times 10^{-3} > \epsilon_y$$

$$\therefore {}^2F_a^{(2)} = 1.5533 \times 10^4 \text{ N}$$

$${}^2F_b^{(2)} = 2.0111 \times 10^4 \text{ N}$$

$$({}^1K_a + {}^1K_b)\,\Delta u^{(3)} = {}^2R - {}^2F_a^{(2)} - {}^2F_b^{(2)}$$

$$\Delta u^{(3)} = 1.4521 \times 10^{-3} \text{ cm}$$

The procedure is repeated, and the results of successive iterations are tabulated in the accompanying table.

i	$\Delta u^{(i)}$ (cm)	${}^2u^{(i)}$ (cm)
3	1.4521×10^{-3}	1.6985×10^{-2}
4	9.5832×10^{-4}	1.7944×10^{-2}
5	6.3249×10^{-4}	1.8576×10^{-2}
6	4.1744×10^{-4}	1.8994×10^{-2}
7	2.7551×10^{-4}	1.9269×10^{-2}

After seven iterations, we have

$${}^2u \doteq {}^2u^{(7)} = 1.9269 \times 10^{-2} \text{ cm}$$

6.2 FORMULATION OF THE CONTINUUM MECHANICS INCREMENTAL EQUATIONS OF MOTION

The objective in the introductory discussion of nonlinear analysis in Section 6.1 was to describe various nonlinearities and the form of the basic finite element equations that are used to analyze the nonlinear response of a structural system. To show the procedure of analysis, we simply stated the finite element equations, discussed their solution, and gave a

physical argument why the nonlinear response is appropriately predicted using these equations. We demonstrated the applicability of the approach in the solution of two very simple problems merely to give some insight into the steps of analysis used. In each of these analyses the applicable finite element matrices and vectors were developed using physical arguments.

The physical approach of analysis used in Examples 6.3 and 6.4 is very instructive and yields insight into the analysis; however, when considering a more complex solution, a consistent continuum-mechanics-based approach should be employed to develop the governing finite element equations. The objective in this section is to present the governing continuum mechanics equations for a displacement-based finite element solution. As in Section 4.2.1, we use the principle of virtual work but now include the possibility that the body considered undergoes large displacements and rotations and large strains and that the stress-strain relationship is nonlinear. The governing continuum mechanics equations to be presented can therefore be regarded as an extension of the basic equation given in (4.7). In the linear analysis of a general body, the equation in (4.7) was used as the basis for the development of the governing linear finite element equations [given in (4.17) to (4.27)]. Considering the nonlinear analysis of a general body, after having developed suitable continuum mechanics equations, we will proceed in a completely analogous manner to establish the nonlinear finite element equations that govern the nonlinear response of the body (see Section 6.3).

6.2.1 The Basic Problem

In Section 6.1 we underlined the fact that in a nonlinear analysis the equilibrium of the body considered must be established in the current configuration. We also pointed out that in general it is necessary to employ an incremental formulation and that a time variable is used to conveniently describe the loading and the motion of the body.

In the development to follow, we consider the motion of a general body in a stationary Cartesian coordinate system, as shown in Fig. 6.2, and assume that the body can experience large displacements, large strains, and a nonlinear constitutive response. The aim is to evaluate the equilibrium positions of the complete body at the discrete time points $0, \Delta t, 2\,\Delta t, 3\,\Delta t, \ldots$, where Δt is an increment in time. To develop the solution strategy, assume that the solutions for the static and kinematic variables for all time steps from time 0 to time t, inclusive, have been obtained. Then the solution process for the next required equilibrium position corresponding to time $t + \Delta t$ is typical and is applied repetitively until the complete solution path has been solved for. Hence, in the analysis we follow all particles of the body in their motion, from the original to the final configuration of the body, which means that we adopt a *Lagrangian* (or *material*) *formulation* of the problem. This approach stands in contrast to an *Eulerian formulation* which is usually used in the analysis of fluid mechanics problems, in which attention is focused on the motion of the material through a stationary control volume. Considering the analysis of solids and structures, a Lagrangian formulation usually represents a more natural and effective analysis approach than an Eulerian formulation. For example, using an Eulerian formulation of a structural problem with large displacements, new control volumes have to be created (because the boundaries of the solid change continuously), and the nonlinearities in the convective acceleration terms are difficult to deal with (see Section 7.4).

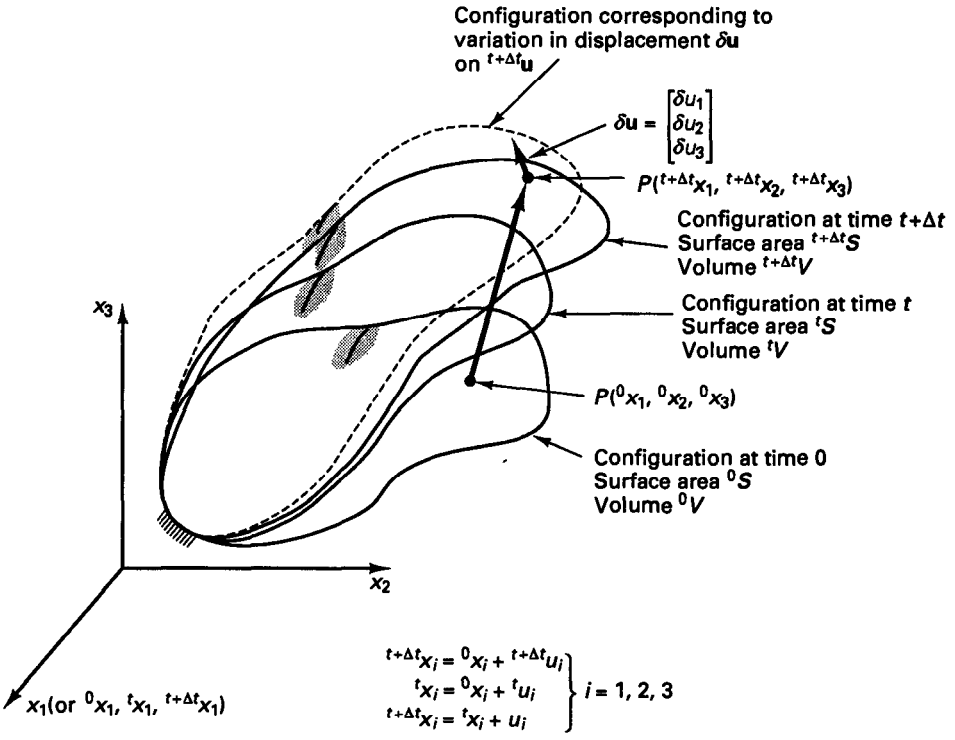

Figure 6.2 Motion of body in Cartesian coordinate frame

In our Lagrangian incremental analysis approach we express the equilibrium of the body at time $t + \Delta t$ using the principle of virtual displacements. Using tensor notation (see Section 2.4), this principle requires that

$$\int_{^{t+\Delta t}V} {}^{t+\Delta t}\tau_{ij}\, \delta_{t+\Delta t}e_{ij}\, d^{t+\Delta t}V = {}^{t+\Delta t}\mathcal{R} \tag{6.13}$$

where

$^{t+\Delta t}\tau_{ij}$ = Cartesian components of the *Cauchy stress* tensor (forces per unit areas in the deformed geometry)

$\delta_{t+\Delta t}e_{ij} = \frac{1}{2}\left(\frac{\partial \delta u_i}{\partial\, ^{t+\Delta t}x_j} + \frac{\partial \delta u_j}{\partial\, ^{t+\Delta t}x_i}\right)$ = strain tensor corresponding to virtual displacements

δu_i = components of virtual displacement vector imposed on configuration at time $t + \Delta t$, a function of $^{t+\Delta t}x_j$, $j = 1, 2, 3$

$^{t+\Delta t}x_i$ = Cartesian coordinates of material point at time $t + \Delta t$

$^{t+\Delta t}V$ = volume at time $t + \Delta t$

and

$$\boxed{{}^{t+\Delta t}\mathcal{R} = \int_{{}^{t+\Delta t}V} {}^{t+\Delta t}f_i^B \, \delta u_i \, d^{t+\Delta t}V + \int_{{}^{t+\Delta t}S_f} {}^{t+\Delta t}f_i^S \, \delta u_i^S \, d^{t+\Delta t}S} \tag{6.14}$$

where

${}^{t+\Delta t}f_i^B$ = components of externally applied forces per unit volume at time $t + \Delta t$
${}^{t+\Delta t}f_i^S$ = components of externally applied surface tractions per unit surface area at time $t + \Delta t$
${}^{t+\Delta t}S_f$ = surface at time $t + \Delta t$ on which external tractions are applied
δu_i^S = δu_i evaluated on the surface ${}^{t+\Delta t}S_f$ (the δu_i components are zero at and corresponding to the prescribed displacements on the surface ${}^{t+\Delta t}S_u$)

In (6.13), the left-hand side is the internal virtual work and the right-hand side is the external virtual work. The relation is derived as in linear infinitesimal displacement analysis (see Example 4.2), but the current configuration at time $t + \Delta t$ (with the stresses and forces at that time) is used. Hence, the derivation of (6.13) is based on the following equilibrium equations.

Within ${}^{t+\Delta t}V$ for $i = 1, 2, 3$,

$$\frac{\partial {}^{t+\Delta t}\tau_{ij}}{\partial {}^{t+\Delta t}x_j} + {}^{t+\Delta t}f_i^B = 0 \qquad \text{sum over } j = 1, 2, 3 \tag{6.15a}$$

and on the surface ${}^{t+\Delta t}S_f$, for $i = 1, 2, 3$,

$${}^{t+\Delta t}\tau_{ij} \, {}^{t+\Delta t}n_j = {}^{t+\Delta t}f_i^S \qquad \text{sum over } j = 1, 2, 3 \tag{6.15b}$$

where the ${}^{t+\Delta t}n_j$ are the components of the unit normal to the surface ${}^{t+\Delta t}S_f$ at time $t + \Delta t$.

As shown in Example 4.2, the equation (6.15a) is multiplied by arbitrary continuous virtual displacements δu_i that are zero at and corresponding to the prescribed displacements. The integration of the expression obtained from (6.15a) over the volume at time $t+\Delta t$ and the use of the divergence theorem and (6.15b) then directly yield the relation in (6.13).

We note that the strain tensor components $\delta_{t+\Delta t}e_{ij}$ corresponding to the imposed virtual displacements are like the components of the infinitesimal strain tensor, but the derivatives are with respect to the current coordinates at time $t + \Delta t$. The use of the strain tensor $\delta_{t+\Delta t}e_{ij}$ in (6.13) is the *direct* result of the transformation by the divergence theorem used in the derivation of (6.13), and this strain tensor is obtained irrespective of the magnitude of the virtual displacements.

However, we now recognize that the virtual displacements δu_i may be thought of as a *variation* in the real displacements ${}^{t+\Delta t}u_i$ (subject to the constraint that these variations must be zero at and corresponding to the prescribed displacements). These displacement variations result in variations in the current strains of the body, and we shall later, in particular, use the variation in the Green-Lagrange strain components corresponding to δu_i (see Example 6.10).

It is most important to recognize that the virtual work principle stated in (6.13) is simply an application of the equation in (4.7) (used in linear analysis) to the body considered in the configuration at time $t + \Delta t$. Therefore, all previous discussions and results

pertaining to the use of the virtual work principle in linear analysis are now directly applicable, with the current configuration at time $t + \Delta t$ being considered.[1]

A fundamental difficulty in the general application of (6.13) is that the configuration of the body at time $t + \Delta t$ is unknown. This is an important difference compared with linear analysis in which it is assumed that the displacements are infinitesimally small so that in (6.13) to (6.15) the original configuration is used. The continuous change in the configuration of the body entails some important consequences for the development of an incremental analysis procedure. For example, an important consideration must be that the Cauchy stresses at time $t + \Delta t$ cannot be obtained by simply adding to the Cauchy stresses at time t a stress increment that is due only to the straining of the material. Namely, the calculation of the Cauchy stresses at time $t + \Delta t$ must also take into account the rigid body rotation of the material because the components of the Cauchy stress tensor also change when the material is subjected to only a rigid body rotation.

The fact that the configuration of the body changes continuously in a large deformation analysis is dealt with in an elegant manner by using appropriate stress and strain measures and constitutive relations, as discussed in detail in the next sections.

Considering the discussions to follow, we recognize that a difficult point in the presentation of continuum mechanics relations for general large deformation analysis is the use of an effective notation because there are many different quantities that need to be dealt with. The symbols used should display all necessary information but should do so in a compact manner in order that the equations can be read with relative ease. For effective use of a notation, an understanding of the convention employed is most helpful, and for this purpose we summarize here briefly some basic facts and conventions used in our notation.

In our analysis we consider the motion of the body in a fixed (stationary) Cartesian coordinate system as displayed in Fig. 6.2. All kinematic and static variables are measured in this coordinate system, and throughout our description we use tensor notation.

The coordinates of a generic point P in the body at time 0 are ${}^0x_1$, ${}^0x_2$, ${}^0x_3$; at time t they are ${}^tx_1$, ${}^tx_2$, ${}^tx_3$; and at time $t + \Delta t$ they are ${}^{t+\Delta t}x_1$, ${}^{t+\Delta t}x_2$, ${}^{t+\Delta t}x_3$, where the left superscripts refer to the configuration of the body and the subscripts to the coordinate axes.

The notation for the displacements of the body is similar to the notation for the coordinates: at time t the displacements are ${}^tu_i$, $i = 1, 2, 3$, and at time $t + \Delta t$ the displacements are ${}^{t+\Delta t}u_i$, $i = 1, 2, 3$. Therefore, we have

$$\left.\begin{aligned} {}^tx_i &= {}^0x_i + {}^tu_i \\ {}^{t+\Delta t}x_i &= {}^0x_i + {}^{t+\Delta t}u_i \end{aligned}\right\} \qquad i = 1, 2, 3 \tag{6.16}$$

The increments in the displacements from time t to time $t + \Delta t$ are denoted as

$$ {}_tu_i = {}^{t+\Delta t}u_i - {}^tu_i; \qquad i = 1, 2, 3 \tag{6.17}$$

During motion of the body, its volume, surface area, mass density, stresses, and strains are changing continuously. We denote the specific mass, area, and volume of the body at times 0, t, and $t + \Delta t$ as ${}^0\rho$, ${}^t\rho$, ${}^{t+\Delta t}\rho$; ${}^0A$, ${}^tA$, ${}^{t+\Delta t}A$; and ${}^0V$, ${}^tV$, ${}^{t+\Delta t}V$, respectively.

Since the configuration of the body at time $t + \Delta t$ is not known, we will refer applied forces, stresses, and strains to a known equilibrium configuration. In analogy to the notation

[1]We may imagine that in considering the moving body, a picture is taken at time $t + \Delta t$ and then the principle of virtual displacements is applied to the state of the body in that picture.

used for coordinates and displacements, a left superscript indicates in which configuration the quantity (body force, surface traction, stress, etc.) occurs; in addition, a left subscript indicates the configuration with respect to which the quantity is measured. For example, the surface and body force components at time $t + \Delta t$, but measured in configuration 0, are ${}^{t+\Delta t}_{0}f_i^S$, ${}^{t+\Delta t}_{0}f_i^B$, $i = 1, 2, 3$. Here we have the exception that if the quantity under consideration occurs in the same configuration in which it is also measured, the left subscript may not be used; e.g., for the Cauchy stresses we have

$$ {}^{t+\Delta t}\tau_{ij} \equiv {}^{t+\Delta t}_{t+\Delta t}\tau_{ij} $$

In the formulation of the governing equilibrium equations we also need to consider derivatives of displacements and coordinates. In our notation a comma denotes differentiation with respect to the coordinate following, and the left subscript denoting time indicates the configuration in which this coordinate is measured; thus we have, for example,

$$ {}^{t+\Delta t}_{0}u_{i,j} = \frac{\partial {}^{t+\Delta t}u_i}{\partial {}^{0}x_j} $$

and

$$ {}^{0}_{t+\Delta t}x_{m,n} = \frac{\partial {}^{0}x_m}{\partial {}^{t+\Delta t}x_n} \tag{6.18} $$

Using these conventions, we shall define new symbols when they are first encountered.

6.2.2 The Deformation Gradient, Strain, and Stress Tensors

We mentioned in the previous section that in a large deformation analysis special attention must be given to the fact that the configuration of the body is changing continuously. This change in configuration can be dealt with in an elegant manner by defining auxiliary stress and strain measures. The objective in defining them is to express the internal virtual work in (6.13) in terms of an integral over a volume that is known and to be able to incrementally decompose the stresses and strains in an effective manner. There are various different stress and strain tensors that, in principle, could be used (see L. E. Malvern [A], Y. C. Fung [A], A. E. Green and W. Zerna [A], and R. Hill [A]). However, if the objective is to obtain an effective overall finite element solution procedure, only a few stress and strain measures need be considered. In the following we first consider the motion of a general body and define kinematic measures of this motion. We then introduce appropriate strain and the corresponding stress tensors. These are used later in the chapter to develop the incremental general finite element equations.

Consider the body in Fig. 6.2 at a generic time t. A fundamental measure of the deformation of the body is given by the *deformation gradient,* defined as[2]

[2] The deformation gradient is denoted as $\mathbf{F}$ in other books, but we use the notation ${}_0\mathbf{X}$ throughout this text because this symbol more naturally indicates that the differentiations of the coordinates ${}^{t}x_i$ with respect to the coordinates ${}^{0}x_j$ are performed.

$$\boxed{{}_0^t\mathbf{X} = \begin{bmatrix} \frac{\partial {}^t x_1}{\partial {}^0 x_1} & \frac{\partial {}^t x_1}{\partial {}^0 x_2} & \frac{\partial {}^t x_1}{\partial {}^0 x_3} \\ \frac{\partial {}^t x_2}{\partial {}^0 x_1} & \frac{\partial {}^t x_2}{\partial {}^0 x_2} & \frac{\partial {}^t x_2}{\partial {}^0 x_3} \\ \frac{\partial {}^t x_3}{\partial {}^0 x_1} & \frac{\partial {}^t x_3}{\partial {}^0 x_2} & \frac{\partial {}^t x_3}{\partial {}^0 x_3} \end{bmatrix}} \tag{6.19}$$

or

$${}_0^t\mathbf{X} = ({}_0\nabla {}^t\mathbf{x}^T)^T \tag{6.20}$$

where ${}_0\nabla$ is the gradient operator

$${}_0\nabla = \begin{bmatrix} \frac{\partial}{\partial {}^0 x_1} \\ \frac{\partial}{\partial {}^0 x_2} \\ \frac{\partial}{\partial {}^0 x_3} \end{bmatrix}; \qquad {}^t\mathbf{x}^T = [{}^t x_1 \quad {}^t x_2 \quad {}^t x_3] \tag{6.21}$$

The deformation gradient describes the stretches and rotations that the material fibers have undergone from time 0 to time t. Namely, let $d^0\mathbf{x}$ be a differential material fiber at time 0; then, by the chain rule of differentiation, this material fiber at time t is given by

$$d^t\mathbf{x} = {}_0^t\mathbf{X}\, d^0\mathbf{x} \tag{6.22}$$

Using chain differentiation, it also follows that

$$d^0\mathbf{x} = {}_t^0\mathbf{X}\, d^t\mathbf{x} \tag{6.23}$$

where ${}_t^0\mathbf{X}$ is the inverse deformation gradient. From (6.22) and (6.23) we obtain

$$d^0\mathbf{x} = ({}_t^0\mathbf{X})({}_0^t\mathbf{X})\, d^0\mathbf{x} \tag{6.24}$$

and hence [because (6.24) must hold for any differential length $d^0\mathbf{x}$], we have

$${}_t^0\mathbf{X} = ({}_0^t\mathbf{X})^{-1} \tag{6.25}$$

Therefore, the inverse deformation gradient ${}_t^0\mathbf{X}$ is actually the inverse of *the* deformation gradient ${}_0^t\mathbf{X}$.

An application of (6.18) is given by the evaluation of the mass density ${}^t\rho$ of the body at time t, namely,

$$\boxed{{}^t\rho = \frac{{}^0\rho}{\det ({}_0^t\mathbf{X})}} \tag{6.26}$$

We prove and illustrate this relationship in the following examples.

EXAMPLE 6.5: Consider the general motion of the body in Fig. 6.2 and establish that the mass density of the body changes as a function of the determinant of the deformation gradient,

$$ {}^t\rho = \frac{{}^0\rho}{\det ({}^t_0\mathbf{X})} $$

Any infinitesimal volume of material at time 0 can be represented using (see Fig. E6.5)

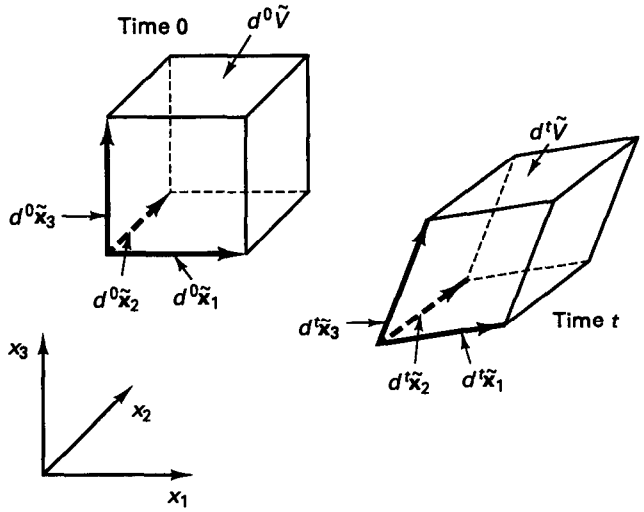

Figure E6.5 Infinitesimal volumes at times 0 and t

$$ d^0\tilde{\mathbf{x}}_1 = \begin{bmatrix} 1 \\ 0 \\ 0 \end{bmatrix} ds_1; \qquad d^0\tilde{\mathbf{x}}_2 = \begin{bmatrix} 0 \\ 1 \\ 0 \end{bmatrix} ds_2; \qquad d^0\tilde{\mathbf{x}}_3 = \begin{bmatrix} 0 \\ 0 \\ 1 \end{bmatrix} ds_3 $$

and

$$ d^0\tilde{\mathbf{V}} = ds_1\, ds_2\, ds_3 $$

Using (6.22), we have after deformation,

$$ d^t\tilde{\mathbf{x}}_i = {}^t_0\mathbf{X}\, d^0\tilde{\mathbf{x}}_i \qquad i = 1, 2, 3 $$

where we note that of course the same deformation gradient applies to all material fibers of that infinitesimal volume, and we obtain

$$ \begin{aligned} d^t\tilde{V} &= (d^t\tilde{\mathbf{x}}_1 \times d^t\tilde{\mathbf{x}}_2) \cdot d^t\tilde{\mathbf{x}}_3 \\ &= (\det {}^t_0\mathbf{X})\, ds_1\, ds_2\, ds_3 \\ &= \det {}^t_0\mathbf{X}\, d^0\tilde{V} \end{aligned} $$

But if we assume that no mass is lost during the deformation, we have

$$ {}^t\rho\, d^t\tilde{V} = {}^0\rho\, d^0\tilde{V} $$

and hence,

$$ {}^t\rho = \frac{{}^0\rho}{\det {}^t_0\mathbf{X}} $$

EXAMPLE 6.6: Consider the element in Fig. E6.6. Evaluate the deformation gradient and the mass density corresponding to the configuration at time t.

The displacement interpolation functions for this element were given in Fig. 5.4. Since the ${}^0x_1$, ${}^0x_2$ axes correspond to the r, s axes, respectively, we have

$$h_1 = \tfrac{1}{4}(1 + {}^0x_1)(1 + {}^0x_2); \qquad h_2 = \tfrac{1}{4}(1 - {}^0x_1)(1 + {}^0x_2)$$

$$h_3 = \tfrac{1}{4}(1 - {}^0x_1)(1 - {}^0x_2); \qquad h_4 = \tfrac{1}{4}(1 + {}^0x_1)(1 - {}^0x_2)$$

and

$$\frac{\partial h_1}{\partial {}^0x_1} = \frac{1}{4}(1 + {}^0x_2); \qquad \frac{\partial h_2}{\partial {}^0x_1} = -\frac{1}{4}(1 + {}^0x_2)$$

$$\frac{\partial h_3}{\partial {}^0x_1} = -\frac{1}{4}(1 - {}^0x_2); \qquad \frac{\partial h_4}{\partial {}^0x_1} = \frac{1}{4}(1 - {}^0x_2)$$

$$\frac{\partial h_1}{\partial {}^0x_2} = \frac{1}{4}(1 + {}^0x_1); \qquad \frac{\partial h_2}{\partial {}^0x_2} = \frac{1}{4}(1 - {}^0x_1)$$

$$\frac{\partial h_3}{\partial {}^0x_2} = -\frac{1}{4}(1 - {}^0x_1); \qquad \frac{\partial h_4}{\partial {}^0x_2} = -\frac{1}{4}(1 + {}^0x_1)$$

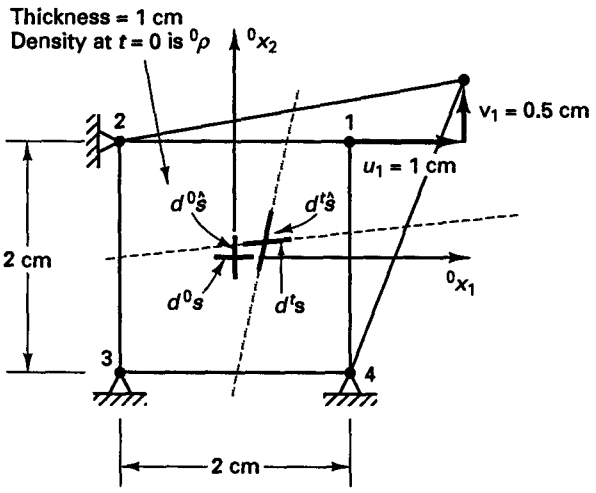

Figure E6.6 Four-node element subjected to large deformations

Now we use

$${}^tx_i = \sum_{k=1}^{4} h_k \, {}^tx_i^k$$

and hence,

$$\frac{\partial {}^tx_i}{\partial {}^0x_j} = \sum_{k=1}^{4} \left(\frac{\partial h_k}{\partial {}^0x_j}\right) {}^tx_i^k$$

The nodal point coordinates at time t are

$${}^tx_1^1 = 2; \qquad {}^tx_2^1 = 1.5; \qquad {}^tx_1^2 = -1; \qquad {}^tx_2^2 = 1$$

$${}^tx_1^3 = -1; \qquad {}^tx_2^3 = -1; \qquad {}^tx_1^4 = 1; \qquad {}^tx_2^4 = -1$$

Hence,

$$\frac{\partial {}^tx_1}{\partial {}^0x_1} = \frac{1}{4}[(1 + {}^0x_2)(2) - (1 + {}^0x_2)(-1) - (1 - {}^0x_2)(-1) + (1 - {}^0x_2)(1)]$$

$$= \frac{1}{4}(5 + {}^0x_2)$$

and

$$\frac{\partial {}^tx_1}{\partial {}^0x_2} = \frac{1}{4}(1 + {}^0x_1); \qquad \frac{\partial {}^tx_2}{\partial {}^0x_1} = \frac{1}{8}(1 + {}^0x_2)$$

$$\frac{\partial {}^tx_2}{\partial {}^0x_2} = \frac{1}{8}(9 + {}^0x_1)$$

so that the deformation gradient is

$${}_0^t\mathbf{X} = \frac{1}{4}\begin{bmatrix}(5 + {}^0x_2) & (1 + {}^0x_1) \\ \frac{1}{2}(1 + {}^0x_2) & \frac{1}{2}(9 + {}^0x_1)\end{bmatrix}$$

and using (6.26), the mass density in the deformed configuration is

$${}^t\rho = \frac{32\,{}^0\rho}{(5 + {}^0x_2)(9 + {}^0x_1) - (1 + {}^0x_1)(1 + {}^0x_2)}$$

The deformation gradient is also used to measure the stretch of a material fiber and the change in angle between adjacent material fibers due to the deformation. In this calculation we use the *right Cauchy-Green deformation* tensor,

$$\boxed{{}_0^t\mathbf{C} = {}_0^t\mathbf{X}^T\,{}_0^t\mathbf{X}} \tag{6.27}$$

We note that ${}_0^t\mathbf{C}$ is, in general, not equal to the *left Cauchy-Green deformation* tensor,

$${}_0^t\mathbf{B} = {}_0^t\mathbf{X}\,{}_0^t\mathbf{X}^T \tag{6.28}$$

EXAMPLE 6.7: The *stretch* ${}^t\lambda$ of a line element of a general body in motion is defined as ${}^t\lambda = {}^ds/{}^0s$, where ${}^0s$ and ${}^ts$ are the original and current lengths of the line element as shown in Fig. E6.7. Prove that

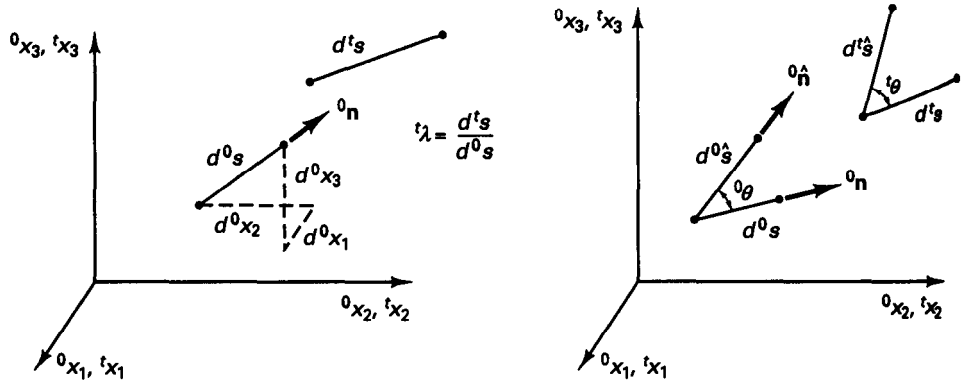

Figure E6.7 Stretch and rotation of line elements

$$ {}^t\lambda = ({}^0\mathbf{n}^T\, {}_0^t\mathbf{C}\, {}^0\mathbf{n})^{1/2} \tag{a} $$

where ${}^0\mathbf{n}$ is a vector of the direction cosines of the line element at time 0. Also, prove that considering two line elements emanating from the same material point, the angle ${}^t\theta$ between the line elements at time t is given by

$$ \cos {}^t\theta = \frac{{}^0\mathbf{n}^T\, {}_0^t\mathbf{C}\, {}^0\hat{\mathbf{n}}}{{}^t\lambda\, {}^t\hat{\lambda}} \tag{b} $$

where the hat denotes the second line element (see Fig. E6.7).

As an example, apply the formulas in (a) and (b) to evaluate the stretches of the specific line elements d^0s and $d^t\hat{s}$ shown in Fig. E6.6 and evaluate also the angular distortion between them.

To prove (a), we recognize that

$$ (d^ts)^2 = d^t\mathbf{x}^T\, d^t\mathbf{x}; \qquad d^t\mathbf{x} = {}_0^t\mathbf{X}\, d^0\mathbf{x} $$

so that using (6.27),

$$ (d^ts)^2 = d^0\mathbf{x}^T\, {}_0^t\mathbf{C}\, d^0\mathbf{x} $$

Hence,

$$ {}^t\lambda^2 = \frac{d^0\mathbf{x}^T}{d^0s}\, {}_0^t\mathbf{C} \frac{d^0\mathbf{x}}{d^0s} $$

and since

$$ {}^0\mathbf{n} = \frac{d^0\mathbf{x}}{d^0s} $$

we have

$$ {}^t\lambda = ({}^0\mathbf{n}^T\, {}_0^t\mathbf{C}\, {}^0\mathbf{n})^{1/2} $$

To prove (b) we use (2.50)

$$ d^t\mathbf{x}^T\, d^t\hat{\mathbf{x}} = (d^ts)(d^t\hat{s}) \cos {}^t\theta $$

Hence,

$$ \cos {}^t\theta = \frac{d^0\mathbf{x}^T\, {}_0^t\mathbf{X}^T\, {}_0^t\hat{\mathbf{X}}\, d^0\hat{\mathbf{x}}}{(d^ts)(d^t\hat{s})} \tag{c} $$

Since ${}_0^t\mathbf{X} \equiv {}_0^t\hat{\mathbf{X}}$ (it is the deformation gradient at the location of the differential line elements), we obtain from (c),

$$ \cos {}^t\theta = \frac{{}^0\mathbf{n}^T\, {}_0^t\mathbf{C}\, {}^0\hat{\mathbf{n}}}{{}^t\lambda\, {}^t\hat{\lambda}} $$

It should be noted that the relations in (a) and (b) show that when ${}_0^t\mathbf{C} = \mathbf{I}$, the stretches of the line elements are equal to 1 and the angle between line elements has not changed during the motion. Hence, when the Cauchy-Green deformation tensor is equal to the identity matrix, the motion could have been at most a rigid body motion.

If we apply (a) and (b) to the line elements depicted in Fig. E6.6, we obtain at ${}^0x_1 = 0$, ${}^0x_2 = 0$ (see Example 6.6)

$$ {}_0^t\mathbf{C} = \frac{1}{16}\begin{bmatrix} 25.25 & 7.25 \\ 7.25 & 21.25 \end{bmatrix} $$

$$ {}^0\mathbf{n} = \begin{bmatrix} 1 \\ 0 \end{bmatrix}; \qquad {}^0\hat{\mathbf{n}} = \begin{bmatrix} 0 \\ 1 \end{bmatrix} $$

Hence, using (a),

$$ {}^t\lambda = 1.256; \qquad {}^t\hat{\lambda} = 1.152 $$

and using (b),

$$ \cos {}^t\theta = 0.313; \qquad {}^t\theta = 71.75^\circ $$

Therefore, the angular distortion between the line elements d^0s and $d^0\hat{s}$ due to the motion from time 0 to time t is 18.25 degrees.

A most important property of the deformation gradient is that it can always be decomposed into a unique product of two matrices, a symmetric stretch matrix ${}^{t}_{0}\mathbf{U}$ and an orthogonal matrix ${}^{t}_{0}\mathbf{R}$ corresponding to a rotation such that

$$\boxed{{}^{t}_{0}\mathbf{X} = {}^{t}_{0}\mathbf{R}\,{}^{t}_{0}\mathbf{U}} \tag{6.29}$$

We can interpret (6.29), *conceptually*, to mean that the total deformation is obtained by first applying the stretch and then the rotation. That is, we could write (6.29) also as ${}^{t}_{0}\mathbf{X} = {}^{t}_{\tau}\mathbf{R}\,{}^{\tau}_{0}\mathbf{U}$, where τ corresponds to an intermediate (conceptual) time. Then we realize that the decomposition is really an application of the chain rule ${}^{t}_{0}\mathbf{X} = {}^{t}_{\tau}\mathbf{X}\,{}^{\tau}_{0}\mathbf{X}$, where ${}^{t}_{\tau}\mathbf{X} \equiv {}^{t}_{\tau}\mathbf{R}$ and ${}^{\tau}_{0}\mathbf{X} \equiv {}^{\tau}_{0}\mathbf{U}$. However, the state corresponding to τ is only conceptual, and we therefore usually use the notation in (6.29).

The relation in (6.29) is referred to as the *polar decomposition* of the deformation gradient, and we prove and demonstrate this property in the following examples.

To simplify the notation in the following discussion of continuum mechanics relations, we shall frequently not show the superscripts and subscripts t and 0 but always imply them, and when there is doubt, we shall also actually show them. For example, (6.29) is written as $\mathbf{X} = \mathbf{RU}$.

EXAMPLE 6.8: Show that the deformation gradient $\mathbf{X}$ can always be decomposed as follows:

$$\mathbf{X} = \mathbf{RU} \tag{a}$$

where $\mathbf{R}$ is an orthogonal (rotation) matrix and $\mathbf{U}$ is a stretch (symmetric) matrix.

To prove the relationship in (a), we consider the Cauchy-Green deformation tensor $\mathbf{C}$ and represent this tensor in its principal coordinate axes. For this purpose we solve the eigenproblem

$$\mathbf{Cp} = \lambda\mathbf{p} \tag{b}$$

The complete solution of (b) can be written as (see Section 2.5)

$$\mathbf{CP} = \mathbf{PC}'$$

where the columns of $\mathbf{P}$ are the eigenvectors of $\mathbf{C}$, and $\mathbf{C}'$ is a diagonal matrix storing the corresponding eigenvalues. We also have

$$\mathbf{P}^{T}\mathbf{CP} = \mathbf{C}' \tag{c}$$

and $\mathbf{C}'$ is the representation of the Cauchy-Green deformation tensor in its principal coordinate axes. The representation of the deformation gradient in this coordinate system, denoted as $\mathbf{X}'$, is similarly obtained

$$\mathbf{X}' = \mathbf{P}^{T}\mathbf{XP} \tag{d}$$

where we note that (c) and (d) are really tensor transformations from the original to a new coordinate system (see Section 2.4).

Using these relations and $\mathbf{C} = \mathbf{X}^{T}\mathbf{X}$, we have

$$\mathbf{C}' = \mathbf{X}'^{T}\mathbf{X}'$$

and we note that the matrix

$$\mathbf{R}' = \mathbf{X}'(\mathbf{C}')^{-1/2}$$

is an orthogonal matrix; i.e., $\mathbf{R}'^T\mathbf{R}' = \mathbf{I}$. Hence, we can write

$$\mathbf{X}' = \mathbf{R}'\mathbf{U}' \tag{e}$$

where

$$\mathbf{U}' = (\mathbf{C}')^{1/2}$$

and to evaluate $\mathbf{U}'$ we use the positive values of the square roots of the diagonal elements of $\mathbf{C}'$. The positive values must be used because the diagonal values in $\mathbf{U}'$ represent the stretches in the new coordinate system.

The relation in (e) is the decomposition of the deformation gradient $\mathbf{X}'$ into the product of the orthogonal matrix $\mathbf{R}'$ and the stretch matrix $\mathbf{U}'$. This decomposition has been accomplished in the principal axes of $\mathbf{C}$ but is also valid in any other (admissible) coordinate system because the deformation gradient is a tensor (see Section 2.4). Indeed, we can now obtain $\mathbf{R}$ and $\mathbf{U}$ directly corresponding to the decomposition in (a); i.e.,

$$\mathbf{R} = \mathbf{P}\mathbf{R}'\mathbf{P}^T$$

$$\mathbf{U} = \mathbf{P}\mathbf{U}'\mathbf{P}^T$$

where we used the inverse of the transformation employed in (d).

EXAMPLE 6.9: Consider the four-node element and its deformation shown in Fig. E6.9. (a) Evaluate the deformation gradient and its polar decomposition at time t. (b) Assume that the motion from time t to time $t + \Delta t$ consists only of a counterclockwise rigid body rotation of 45 degrees. Evaluate the new deformation gradient.

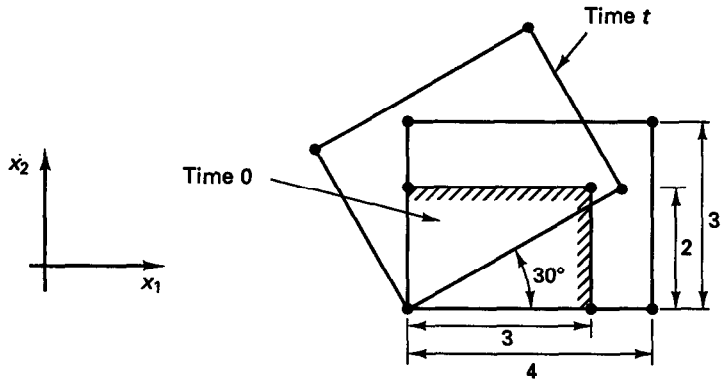

Figure E6.9 Four-node element subjected to stretching and rotation

To evaluate the deformation gradient at time t, we can here conveniently use ${}^{\delta}\mathbf{X} = {}^{t}_{\tau}\mathbf{R}\,{}^{\delta}\mathbf{U}$, where the hypothetical (or conceptual) configuration τ corresponds to the stretching of the fibers only. Hence,

$${}^{t}_{\tau}\mathbf{R} = \begin{bmatrix} \frac{\sqrt{3}}{2} & \frac{-1}{2} \\ \frac{1}{2} & \frac{\sqrt{3}}{2} \end{bmatrix}; \qquad {}^{\delta}\mathbf{U} = \begin{bmatrix} \frac{4}{3} & 0 \\ 0 & \frac{3}{2} \end{bmatrix}$$

and
$$ {}^{t}_{0}\mathbf{X} = \begin{bmatrix} \frac{2}{\sqrt{3}} & -\frac{3}{4} \\ \frac{2}{3} & \frac{3\sqrt{3}}{4} \end{bmatrix} $$

Of course, the same result is also obtained by writing ${}^{t}x_i$ in terms of ${}^{0}x_j$, $i = 1, 2; j = 1, 2$, and using the definition of ${}^{t}_{0}\mathbf{X}$ given in (6.19).

Let us next subject the element to the counterclockwise rotation of 45 degrees. The deformation gradient is then

$$ {}^{t+\Delta t}_{0}\mathbf{X} = \begin{bmatrix} \cos 45^\circ & -\sin 45^\circ \\ \sin 45^\circ & \cos 45^\circ \end{bmatrix} \begin{bmatrix} \frac{2}{\sqrt{3}} & -\frac{3}{4} \\ \frac{2}{3} & \frac{3\sqrt{3}}{4} \end{bmatrix} $$
$$ = \frac{1}{\sqrt{2}} \begin{bmatrix} \frac{2\sqrt{3}-2}{3} & -\frac{3+3\sqrt{3}}{4} \\ \frac{2\sqrt{3}+2}{3} & \frac{-3+3\sqrt{3}}{4} \end{bmatrix} $$

The proof in Example 6.8 also indicates how any deformation gradient can be decomposed into the product in (6.29). Assume that $\mathbf{X}$ is given and we want to find $\mathbf{R}$ and $\mathbf{U}$; then we may calculate $\mathbf{C} = \mathbf{X}^T\mathbf{X} = \mathbf{U}^2$ and, using (2.109), we have (for $n = 2$ or 3), $\mathbf{U} = \sum_{i=1}^{n} \sqrt{\lambda_i}\, \mathbf{p}_i\mathbf{p}_i^T$ with $\mathbf{C}\mathbf{p}_i = \lambda_i\mathbf{p}_i$. With $\mathbf{U}$ given, we obtain $\mathbf{R}$ from $\mathbf{R} = \mathbf{X}\mathbf{U}^{-1}$.

The preceding relations can now be used to evaluate additional kinematic relations that describe the motion of the body. That is, it can be proven (see Exercise 6.7) that we also have

$$ \mathbf{X} = \mathbf{V}\mathbf{R} \tag{6.30}^{3} $$

where $\mathbf{V}$ is also a symmetric matrix

$$ \mathbf{V} = \mathbf{R}\mathbf{U}\mathbf{R}^T \tag{6.31} $$

We refer to $\mathbf{U}$ as the right stretch matrix and to $\mathbf{V}$ as the left stretch matrix.

Example 6.8 shows that we have the spectral decomposition of $\mathbf{U}$,

$$ \mathbf{U} = \mathbf{R}_L\mathbf{\Lambda}\mathbf{R}_L^T \tag{6.32} $$

Physically, $\mathbf{\Lambda}$ corresponds to the principal stretches and $\mathbf{R}_L$ stores the directions of these stretches, with the rigid body rotation removed since this rotation appears in $\mathbf{R}$. (In Example 6.8, the matrix $\mathbf{P}$ is equal to $\mathbf{R}_L$.) We also have

$$ \mathbf{V} = \mathbf{R}_E\mathbf{\Lambda}\mathbf{R}_E^T \tag{6.33} $$

where
$$ \mathbf{R}_E = \mathbf{R}\mathbf{R}_L \tag{6.34} $$

We note that $\mathbf{R}_E$ stores the base vectors of the principal stretches in the stationary coordinate system x_i.

[3] Note that since we can write (6.30) as ${}^{t}_{0}\mathbf{X} = {}^{t}_{\tau}\mathbf{V}\,{}^{\tau}_{0}\mathbf{R}$, *conceptually*, the fibers can be thought of as being first rotated and then stretched [in contrast to the conceptual interpretation of (6.29)].

To proceed further with our description of the motion of the material particles in the body, we consider next the time rates of change of the quantities defined above. For this development we define

$$\dot{\mathbf{R}} = \boldsymbol{\Omega}_R \mathbf{R} \tag{6.35}$$

$$\dot{\mathbf{R}}_L = \mathbf{R}_L \boldsymbol{\Omega}_L \tag{6.36}$$

$$\dot{\mathbf{R}}_E = \mathbf{R}_E \boldsymbol{\Omega}_E \tag{6.37}$$

where $\boldsymbol{\Omega}_R$, $\boldsymbol{\Omega}_L$, and $\boldsymbol{\Omega}_E$ are skew-symmetric spin tensors, and clearly, using (6.34),

$$\boldsymbol{\Omega}_R = \mathbf{R}_E(\boldsymbol{\Omega}_E - \boldsymbol{\Omega}_L)\mathbf{R}_E^T \tag{6.38}$$

The *velocity gradient* $\mathbf{L}$ is defined as the gradient of the velocity field with respect to the *current* position ${}^t x_j$ of the material particles,

$$\mathbf{L} = \left[\frac{\partial {}^t\dot{u}_i}{\partial {}^t x_j}\right] \tag{6.39}$$

or

$$\mathbf{L} = \dot{\mathbf{X}}\mathbf{X}^{-1} \tag{6.40}$$

The symmetric part of $\mathbf{L}$ is the *velocity strain tensor* $\mathbf{D}$ (also called the rate-of-deformation tensor or stretching tensor), and the skew-symmetric part is the *spin tensor* $\mathbf{W}$ (also called the vorticity tensor). Hence,

$$\mathbf{L} = \mathbf{D} + \mathbf{W} \tag{6.41}$$

Using the polar decomposition of $\mathbf{X}$ we obtain from (6.40),

$$\mathbf{D} = \tfrac{1}{2}\mathbf{R}(\dot{\mathbf{U}}\mathbf{U}^{-1} + \mathbf{U}^{-1}\dot{\mathbf{U}})\mathbf{R}^T \tag{6.42}$$

$$\mathbf{W} = \boldsymbol{\Omega}_R + \tfrac{1}{2}\mathbf{R}(\dot{\mathbf{U}}\mathbf{U}^{-1} - \mathbf{U}^{-1}\dot{\mathbf{U}})\mathbf{R}^T \tag{6.43}$$

Substituting for $\mathbf{U}$ from (6.32), we can write

$$\mathbf{D} = \mathbf{R}_E \mathbf{D}_E \mathbf{R}_E^T \tag{6.44}$$

$$\mathbf{W} = \mathbf{R}_E \mathbf{W}_E \mathbf{R}_E^T \tag{6.45}$$

where

$$\mathbf{D}_E = \dot{\boldsymbol{\Lambda}}\boldsymbol{\Lambda}^{-1} + \tfrac{1}{2}(\boldsymbol{\Lambda}^{-1}\boldsymbol{\Omega}_L\boldsymbol{\Lambda} - \boldsymbol{\Lambda}\boldsymbol{\Omega}_L\boldsymbol{\Lambda}^{-1}) \tag{6.46}$$

$$\mathbf{W}_E = \boldsymbol{\Omega}_E - \tfrac{1}{2}(\boldsymbol{\Lambda}^{-1}\boldsymbol{\Omega}_L\boldsymbol{\Lambda} + \boldsymbol{\Lambda}\boldsymbol{\Omega}_L\boldsymbol{\Lambda}^{-1}) \tag{6.47}$$

Hence, we obtain for the elements of $\dot{\boldsymbol{\Lambda}}$,

$$[\dot{\boldsymbol{\Lambda}}]_{\alpha\alpha} = \lambda_\alpha [\mathbf{D}_E]_{\alpha\alpha} \qquad \text{no sum on } \alpha \tag{6.48}$$

where the λ_α are the stretches, and for the elements of $\boldsymbol{\Omega}_L$ and $\boldsymbol{\Omega}_E$, assuming that $\lambda_\alpha \neq \lambda_\beta$,

$$[\boldsymbol{\Omega}_L]_{\alpha\beta} = \frac{2\lambda_\beta\lambda_\alpha}{\lambda_\beta^2 - \lambda_\alpha^2}[\mathbf{D}_E]_{\alpha\beta} \tag{6.49}$$

$$[\boldsymbol{\Omega}_E]_{\alpha\beta} = [\mathbf{W}_E]_{\alpha\beta} + \frac{\lambda_\beta^2 + \lambda_\alpha^2}{\lambda_\beta^2 - \lambda_\alpha^2}[\mathbf{D}_E]_{\alpha\beta} \tag{6.50}$$

We note that $\mathbf{D}_E$ and $\mathbf{W}_E$ are the velocity strain and spin tensors referred to the principal axes of the deformation at time t. Hence, by representing the velocity strain and spin tensors in the basis given by $\mathbf{R}_E$, we obtain relationships that we can use directly to evaluate the components of $\dot{\boldsymbol{\Lambda}}$, $\boldsymbol{\Omega}_L$, and $\boldsymbol{\Omega}_E$.

We now want to define strain tensors that are valuable in finite element analysis. The *Green-Lagrange strain* tensor ${}_0^t\boldsymbol{\epsilon}$ is defined as

$$ {}_0^t\boldsymbol{\epsilon} = {}_0^t\mathbf{R}_L[\tfrac{1}{2}({}^t\boldsymbol{\Lambda}^2 - \mathbf{I})]{}_0^t\mathbf{R}_L^T \tag{6.51} $$

The *Hencky (or logarithmic) strain* tensor is defined as

$$ {}_0^t\mathbf{E}^H = {}_0^t\mathbf{R}_L(\ln {}^t\boldsymbol{\Lambda}){}_0^t\mathbf{R}_L^T \tag{6.52} $$

We note that since ${}_0^t\mathbf{R}$ does not enter the definitions in (6.51) and (6.52), both strain tensors are independent of the rigid body motions of the particles.

The Green-Lagrange strain tensor is frequently written in terms of the right stretch tensor ${}_0^t\mathbf{U}$; that is, using (6.51), we obtain

$$ \boxed{\begin{aligned} {}_0^t\boldsymbol{\epsilon} &= \tfrac{1}{2}[({}_0^t\mathbf{R}_L\,{}^t\boldsymbol{\Lambda}\,{}_0^t\mathbf{R}_L^T)({}_0^t\mathbf{R}_L\,{}^t\boldsymbol{\Lambda}\,{}_0^t\mathbf{R}_L^T) - \mathbf{I}] \\ &= \tfrac{1}{2}({}_0^t\mathbf{U}\,{}_0^t\mathbf{U} - \mathbf{I}) \end{aligned}} \tag{6.53} $$

Also, we can write the Green-Lagrange strain tensor in terms of the Cauchy-Green deformation tensor,

$$ \begin{aligned} {}_0^t\boldsymbol{\epsilon} &= \tfrac{1}{2}({}_0^t\mathbf{U}\,{}_0^t\mathbf{R}^T\,{}_0^t\mathbf{R}\,{}_0^t\mathbf{U} - \mathbf{I}) \\ &= \boxed{\tfrac{1}{2}({}_0^t\mathbf{X}^T\,{}_0^t\mathbf{X} - \mathbf{I})} \\ &= \tfrac{1}{2}({}_0^t\mathbf{C} - \mathbf{I}) \end{aligned} \tag{6.54} $$

Furthermore, evaluating the components in terms of displacements [i.e., using (6.16) and (6.19) in (6.54)], we have,

$$ \boxed{{}_0^t\epsilon_{ij} = \tfrac{1}{2}({}_0^tu_{i,j} + {}_0^tu_{j,i} + {}_0^tu_{k,i}\,{}_0^tu_{k,j})} \tag{6.55} $$

We should note that in the definition of the Green-Lagrange strain tensor, all derivatives are with respect to the *initial* coordinates of the material particles. For this reason, we say that the strain tensor is defined with respect to the initial coordinates of the body. Also note that, although only up to quadratic terms of displacement derivatives appear in (6.55), this is the complete strain tensor; i.e., we have not neglected any higher-order terms.

The Green-Lagrange and Hencky strain tensors are clearly of the general form

$$ \mathbf{E}_g = \mathbf{R}_L g(\boldsymbol{\Lambda})\mathbf{R}_L^T \tag{6.56} $$

where $g(\boldsymbol{\Lambda}) = \text{diag}\,[g(\lambda_i)]$. Hence, the rate of change of the strain tensors can be written as

$$ \dot{\mathbf{E}}_g = \mathbf{R}_L\dot{\mathbf{E}}_L\mathbf{R}_L^T \tag{6.57} $$

where we have

$$ \dot{\mathbf{E}}_L = \dot{\boldsymbol{\Lambda}}g'(\boldsymbol{\Lambda}) + \boldsymbol{\Omega}_L g(\boldsymbol{\Lambda}) - g(\boldsymbol{\Lambda})\boldsymbol{\Omega}_L \tag{6.58} $$

Expanding this equation, we can identify the components of $\dot{\mathbf{E}}_L$ as

$$ [\dot{\mathbf{E}}_L]_{\alpha\beta} = \gamma_{\alpha\beta}[\mathbf{D}_E]_{\alpha\beta} \tag{6.59} $$

where for the Green-Lagrange strain tensor,

$$\gamma_{\alpha\beta} = \lambda_\alpha \lambda_\beta \tag{6.60}$$

and for the Hencky strain tensor,

$$\gamma_{\alpha\beta} = \begin{cases} 1 & \text{if } \lambda_\alpha = \lambda_\beta \\ \dfrac{2\lambda_\alpha\lambda_\beta}{\lambda_\beta^2 - \lambda_\alpha^2} \ln \dfrac{\lambda_\beta}{\lambda_\alpha} & \text{otherwise} \end{cases} \tag{6.61}$$

Using (6.57) and (6.59), we can now establish an important relationship between the time rate of change of the Green-Lagrange strain tensor ${}_0^t\dot{\boldsymbol{\epsilon}}$ and the velocity strain tensor ${}^t\mathbf{D}$. Using (6.57), (6.59), (6.60), and (6.44), we obtain

$${}_0^t\mathbf{R}_L^T \, {}_0^t\dot{\boldsymbol{\epsilon}} \, {}_0^t\mathbf{R}_L = {}^t\boldsymbol{\Lambda} \, {}_0^t\mathbf{R}_E^T \, {}^t\mathbf{D} \, {}_0^t\mathbf{R}_E \, {}^t\boldsymbol{\Lambda} \tag{6.62}$$

and hence, using (6.32) and (6.34),

$$\boxed{{}_0^t\dot{\boldsymbol{\epsilon}} = {}_0^t\mathbf{X}^T \, {}^t\mathbf{D} \, {}_0^t\mathbf{X}} \qquad \boxed{{}^t\mathbf{D} = {}_t^0\mathbf{X}^T \, {}_0^t\dot{\boldsymbol{\epsilon}} \, {}_t^0\mathbf{X}} \tag{6.63}$$

or in component form (with super- and subscripts)

$$\boxed{{}_0^t\dot{\epsilon}_{ij} = {}_0^t x_{m,i} \, {}_0^t x_{n,j} \, {}^t D_{mn}} \qquad \boxed{{}^t D_{mn} = {}_t^0 x_{i,m} \, {}_t^0 x_{j,n} \, {}_0^t\dot{\epsilon}_{ij}} \tag{6.64}$$

Of course, we can obtain the same result, but with less insight, by simply differentiating the Green-Lagrange strain tensor with respect to time,

$${}_0^t\dot{\boldsymbol{\epsilon}} = \tfrac{1}{2}({}_0^t\dot{\mathbf{X}}^T \, {}_0^t\mathbf{X} + {}_0^t\mathbf{X}^T \, {}_0^t\dot{\mathbf{X}}) \tag{6.65}$$

Using (6.40) and (6.41) to substitute into (6.65), we directly obtain (6.63). We demonstrate this derivation for virtual displacement increments, or variations in the current displacements, in the following example.

EXAMPLE 6.10: Consider a body in its deformed configuration at time t (see Fig. E6.10). The current coordinates of the material particles of the body are ${}^t x_i$, $i = 1, 2, 3$, and the current displacements are ${}^t u_i = {}^t x_i - {}^0 x_i$.

Assume that a virtual displacement field is applied, which we denote as δu_i (see Fig. E6.10). This virtual displacement field can be thought of as a variation on the current displacements; hence, we may write $\delta u_i \equiv \delta {}^t u_i$ However, the variation on the current displacements must correspond to a variation on the current Green-Lagrange strain components, $\delta {}_0^t\epsilon_{ij}$, and also to a small strain tensor $\delta {}_t e_{mn}$ referred to the current configuration. Evaluate the components $\delta {}_0^t\epsilon_{ij}$ and show that

$$\delta {}_0^t\epsilon_{ij} = {}_0^t x_{m,i} \, {}_0^t x_{n,j} \, \delta {}_t e_{mn} \tag{a}$$

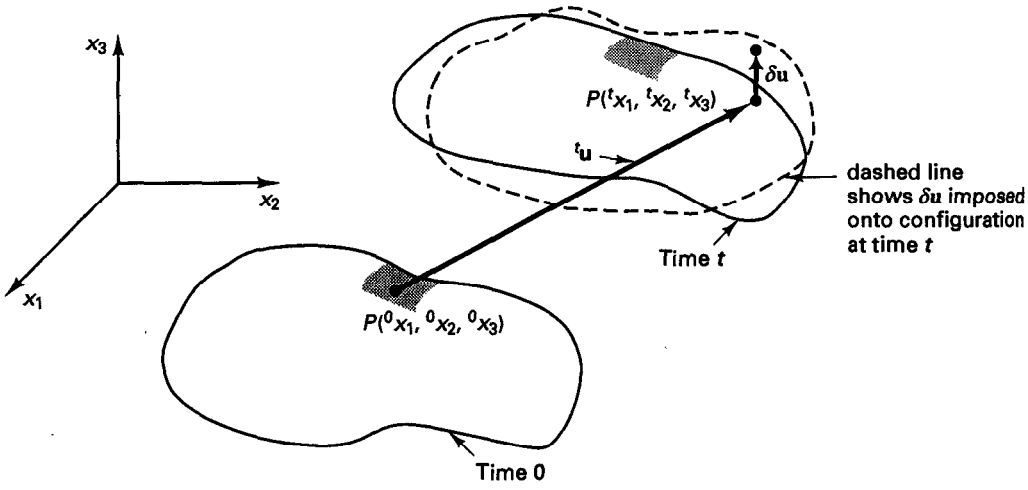

Figure E6.10 Body at time t subjected to virtual displacement field given by $\delta \mathbf{u}$. Note that $\delta \mathbf{u}$ is a function of ${}^tx_i$, $i = 1,2,3$, and we can think of δu_i as a variation on ${}^tu_i$.

where
$$\delta_t e_{mn} = \frac{1}{2}\left(\frac{\partial \delta u_m}{\partial {}^tx_n} + \frac{\partial \delta u_n}{\partial {}^tx_m}\right)$$

We use the definition of the Green-Lagrange strain in (6.54) to obtain

$$\delta {}^t_0\boldsymbol{\epsilon} = \tfrac{1}{2}[(\delta {}^t_0\mathbf{X}^T)({}^t_0\mathbf{X}) + ({}^t_0\mathbf{X}^T)(\delta {}^t_0\mathbf{X})] \tag{b}$$

Let us define $\delta_t\mathbf{u}$ to be

$$\delta_t\mathbf{u} = \begin{bmatrix} \dfrac{\partial \delta u_1}{\partial {}^tx_1} & \dfrac{\partial \delta u_1}{\partial {}^tx_2} & \cdots \\ \dfrac{\partial \delta u_2}{\partial {}^tx_1} & \dfrac{\partial \delta u_2}{\partial {}^tx_2} & \cdots \\ & \cdots & \end{bmatrix}$$

then
$$\delta {}^t_0\mathbf{X} = \delta_t\mathbf{u}\ {}^t_0\mathbf{X}$$

and hence (b) can be written as

$$\begin{aligned} \delta {}^t_0\boldsymbol{\epsilon} &= \tfrac{1}{2}[{}^t_0\mathbf{X}^T(\delta_t\mathbf{u})^T\ {}^t_0\mathbf{X} + {}^t_0\mathbf{X}^T(\delta_t\mathbf{u})\ {}^t_0\mathbf{X}] \\ &= {}^t_0\mathbf{X}^T\{\tfrac{1}{2}[(\delta_t\mathbf{u})^T + \delta_t\mathbf{u}]\}\ {}^t_0\mathbf{X} \\ &= {}^t_0\mathbf{X}^T\ \delta_t\mathbf{e}\ {}^t_0\mathbf{X} \end{aligned}$$

which is (a) in matrix form.

Note that a simple closed-form relationship cannot be established between the time rate of change of the Hencky strain tensor and the velocity strain tensor [because of the complex expression in (6.61)]. We shall use the Hencky strain measure only later for large strain inelastic analysis, and the appropriate relationships will then be evaluated based on work conjugacy (see Section 6.6.4).

However, we shall use the Green-Lagrange strain tensor frequently and now want to define the appropriate stress tensor to use with this strain tensor. The stress measure to use is the *second Piola-Kirchhoff stress* tensor ${}_0^t\mathbf{S}$, which is work-conjugate with the Green-Lagrange strain tensor.[4]

Consider the stress power per unit reference volume ${}^tJ\,{}^t\boldsymbol{\tau} \cdot {}^t\mathbf{D}$,[5] where ${}^t\boldsymbol{\tau}$ is the Cauchy stress tensor and ${}^tJ = \det {}_0^t\mathbf{X}$. Then the second Piola-Kirchhoff stress tensor ${}_0^t\mathbf{S}$ is given by

$$ {}^tJ\,{}^t\boldsymbol{\tau} \cdot {}^t\mathbf{D} = {}_0^t\mathbf{S} \cdot {}_0^t\dot{\boldsymbol{\epsilon}} \tag{6.66} $$

To find the explicit expression for ${}_0^t\mathbf{S}$, we substitute from (6.63) to obtain

$$ {}^tJ\,{}^t\boldsymbol{\tau} \cdot {}^t\mathbf{D} = {}_0^t\mathbf{S} \cdot ({}_0^t\mathbf{X}^T\,{}^t\mathbf{D}\,{}_0^t\mathbf{X}) \tag{6.67} $$

Since this relationship must hold for any ${}^t\mathbf{D}$, we have[6]

$$ \boxed{{}_0^t\mathbf{S} = \frac{{}^0\rho}{{}^t\rho}\,{}_t^0\mathbf{X}\,{}^t\boldsymbol{\tau}\,{}_t^0\mathbf{X}^T} \qquad \boxed{{}^t\boldsymbol{\tau} = \frac{{}^t\rho}{{}^0\rho}\,{}_0^t\mathbf{X}\,{}_0^t\mathbf{S}\,{}_0^t\mathbf{X}^T} \tag{6.68} $$

or in component forms

$$ \boxed{{}_0^tS_{ij} = \frac{{}^0\rho}{{}^t\rho}\,{}_t^0x_{i,m}\,{}_t^0x_{j,n}\,{}^t\tau_{mn}} \qquad \boxed{{}^t\tau_{mn} = \frac{{}^t\rho}{{}^0\rho}\,{}_0^tx_{m,i}\,{}_0^tx_{n,j}\,{}_0^tS_{ij}} \tag{6.69} $$

There has been much discussion about the physical nature of the second Piola-Kirchhoff stress tensor. However, although it is possible to relate the transformation on the Cauchy stress tensor in (6.68) to some geometry arguments as discussed in the next example, it should be recognized that the second Piola-Kirchhoff stresses have little physical meaning and, in practice, Cauchy stresses must be calculated.

[4] We use extensively in this book the second Piola-Kirchhoff stress tensor ${}_0^t\mathbf{S}$ defined by (6.66) and (6.68). The first Piola-Kirchhoff stress tensor is given by ${}_0^t\mathbf{S}\,{}_0^t\mathbf{X}^T$ (or the transpose thereof). In addition, we also have the Kirchhoff stress tensor given by ${}^tJ\,{}^t\boldsymbol{\tau}$ (see, for example, L. E. Malvern [A]).

[5] Note that here and in the following we use the notation that with $\mathbf{a}$ and $\mathbf{b}$ second-order tensors we have $\mathbf{a} \cdot \mathbf{b} = \mathbf{a}_{ij}\mathbf{b}_{ij}$ [sum over all i, j; see (2.79)].

[6] Here we use ${}_0^t\mathbf{S} \cdot ({}_0^t\mathbf{X}^T\,{}^t\mathbf{D}\,{}_0^t\mathbf{X}) = ({}_0^t\mathbf{X}\,{}_0^t\mathbf{S}\,{}_0^t\mathbf{X}^T) \cdot {}^t\mathbf{D}$, as can be easily proven by writing the matrices in component forms (see Exercise 2.14).

EXAMPLE 6.11: Figure E6.11 shows a generic body in the configurations at times 0 and t. Let $d^t\mathbf{T}$ be the actual force on a surface area d^tS in the configuration at time t, and let us define a (fictitious) force

$$d^0\mathbf{T} = {}^0_t\mathbf{X}\, d^t\mathbf{T}; \qquad {}^0_t\mathbf{X} = \left[\frac{\partial {}^0x_i}{\partial {}^tx_j}\right] \tag{a}$$

which acts on the surface area d^0S, where d^0S has become d^tS and ${}^0_t\mathbf{X}$ is the inverse of the deformation gradient, ${}^0_t\mathbf{X} = {}^t_0\mathbf{X}^{-1}$. Show that the second Piola-Kirchhoff stresses measured in the original configuration are the stress components corresponding to $d^0\mathbf{T}$.

Let the unit normals to the surface areas d^0S and d^tS be ${}^0\mathbf{n}$ and ${}^t\mathbf{n}$, respectively. Force equilibrium (of the wedge ABC in Fig. E6.11) in the configuration at time t requires that

$$d^t\mathbf{T} = {}^t\boldsymbol{\tau}^T\, {}^t\mathbf{n}\, d^tS \tag{b}$$

and similarly in the configuration at time 0

$$d^0\mathbf{T} = {}^t_0\mathbf{S}^T\, {}^0\mathbf{n}\, d^0S \tag{c}$$

The relations in (b) and (c) are referred to as *Cauchy's formula.* However, it can be shown that the following kinematic relationship exists:

$${}^t\mathbf{n}\, d^tS = \frac{{}^0\rho}{{}^t\rho}\, {}^0_t\mathbf{X}^T\, {}^0\mathbf{n}\, d^0S \tag{d}$$

This relation is referred to as *Nanson's formula.* Now using (a) to (d), we obtain

$${}^t_0\mathbf{S}^T\, {}^0\mathbf{n}\, d^0S = {}^0_t\mathbf{X}\, {}^t\boldsymbol{\tau}^T \frac{{}^0\rho}{{}^t\rho}\, {}^0_t\mathbf{X}^T\, {}^0\mathbf{n}\, d^0S$$

or

$$\left({}^t_0\mathbf{S}^T - \frac{{}^0\rho}{{}^t\rho}\, {}^0_t\mathbf{X}\, {}^t\boldsymbol{\tau}^T\, {}^0_t\mathbf{X}^T\right){}^0\mathbf{n}\, d^0S = \mathbf{0}$$

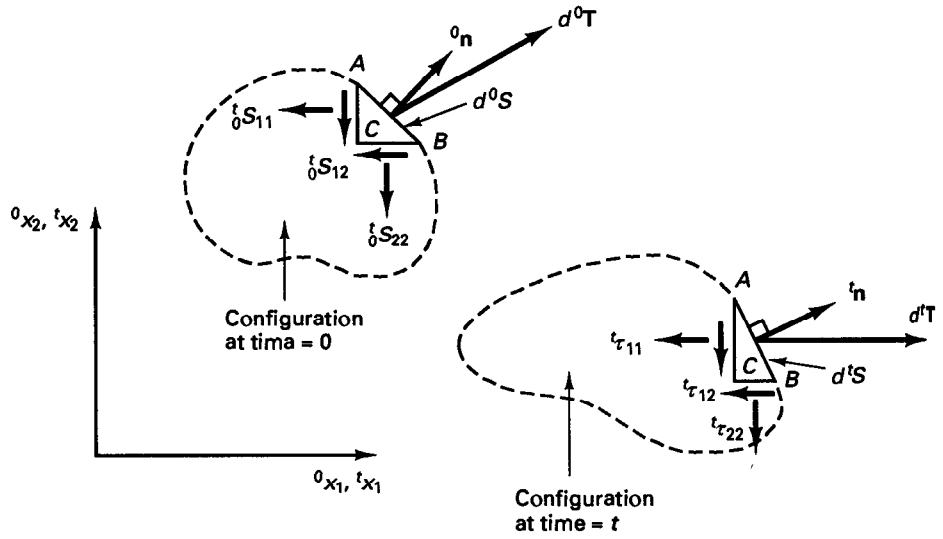

Figure E6.11 Second Piola-Kirchhoff and Cauchy stresses in two-dimensional action

However, this relationship must hold for any surface area and also any "interior surface area" that could be created by a cut in the body. Hence, the normal ${}^0\mathbf{n}$ is arbitrary and can be chosen to be in succession equal to the unit coordinate vectors. It follows that

$$ {}_0^t\mathbf{S} = \frac{{}^0\rho}{{}^t\rho} {}_t^0\mathbf{X}\, {}^t\boldsymbol{\tau}\, {}_t^0\mathbf{X}^T $$

where we used the property that the matrices ${}^t\boldsymbol{\tau}$ and ${}_0^t\mathbf{S}$ are symmetric.

Finally, we may interpret the force defined in (a). We note that the force $d^0\mathbf{T}$, which is balanced by the second Piola-Kirchhoff stresses on the wedge ABC, is related to the actual force $d^t\mathbf{T}$ in the same way as an original fiber in d^0S is deformed

$$ d^0\mathbf{x} = {}_t^0\mathbf{X}\, d^t\mathbf{x} $$

We may therefore say that in using (a) to obtain $d^0\mathbf{T}$, the force $d^t\mathbf{T}$ is "stretched and rotated" in the same way that $d^t\mathbf{x}$ is stretched and rotated to obtain $d^0\mathbf{x}$.

We note that the components of the Green-Lagrange strain tensor and second Piola-Kirchhoff stress tensor do not change when the material is subjected to only a rigid body translation because such motion does not change the deformation gradient.

The definition of the second Piola-Kirchhoff stress tensor also implies that the components do not change when the body being considered is undergoing a rigid body rotation. Since the invariance of the Green-Lagrange strain tensor components and second Piola-Kirchhoff stress tensor components in rigid body rotations is of great importance, we consider these properties in the following four examples.

Of course, the invariance of the Green-Lagrange strain tensor components with respect to rigid body rotations already follows from (6.53), since, as we pointed out earlier, the rigid body rotation of the fibers expressed in the matrix ${}_0^t\mathbf{R}$ does not enter the definition of (6.53). To gain further insight, let us consider the following example.

EXAMPLE 6.12: Show that the components of the Green-Lagrange strain tensor are invariant under a rigid body rotation of the material.

Let the Green-Lagrange strain tensor components at time t be given by

$$ {}_0^t\boldsymbol{\epsilon} = \tfrac{1}{2}({}_0^t\mathbf{X}^T\, {}_0^t\mathbf{X} - \mathbf{I}) \tag{a} $$

where ${}_0^t\mathbf{X}$ is the deformation gradient at time t corresponding to the *stationary* coordinate system x_i, $i = 1, 2, 3$.

Assume that the material is subjected to a rigid body rotation from time t to time $t + \Delta t$. Then corresponding to the stationary coordinate system x_i, we have

$$ {}_0^{t+\Delta t}\mathbf{X} = \mathbf{R}\, {}_0^t\mathbf{X} \tag{b} $$

where $\mathbf{R}$ corresponds to the rotation, and then

$$ {}_0^{t+\Delta t}\boldsymbol{\epsilon} = \tfrac{1}{2}({}_0^{t+\Delta t}\mathbf{X}^T\, {}_0^{t+\Delta t}\mathbf{X} - \mathbf{I}) \tag{c} $$

Substituting (b) into (c) and comparing the result with (a), we obtain

$$ {}_0^{t+\Delta t}\boldsymbol{\epsilon} = {}_0^t\boldsymbol{\epsilon} $$

EXAMPLE 6.13: A four-node element is stretched until time t and then undergoes without distortion a large rigid body rotation from time t to time $t + \Delta t$ as depicted in Fig. E6.13. Show explicitly that for the element the components of the Green-Lagrange strain tensor at time t and time $t + \Delta t$ are exactly equal.

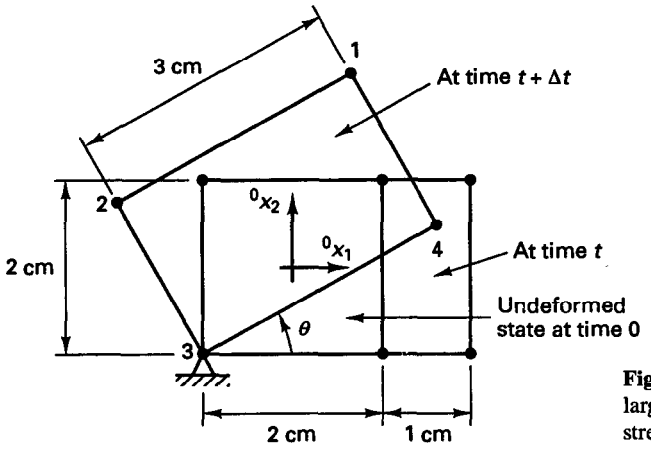

Figure E6.13 Element subjected to large rigid body rotation after initial stretch

The Green-Lagrange strain components at time t can be evaluated by inspection using (6.51),

$$ {}^t_0\epsilon_{22} = 0; \qquad {}^t_0\epsilon_{12} = {}^t_0\epsilon_{21} = 0 $$

and

$$ {}^t_0\epsilon_{11} = \frac{1}{2}\left[\left(\frac{3}{2}\right)^2 - 1\right] $$

$$ = \tfrac{5}{8} $$

Hence,

$$ {}^t_0\boldsymbol{\epsilon} = \begin{bmatrix} \frac{5}{8} & 0 \\ 0 & 0 \end{bmatrix} $$

Alternatively, we can use (6.54), where we first evaluate the deformation gradient as in Example 6.6:

$$ {}^t_0\mathbf{X} = \begin{bmatrix} \frac{3}{2} & 0 \\ 0 & 1 \end{bmatrix} $$

Hence,

$$ {}^t_0\mathbf{C} = \begin{bmatrix} \frac{9}{4} & 0 \\ 0 & 1 \end{bmatrix} $$

and as before,

$$ {}^t_0\boldsymbol{\epsilon} = \begin{bmatrix} \frac{5}{8} & 0 \\ 0 & 0 \end{bmatrix} \qquad \text{(a)} $$

After the rigid body rotation the nodal point coordinates are

Node	$^{t+\Delta t}x_1$	$^{t+\Delta t}x_2$
1	$3\cos\theta - 1 - 2\sin\theta$	$3\sin\theta - 1 + 2\cos\theta$
2	$-1 - 2\sin\theta$	$2\cos\theta - 1$
3	-1	-1
4	$3\cos\theta - 1$	$3\sin\theta - 1$

Thus, using again the procedure in Example 6.6 to evaluate the deformation gradient, we obtain

$$ {}^{t+\Delta t}_{0}\mathbf{X} = \frac{1}{4}\left[\begin{array}{l|l} (1 + {}^{0}x_2)(3\cos\theta - 1 - 2\sin\theta) & (1 + {}^{0}x_1)(3\cos\theta - 1 - 2\sin\theta) \\ -(1 + {}^{0}x_2)(-1 - 2\sin\theta) & +(1 - {}^{0}x_1)(-1 - 2\sin\theta) \\ -(1 - {}^{0}x_2)(-1) & -(1 - {}^{0}x_1)(-1) \\ +(1 - {}^{0}x_2)(3\cos\theta - 1) & -(1 + {}^{0}x_1)(3\cos\theta - 1) \\ \hline (1 + {}^{0}x_2)(3\sin\theta - 1 + 2\cos\theta) & (1 + {}^{0}x_1)(3\sin\theta - 1 + 2\cos\theta) \\ -(1 + {}^{0}x_2)(2\cos\theta - 1) & +(1 - {}^{0}x_1)(2\cos\theta - 1) \\ -(1 - {}^{0}x_2)(-1) & -(1 - {}^{0}x_1)(-1) \\ +(1 - {}^{0}x_2)(3\sin\theta - 1) & -(1 + {}^{0}x_1)(3\sin\theta - 1) \end{array}\right] \tag{b} $$

or

$$ {}^{t+\Delta t}_{0}\mathbf{X} = \begin{bmatrix} \frac{3}{2}\cos\theta & -\sin\theta \\ \frac{3}{2}\sin\theta & \cos\theta \end{bmatrix} \tag{c} $$

In reference to (6.29) we note that this deformation gradient can be written as

$$ {}^{t+\Delta t}_{0}\mathbf{X} = {}^{t+\Delta t}_{t}\mathbf{R}\ {}^{t}_{0}\mathbf{U} \tag{d} $$

where

$$ {}^{t+\Delta t}_{t}\mathbf{R} = \begin{bmatrix} \cos\theta & -\sin\theta \\ \sin\theta & \cos\theta \end{bmatrix}; \qquad {}^{t}_{0}\mathbf{U} = \begin{bmatrix} \frac{3}{2} & 0 \\ 0 & 1 \end{bmatrix} $$

This decomposition certainly corresponds to the actual physical situation, in which we measured a stretch in the ${}^{0}x_1$ direction and then a rotation. Therefore, we could have established ${}^{t+\Delta t}_{0}\mathbf{X}$ using (d) instead of performing all the calculations leading to (b) and thus (c)!

Using (d) and (6.27), we obtain

$$ {}^{t+\Delta t}_{0}\mathbf{C} = \begin{bmatrix} \frac{9}{4} & 0 \\ 0 & 1 \end{bmatrix} $$

and thus using (6.54), we have

$$ {}^{t+\Delta t}_{0}\boldsymbol{\epsilon} = \begin{bmatrix} \frac{5}{8} & 0 \\ 0 & 0 \end{bmatrix} \tag{e} $$

Hence ${}^{t}_{0}\boldsymbol{\epsilon}$ in (a) is equal to ${}^{t+\Delta t}_{0}\boldsymbol{\epsilon}$ in (e), which shows that the Green-Lagrange strain components did not change as a result of the rigid body rotation.

EXAMPLE 6.14: Show that the components of the second Piola-Kirchhoff stress tensor are invariant under a rigid body rotation of the material.

Here we consider a stationary coordinate system x_i, $i = 1, 2, 3$ and assume that the second Piola-Kirchhoff stress components are given in ${}^{t}_{0}\mathbf{S}$. Let the Cauchy stress, deformation gradient, and mass density at time t be ${}^{t}\boldsymbol{\tau}$, ${}^{t}_{0}\mathbf{X}$, and ${}^{t}\rho$. Hence,

$$ {}^{t}_{0}\mathbf{S} = \frac{{}^{0}\rho}{{}^{t}\rho}\,{}^{0}_{t}\mathbf{X}\ {}^{t}\boldsymbol{\tau}\ {}^{0}_{t}\mathbf{X}^{T} \tag{a} $$

where ${}^{0}_{t}\mathbf{X}$ is the inverse deformation gradient.

If a rigid body rotation is applied to the material from time t to time $t + \Delta t$, the deformation gradient changes to

$$ {}^{t+\Delta t}_{0}\mathbf{X} = \mathbf{R}\ {}^{t}_{0}\mathbf{X} $$

where $\mathbf{R}$ is an orthogonal (rotation) matrix, and hence

$$ {}^{0}_{t+\Delta t}\mathbf{X} = {}^{0}_{t}\mathbf{X}\mathbf{R}^{T} \tag{b} $$

Equations (a) and (b) show that

$$ {}^{t+\Delta t}_{0}\mathbf{S} = \frac{{}^{0}\rho}{{}^{t}\rho}\, {}^{0}_{t}\mathbf{X}\mathbf{R}^{T}\, {}^{t+\Delta t}\boldsymbol{\tau}\mathbf{R}\, {}^{0}_{t}\mathbf{X}^{T} \tag{c} $$

During the rigid body rotation of the material, the stress components remain constant in the rotating coordinate system. Hence the Cauchy stresses at time $t + \Delta t$ are in the fixed coordinate system,

$$ {}^{t+\Delta t}\boldsymbol{\tau} = \mathbf{R}\, {}^{t}\boldsymbol{\tau}\mathbf{R}^{T} \tag{d} $$

Substituting from (d) into (c), we obtain

$$ {}^{t+\Delta t}_{0}\mathbf{S} = \frac{{}^{0}\rho}{{}^{t}\rho}\, {}^{0}_{t}\mathbf{X}^{T}\, {}^{t}\boldsymbol{\tau}\, {}^{0}_{t}\mathbf{X}^{T} $$

which completes the proof. Note that the reason for the second Piola-Kirchhoff stress components not to change is that the same matrix $\mathbf{R}$ is used in equations (b) and (d).

EXAMPLE 6.15: Figure E6.15 shows a four-node element in the configuration at time 0. The element is subjected to a stress (initial stress) of ${}^{0}\tau_{11}$. Assume that the element is rotated in time 0 to time Δt as a rigid body through a large angle θ and that the stress in a body-attached coordinate system does not change. Hence, the magnitude of ${}^{\Delta t}\bar{\tau}_{11}$ shown in Fig. E6.15 is equal to ${}^{0}\tau_{11}$. Show that the components of the second Piola-Kirchhoff stress tensor did not change as a result of the rigid body rotation.

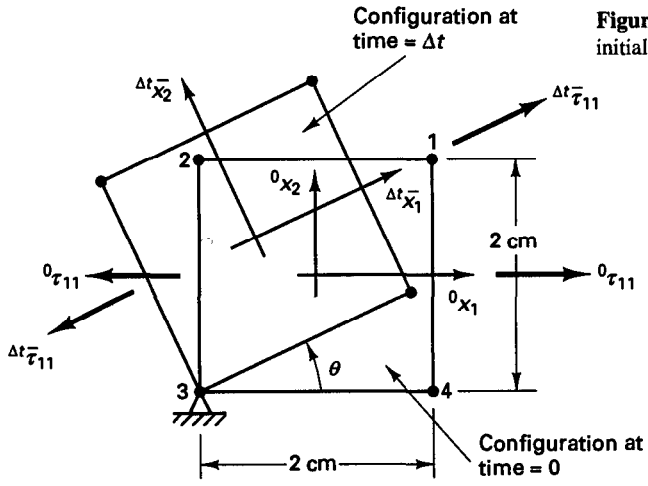

Figure E6.15 Four-node element with initial stress subjected to large rotation

The second Piola-Kirchhoff stress tensor at time 0 is equal to the Cauchy stress tensor because the element deformations are zero,

$$ {}^{0}_{0}\mathbf{S} = \begin{bmatrix} {}^{0}\tau_{11} & 0 \\ 0 & 0 \end{bmatrix} \tag{a} $$

The components of the Cauchy stress tensor at time Δt expressed in the coordinate axes ${}^{0}x_1, {}^{0}x_2$ are

$$ {}^{\Delta t}\boldsymbol{\tau} = \begin{bmatrix} \cos\theta & -\sin\theta \\ \sin\theta & \cos\theta \end{bmatrix} \begin{bmatrix} {}^{\Delta t}\bar{\tau}_{11} & 0 \\ 0 & 0 \end{bmatrix} \begin{bmatrix} \cos\theta & \sin\theta \\ -\sin\theta & \cos\theta \end{bmatrix} \tag{b} $$

This transformation corresponds to a second-order tensor transformation of the components ${}^{\Delta t}\bar{\tau}_{ij}$ from the body-attached coordinate frame ${}^{\Delta t}\bar{x}_1$, ${}^{\Delta t}\bar{x}_2$ to the stationary coordinate frame ${}^0x_1$, ${}^0x_2$ (see Section 2.4).

The relation between the Cauchy stresses and the second Piola-Kirchhoff stresses at time Δt is, according to (6.68),

$$ {}^{\Delta t}\boldsymbol{\tau} = \frac{{}^{\Delta t}\rho}{{}^0\rho} {}^{\Delta t}_0\mathbf{X}\, {}^{\Delta t}_0\mathbf{S}\, {}^{\Delta t}_0\mathbf{X}^T \tag{c} $$

where in this case ${}^{\Delta t}\rho/{}^0\rho = 1$. The deformation gradient can be evaluated as in Example 6.6, where we note that the nodal point coordinates at time t are

$$ {}^{\Delta t}x_1^1 = 2\cos\theta - 1 - 2\sin\theta; \qquad {}^{\Delta t}x_2^1 = 2\sin\theta - 1 + 2\cos\theta $$

$$ {}^{\Delta t}x_1^2 = -1 - 2\sin\theta; \qquad {}^{\Delta t}x_2^2 = 2\cos\theta - 1 $$

$$ {}^{\Delta t}x_1^3 = -1; \qquad {}^{\Delta t}x_2^3 = -1 $$

$$ {}^{\Delta t}x_1^4 = 2\cos\theta - 1; \qquad {}^{\Delta t}x_2^4 = 2\sin\theta - 1 $$

Hence, using the derivatives of the interpolation functions given in Example 6.6, we have

$$ {}^{\Delta t}_0\mathbf{X} = \frac{1}{4}\left[\begin{array}{c|c} (1 + {}^0x_2)(2\cos\theta - 1 - 2\sin\theta) & (1 + {}^0x_1)(2\cos\theta - 1 - 2\sin\theta) \\ -(1 + {}^0x_2)(-1 - 2\sin\theta) & +(1 - {}^0x_1)(-1 - 2\sin\theta) \\ -(1 - {}^0x_2)(-1) & -(1 - {}^0x_1)(-1) \\ +(1 - {}^0x_2)(2\cos\theta - 1) & -(1 + {}^0x_1)(2\cos\theta - 1) \\ \hline (1 + {}^0x_2)(2\sin\theta - 1 + 2\cos\theta) & (1 + {}^0x_1)(2\sin\theta - 1 + 2\cos\theta) \\ -(1 + {}^0x_2)(2\cos\theta - 1) & +(1 - {}^0x_1)(2\cos\theta - 1) \\ -(1 - {}^0x_2)(-1) & -(1 - {}^0x_1)(-1) \\ +(1 - {}^0x_2)(2\sin\theta - 1) & -(1 + {}^0x_1)(2\sin\theta - 1) \end{array}\right] $$

or

$$ {}^{\Delta t}_0\mathbf{X} = \begin{bmatrix} \cos\theta & -\sin\theta \\ \sin\theta & \cos\theta \end{bmatrix} \tag{d} $$

Substituting now from (b) and (d) into (c), we obtain

$$ {}^{\Delta t}_0\mathbf{S} = \begin{bmatrix} {}^{\Delta t}\bar{\tau}_{11} & 0 \\ 0 & 0 \end{bmatrix} \tag{e} $$

But, since ${}^{\Delta t}\bar{\tau}_{11}$ is equal to ${}^0\tau_{11}$, the relations in (a) and (e) show that the components of the second Piola-Kirchhoff stress tensor did not change during the rigid body rotation. The reason there is no change in the second Piola-Kirchhoff stress tensor is that the deformation gradient corresponds in this case to the rotation matrix that is used in the transformation in (b).

It is important to note that in these examples we consider the coordinate system to remain stationary and the body of material to be moving in this coordinate system. This situation is of course quite different from expressing given stress and strain tensors in new coordinate systems.

The above relationships between the stresses and strains show that, using (6.69) for the stress transformation and (6.64) for the strain transformation (but, as in Example 6.10,

using variations in strains rather than time derivatives), we obtain

$$\int_{{}^tV} {}^t\tau_{kl}\, \delta_t e_{kl}\, d^tV = \int_{{}^tV} \left(\frac{{}^t\rho}{{}^0\rho}\, {}^t_0S_{ij}\, {}^t_0x_{k,i}\, {}^t_0x_{l,j} \right) ({}^0_tx_{m,k}\, {}^0_tx_{n,l}\, \delta^t_0\epsilon_{mn})\, d^tV$$

$$= \int_{{}^tV} \frac{{}^t\rho}{{}^0\rho}\, {}^t_0S_{ij}\, \delta_{mi}\, \delta_{nj}\, \delta^t_0\epsilon_{mn}\, d^tV = \int_{{}^0V} {}^t_0S_{ij}\, \delta^t_0\epsilon_{ij}\, d^0V \tag{6.70}$$

where we have also used that ${}^t\rho\, d^tV = {}^0\rho\, d^0V$.

Of course, (6.70) follows from the definition of the second Piola-Kirchhoff stress tensor in (6.66), and indeed (6.70) is but (6.66) in integrated form over the volume of the body (and written for strain variations).

We have used in (6.70) a specific Cartesian coordinate system and should note that (6.70) is of course in component form a general tensor equation. Other suitable coordinate systems could also be chosen [see (6.178)].

Equation (6.70) is the basic expression of the total and updated Lagrangian formulations used in the incremental analysis of solids and structures, which we consider next. An important aspect of (6.70) is that in the final expression the integration is performed over the initial volume of the body. Instead of the initial configuration, any other previously calculated configuration could be used, with the second Piola-Kirchhoff stresses and Green-Lagrange strains then defined with respect to that configuration. More specifically, if the configuration at time τ is to be used, $\tau < t$, and we denote the coordinates at that time by ${}^\tau x_i$, then we would employ

$$\int_{{}^tV} {}^t\tau_{mn}\, \delta_t e_{mn}\, d^tV = \int_{{}^\tau V} {}^t_\tau S_{ij}\, \delta^t_\tau\epsilon_{ij}\, d^\tau V \tag{6.71}$$

where the second Piola-Kirchhoff stresses ${}^t_\tau S_{ij}$ and Green-Lagrange strains ${}^t_\tau\epsilon_{ij}$ are defined as previously discussed, but instead of ${}^0x_i$, the coordinates ${}^\tau x_i$ corresponding to the configuration at time τ are used. We shall employ the relations in (6.70) and (6.71) often in the next sections.

Note that so far we have defined the stress and strain tensors that we shall employ; the use of appropriate constitutive relations is discussed in Section 6.6.

6.2.3 Continuum Mechanics Incremental Total and Updated Lagrangian Formulations, Materially-Nonlinear-Only Analysis

We discussed in Sections 6.1 and 6.2.1 the basic difficulties and the solution approach when a general nonlinear problem is analyzed, and we concluded that, for an effective incremental analysis, appropriate stress and strain measures need to be employed. This led in Section 6.2.2 to the presentation of some stress and strain tensors that are employed effectively in practice, and then to the principle of virtual displacements expressed in terms of second Piola-Kirchhoff stresses and Green-Lagrange strains. We now use this fundamental result in the development of two general continuum mechanics incremental formulations of nonlinear problems. We consider in this section only the continuum mechanics equations without reference to a particular finite element solution scheme. The use of the results and the generalization for incremental formulations with respect to general finite element solution variables are then discussed in Section 6.3.1 (and the sections thereafter).

The basic equation that we want to solve is relation (6.13), which expresses the equilibrium and compatibility requirements of the general body considered in the configuration corresponding to time $t + \Delta t$. [The constitutive equations also enter (6.13), namely, in the calculation of the stresses.] Since in general the body can undergo large displacements and large strains and the constitutive relations are nonlinear, the relation in (6.13) cannot be solved directly; however, an approximate solution can be obtained by referring all variables to a previously calculated known equilibrium configuration and linearizing the resulting equation. This solution can then be improved by iteration.

To develop a governing linearized equation, we recall that the solutions for times 0, $\Delta t, 2\Delta t, \ldots, t$ have already been calculated and that we can employ (6.70) or (6.71) and refer the stresses and strains to one of these known equilibrium configurations. Hence, in principle, any one of the equilibrium configurations already calculated could be used. In practice, however, the choice lies essentially between two formulations which have been termed total Lagrangian (TL) and updated Lagrangian (UL) formulations (see K. J. Bathe, E. Ramm, and E. L. Wilson [A]). The TL formulation has also been referred to as the Lagrangian formulation. In this solution scheme all static and kinematic variables are referred to the initial configuration at time 0. The UL formulation is based on the same procedures that are used in the TL formulation, but in the solution all static and kinematic variables are referred to the last calculated configuration. ***Both the TL and UL formulations include all kinematic nonlinear effects due to large displacements, large rotations, and large strains, but whether the large strain behavior is modeled appropriately depends on the constitutive relations specified (see Section 6.6).*** The only advantage of using one formulation rather than the other lies in its greater numerical efficiency.

Using (6.70), in the TL formulation we consider the basic equation

$$\int_{{}^0V} {}^{t+\Delta t}_{0}S_{ij}\, \delta {}^{t+\Delta t}_{0}\epsilon_{ij}\, d^0V = {}^{t+\Delta t}\mathcal{R} \tag{6.72}$$

whereas in the UL formulation we consider

$$\int_{{}^tV} {}^{t+\Delta t}_{t}S_{ij}\, \delta {}^{t+\Delta t}_{t}\epsilon_{ij}\, d^tV = {}^{t+\Delta t}\mathcal{R} \tag{6.73}$$

in which ${}^{t+\Delta t}\mathcal{R}$ is the external virtual work given in (6.14). This expression also depends in general on the surface area and the volume of the body under consideration. However, for simplicity of discussion we assume for the moment that the loading is deformation-independent, a very important form of such loading being concentrated forces whose directions and intensities are independent of the structural response. Later we shall discuss how to include deformation-dependent loading in the analysis [see (6.83) and (6.84)].

Tables 6.2 and 6.3 summarize the relations used to arrive at the linearized equations of motion about the state at time t in the TL and UL formulations. The linearized equilibrium equations are, in the TL formulation,

$$\int_{{}^0V} {}_0C_{ijrs}\, {}_0e_{rs}\, \delta_0 e_{ij}\, d^0V + \int_{{}^0V} {}_0S_{ij}\, \delta_0 \eta_{ij}\, d^0V = {}^{t+\Delta t}\mathcal{R} - \int_{{}^0V} {}_0S_{ij}\, \delta_0 e_{ij}\, d^0V \tag{6.74}$$

and in the UL formulation

$$\int_{{}^tV} {}_tC_{ijrs}\, {}_te_{rs}\, \delta_t e_{ij}\, d^tV + \int_{{}^tV} {}^t\tau_{ij}\, \delta_t \eta_{ij}\, d^tV = {}^{t+\Delta t}\mathcal{R} - \int_{{}^tV} {}^t\tau_{ij}\, \delta_t e_{ij}\, d^tV \tag{6.75}$$

TABLE 6.2 *Continuum mechanics incremental decomposition: Total Lagrangian formulation*

1. *Equation of motion*

$$\int_{{}^0V} {}^{t+\Delta t}_{0}S_{ij}\,\delta\,{}^{t+\Delta t}_{0}\epsilon_{ij}\,d^0V = {}^{t+\Delta t}\mathcal{R}$$

where

$${}^{t+\Delta t}_{0}S_{ij} = \frac{{}^0\rho}{{}^{t+\Delta t}\rho}\,{}^{t+\Delta t}_{0}x_{i,m}\,{}^{t+\Delta t}\tau_{mn}\,{}^{t+\Delta t}_{0}x_{j,n}; \qquad \delta\,{}^{t+\Delta t}_{0}\epsilon_{ij} = \delta\tfrac{1}{2}({}^{t+\Delta t}_{0}u_{i,j} + {}^{t+\Delta t}_{0}u_{j,i} + {}^{t+\Delta t}_{0}u_{k,i}\,{}^{t+\Delta t}_{0}u_{k,j})$$

2. *Incremental decompositions*

(a) Stresses

$${}^{t+\Delta t}_{0}S_{ij} = {}^{t}_{0}S_{ij} + {}_0S_{ij}$$

(b) Strains

$${}^{t+\Delta t}_{0}\epsilon_{ij} = {}^{t}_{0}\epsilon_{ij} + {}_0\epsilon_{ij}; \qquad {}_0\epsilon_{ij} = {}_0e_{ij} + {}_0\eta_{ij}$$

$${}_0e_{ij} = \tfrac{1}{2}({}_0u_{i,j} + {}_0u_{j,i} + \underbrace{{}^{t}_{0}u_{k,i}\,{}_0u_{k,j} + {}_0u_{k,i}\,{}^{t}_{0}u_{k,j}}); \qquad {}_0\eta_{ij} = \tfrac{1}{2}{}_0u_{k,i}\,{}_0u_{k,j}$$

Initial displacement effect

3. *Equation of motion with incremental decompositions*

Noting that $\delta\,{}^{t+\Delta t}_{0}\epsilon_{ij} = \delta_0\epsilon_{ij}$ the equation of motion is

$$\int_{{}^0V} {}_0S_{ij}\delta_0\epsilon_{ij}\,d^0V + \int_{{}^0V} {}^{t}_{0}S_{ij}\delta_0\eta_{ij}\,d^0V = {}^{t+\Delta t}\mathcal{R} - \int_{{}^0V} {}^{t}_{0}S_{ij}\delta_0e_{ij}\,d^0V$$

4. *Linearization of equation of motion*

Using the approximations ${}_0S_{ij} = {}_0C_{ijrs}\,{}_0e_{rs}$, $\delta_0\epsilon_{ij} = \delta_0e_{ij}$, we obtain as approximate equation of motion:

$$\int_{{}^0V} {}_0C_{ijrs}\,{}_0e_{rs}\delta_0e_{ij}\,d^0V + \int_{{}^0V} {}^{t}_{0}S_{ij}\delta_0\eta_{ij}\,d^0V = {}^{t+\Delta t}\mathcal{R} - \int_{{}^0V} {}^{t}_{0}S_{ij}\delta_0e_{ij}\,d^0V$$

TABLE 6.3 *Continuum mechanics incremental decomposition: Updated Lagrangian formulation*

1. *Equation of motion*

$$\int_{{}^tV} {}^{t+\Delta t}_{t}S_{ij}\,\delta^{t+\Delta t}_{t}\epsilon_{ij}\,d^tV = {}^{t+\Delta t}\mathcal{R}$$

where

$${}^{t+\Delta t}_{t}S_{ij} = \frac{{}^t\rho}{{}^{t+\Delta t}\rho}\,{}^{t+\Delta t}_{t}x_{i,m}\,{}^{t+\Delta t}\tau_{mn}\,{}^{t+\Delta t}_{t}x_{j,n}; \qquad \delta^{t+\Delta t}_{t}\epsilon_{ij} = \delta\tfrac{1}{2}({}_tu_{i,j} + {}_tu_{j,i} + {}_tu_{k,i}\,{}_tu_{k,j})$$

2. *Incremental decompositions*

(a) Stresses

$${}^{t+\Delta t}_{t}S_{ij} = {}^t\tau_{ij} + {}_tS_{ij} \qquad \text{note that } {}^{t}_{t}S_{ij} \equiv {}^t\tau_{ij}$$

(b) Strains

$${}^{t+\Delta t}_{t}\epsilon_{ij} = {}_t\epsilon_{ij}; \qquad {}_t\epsilon_{ij} = {}_te_{ij} + {}_t\eta_{ij}$$

$${}_te_{ij} = \tfrac{1}{2}({}_tu_{i,j} + {}_tu_{j,i}); \qquad {}_t\eta_{ij} = \tfrac{1}{2}{}_tu_{k,i}\,{}_tu_{k,j}$$

3. *Equation of motion with incremental decompositions*

The equation of motion is

$$\int_{{}^tV} {}_tS_{ij}\delta_t\epsilon_{ij}\,d^tV + \int_{{}^tV} {}^t\tau_{ij}\delta_t\eta_{ij}\,d^tV = {}^{t+\Delta t}\mathcal{R} - \int_{{}^tV} {}^t\tau_{ij}\delta_te_{ij}\,d^tV$$

4. *Linearization of equation of motion*

Using the approximations ${}_tS_{ij} = {}_tC_{ijrs}\,{}_te_{rs}$, $\delta_t\epsilon_{ij} = \delta_te_{ij}$, we obtain as approximate equation of motion:

$$\int_{{}^tV} {}_tC_{ijrs}\,{}_te_{rs}\delta_te_{ij}\,d^tV + \int_{{}^tV} {}^t\tau_{ij}\delta_t\eta_{ij}\,d^tV = {}^{t+\Delta t}\mathcal{R} - \int_{{}^tV} {}^t\tau_{ij}\delta_te_{ij}\,d^tV$$

where ${}_0C_{ijrs}$ and ${}_tC_{ijrs}$ are the incremental stress-strain tensors at time t referred to the configurations at times 0 and t, respectively. The derivation of ${}_0C_{ijrs}$ and ${}_tC_{ijrs}$ for various materials is discussed in Section 6.6. We also note that in (6.74) and (6.75) ${}^t_0S_{ij}$ and ${}^t\tau_{ij}$ are the known second Piola-Kirchhoff and Cauchy stresses at time t; and ${}_0e_{ij}$, ${}_0\eta_{ij}$ and ${}_te_{ij}$, ${}_t\eta_{ij}$ are the linear and nonlinear incremental strains which are referred to the configurations at times 0 and t, respectively.

Let us consider in more detail the steps performed in Table 6.2. The steps in Table 6.3 are performed analogously.

In step 2, we incrementally decompose the stresses and strains, which is allowed because all stresses and strains, including the increments, are referred to the original (same) configuration. Also note that we obtain the incremental Green-Lagrange strain components in Table 6.2 by simply using ${}_0\epsilon_{ij} = {}^{t+\Delta t}_0\epsilon_{ij} - {}^t_0\epsilon_{ij}$ and expressing ${}^{t+\Delta t}_0\epsilon_{ij}$ and ${}^t_0\epsilon_{ij}$ in terms of the displacements, where ${}^{t+\Delta t}u_i = {}^tu_i + u_i$.

In step 3, we use $\delta {}^{t+\Delta t}_0\epsilon_{ij} = \delta({}^t_0\epsilon_{ij} + {}_0\epsilon_{ij}) = \delta_0\epsilon_{ij}$; that is, here $\delta {}^t_0\epsilon_{ij} = 0$ because the variation is taken about the configuration at time $t + \Delta t$. We also bring all known quantities to the right-hand side in the principle of virtual work equation. Note that for a given displacement variation the expression $\int_{{}_0V} {}^t_0S_{ij}\, \delta_0 e_{ij}\, d^0V$ is known. So far we have not made any assumption but have merely rewritten the original principle of virtual work equation.

In general, the left-hand side of the principle of virtual work equation given in step 3 is highly nonlinear in the incremental displacements u_i. In step 4, we now linearize the expression, and this linearization is achieved in the following manner.

First, we note that the term $\int_{{}_0V} {}^t_0S_{ij}\, \delta_0\eta_{ij}\, d^0V$ is already linear in the incremental displacements; hence, we keep this term without change. The nonlinear effects are due to the term $\int_{{}_0V} {}_0S_{ij}\, \delta_0\epsilon_{ij}\, d^0V$, which we linearize using a Taylor series expansion,

$$\begin{aligned}
\int_{{}_0V} {}_0S_{ij}\, \delta_0\epsilon_{ij}\, d^0V &= \int_{{}_0V} \left(\left.\frac{\partial {}^t_0S_{ij}}{\partial {}^t_0\epsilon_{rs}}\right|_t {}_0\epsilon_{rs} + \text{higher order terms} \right) \delta({}_0e_{ij} + {}_0\eta_{ij})\, d^0V \\
&= \int_{{}_0V} \left(\underbrace{\left.\frac{\partial {}^t_0S_{ij}}{\partial {}^t_0\epsilon_{rs}}\right|_t}_{\downarrow} \underbrace{({}_0e_{rs} + {}_0\eta_{rs})}_{\downarrow} + \underbrace{\text{higher order terms}}_{\downarrow} \right) \underbrace{\delta({}_0e_{ij} + {}_0\eta_{ij})}_{\downarrow}\, d^0V \\
&\qquad\qquad {}_0C_{ijrs} \qquad \text{Neglect} \qquad \text{Neglect} \qquad \text{Neglect} \\
&= \int_{{}_0V} {}_0C_{ijrs}\, {}_0e_{rs}\, \delta_0 e_{ij}\, d^0V
\end{aligned}$$

This term is now linear in the incremental displacements because $\delta_0 e_{ij}$ is independent of the u_i.

Comparing the UL and TL formulations in Tables 6.2 and 6.3, we observe that they are quite analogous and that, in fact, the only theoretical difference between the two formulations lies in the choice of different reference configurations for the kinematic and static variables. Indeed, if in the numerical solution the appropriate constitutive tensors are employed, identical results are obtained (see Section 6.6).

The choice of using either the UL or the TL formulation in a finite element solution depends, in practice, on their relative numerical effectiveness, which in turn depends on the finite element and the constitutive law used. However, one general observation can be made considering Tables 6.2 and 6.3, namely, that the incremental linear strains ${}_0e_{ij}$ in the TL formulation contain an initial displacement effect that leads to a more complex strain-displacement matrix than in the UL formulation.

The relations in (6.74) and (6.75) can be employed to calculate an increment in the displacements, which then is used to evaluate approximations to the displacements, strains, and stresses corresponding to time $t + \Delta t$. The displacement approximations corresponding to $t + \Delta t$ are obtained simply by adding the calculated increments to the displacements at time t, and the strain approximations are evaluated from the displacements using the available kinematic relations [e.g., relation (6.54) in the TL formulation]. However, the evaluation of the stresses corresponding to time $t + \Delta t$ depends on the specific constitutive relations used and is discussed in detail in Section 6.6.

Assuming that the approximate displacements, strains, and thus stresses have been obtained, we can now check into how much difference there is between the internal virtual work when evaluated with the calculated static and kinematic variables for time $t + \Delta t$ and the external virtual work. Denoting the approximate values with a superscript (1) in anticipation that an iteration will in general be necessary, the error due to linearization is, in the TL formulation,

$$\text{Error} = {}^{t+\Delta t}\mathcal{R} - \int_{{}^0V} {}^{t+\Delta t}_{0}S^{(1)}_{ij}\, \delta\, {}^{t+\Delta t}_{0}\epsilon^{(1)}_{ij}\, d^0V \tag{6.76}$$

and in the UL formulation,

$$\text{Error} = {}^{t+\Delta t}\mathcal{R} - \int_{{}^{t+\Delta t}V^{(1)}} {}^{t+\Delta t}\tau^{(1)}_{ij}\, \delta_{t+\Delta t} e^{(1)}_{ij}\, d^{t+\Delta t}V \tag{6.77}$$

We should note that the right-hand sides of (6.76) and (6.77) are equivalent to the right-hand sides of (6.74) and (6.75), respectively, but in each case the current configurations with the corresponding stress and strain variables are employed. The correspondence in the UL formulation can be seen directly, but when considering the TL formulation, it must be recognized that $\delta_0 e_{ij}$ is equivalent to $\delta\, {}^{t+\Delta t}_{0}\epsilon^{(1)}_{ij}$ when the same current displacements are used (see Exercise 6.29).

These considerations show that the right-hand sides in (6.74) and (6.75) represent an "out-of-balance virtual work" prior to the calculation of the increments in the displacements, whereas the right-hand sides of (6.76) and (6.77) represent the "out-of-balance virtual work" after the solution, as the result of the linearizations performed. In order to further reduce the "out-of-balance virtual work" we need to perform an iteration in which the above solution step is repeated until the difference between the external virtual work and the internal virtual work is negligible within a certain convergence measure. Using the TL formulation, the equation solved repetitively, for $k = 1, 2, 3, \ldots$, is

$$\int_{{}^0V} {}_0C^{(k-1)}_{ijrs}\, \Delta_0 e^{(k)}_{rs}\, \delta_0 e_{ij}\, d^0V + \int_{{}^0V} {}^{t+\Delta t}_{0}S^{(k-1)}_{ij}\, \delta \Delta_0 \eta^{(k)}_{ij}\, d^0V = {}^{t+\Delta t}\mathcal{R} - \int_{{}^0V} {}^{t+\Delta t}_{0}S^{(k-1)}_{ij}\, \delta\, {}^{t+\Delta t}_{0}\epsilon^{(k-1)}_{ij}\, d^0V \tag{6.78}$$

and using the UL formulation, the equation considered is

$$\begin{aligned}\int_{{}^{t+\Delta t}V^{(k-1)}} {}^{t+\Delta t}C^{(k-1)}_{ijrs}\, \Delta_{t+\Delta t} e^{(k)}_{rs}\, \delta_{t+\Delta t} e_{ij}\, d^{t+\Delta t}V + \int_{{}^{t+\Delta t}V^{(k-1)}} {}^{t+\Delta t}\tau^{(k-1)}_{ij}\, \delta \Delta_{t+\Delta t} \eta^{(k)}_{ij}\, d^{t+\Delta t}V \\ = {}^{t+\Delta t}\mathcal{R}_t - \int_{{}^{t+\Delta t}V^{(k-1)}} {}^{t+\Delta t}\tau^{(k-1)}_{ij}\, \delta_{t+\Delta t} e^{(k-1)}_{ij}\, d^{t+\Delta t}V\end{aligned} \tag{6.79}$$

where the case $k = 1$ corresponds to the relations in (6.74) and (6.75) and the displacements are updated as follows:

$$ {}^{t+\Delta t}u_i^{(k)} = {}^{t+\Delta t}u_i^{(k-1)} + \Delta u_i^{(k)}; \qquad {}^{t+\Delta t}u^{(0)} = {}^{t}u \tag{6.80} $$

The relations in (6.78) to (6.80) correspond to the Newton-Raphson iteration already introduced in Section 6.1. Therefore, the expressions in the integrals are all evaluated corresponding to the currently available displacements and corresponding stresses. Note that in (6.79) the Cauchy stresses, the tangent constitutive relation, and the incremental strains are all referred to the configuration and volume at time $t + \Delta t$, end of iteration $(k - 1)$; that is, the quantities are referred to ${}^{t+\Delta t}V^{(k-1)}$, where for $k = 1$, ${}^{t+\Delta t}V^{(0)} = {}^{t}V$.

In an overview of this section, we note once more a very important point. Our objective is to solve the equilibrium relation in (6.13), which can be regarded as an extension of the virtual work principle used in linear analysis. We saw that for a general incremental analysis, certain stress and strain measures can be employed effectively, and this led to a transformation of (6.13) into the updated and total Lagrangian forms. The linearization of these equations then resulted in the relations (6.78) and (6.79). It is most important to recognize that the solution of either (6.78) or (6.79) corresponds entirely to the solution of the relation in (6.13). Namely, provided that the appropriate constitutive relations are employed, identical numerical results are obtained using either (6.78) or (6.79) for solution, and, as mentioned earlier, whether to use the TL or the UL formulation depends in practice only on the relative numerical effectiveness of the two solution approaches.

So far we have assumed that the loading is deformation-independent and can be specified prior to the incremental analysis. Thus, we assumed that the expression in (6.14) can be evaluated using

$$ {}^{t+\Delta t}\mathcal{R} = \int_{{}^0V} {}^{t+\Delta t}_0 f_i^B \, \delta u_i \, d^0V + \int_{{}^0S_f} {}^{t+\Delta t}_0 f_i^S \, \delta u_i^S \, d^0S \tag{6.81} $$

which is possible only for certain types of loading, such as concentrated loading that does not change direction as a function of the deformations. Using the displacement-based isoparametric elements, another important loading condition that can be modeled with (6.81) is the inertia force loading to be included in dynamic analysis. In this case we have

$$ \int_{{}^{t+\Delta t}V} {}^{t+\Delta t}\rho \, {}^{t+\Delta t}\ddot{u}_i \, \delta u_i \, d^{t+\Delta t}V = \int_{{}^0V} {}^0\rho \, {}^{t+\Delta t}\ddot{u}_i \, \delta u_i \, d^0V \tag{6.82} $$

and hence, the mass matrix can be evaluated using the initial configuration of the body. The practical consequence is that in a dynamic analysis the mass matrices of isoparametric elements can be calculated prior to the step-by-step solution.

Assume now that the external virtual work is deformation-dependent and cannot be evaluated using (6.81). If in this case the load (or time) step is small enough, the external virtual work can frequently be approximated to sufficient accuracy using the intensity of loading corresponding to time $t + \Delta t$, but integrating over the volume and area last calculated in the iteration

$$ \int_{{}^{t+\Delta t}V} {}^{t+\Delta t}f_i^B \, \delta u_i \, d^{t+\Delta t}V \doteq \int_{{}^{t+\Delta t}V^{(k-1)}} {}^{t+\Delta t}f_i^B \, \delta u_i \, d^{t+\Delta t}V \tag{6.83} $$

and
$$\int_{t+\Delta t S_f} {}^{t+\Delta t}f_i^S \, \delta u_i^S \, d^{t+\Delta t}S \doteq \int_{t+\Delta t S_f^{(k-1)}} {}^{t+\Delta t}f_i^S \, \delta u_i^S \, d^{t+\Delta t}S \tag{6.84}$$

In order to obtain an iterative scheme that usually converges in fewer iterations, the effect of the unknown incremental displacements in the load terms needs to be included in the stiffness matrix. Depending on the loading considered, a nonsymmetric stiffness matrix is then obtained (see, for example, K. Schweizerhof and E. Ramm [A]), which may require substantially more computations per iteration.

The total and updated Lagrangian formulations are incremental continuum mechanics equations that include all nonlinear effects due to large displacements, large strains, and material nonlinearities; however, in practice, it is often sufficient to account for nonlinear material effects only. In this case, the nonlinear strain components and any updating of surface areas and volumes are neglected in the formulations. Therefore, (6.78) and (6.79) reduce to the same equation of motion, namely,

$$\int_V C_{ijrs}^{(k-1)} \, \Delta e_{rs}^{(k)} \, \delta e_{ij} \, dV = {}^{t+\Delta t}\mathcal{R} - \int_V {}^{t+\Delta t}\sigma_{ij}^{(k-1)} \, \delta e_{ij} \, dV \tag{6.85}$$

where ${}^{t+\Delta t}\sigma_{ij}^{(k-1)}$ is the actual physical stress at time $t + \Delta t$ and end of iteration $(k - 1)$. In this analysis we assume that the volume of the body does not change and therefore ${}^{t+\Delta t}_{0}S_{ij} \equiv {}^{t+\Delta t}\tau_{ij} \equiv {}^{t+\Delta t}\sigma_{ij}$, and there can be no deformation-dependent loading. Since no kinematic nonlinearities are considered in (6.85), it also follows that if the material is linear elastic, the relation in (6.85) is identical to the principle of virtual work discussed in Section 4.2.1 and would lead to a linear finite element solution.

In the above formulations we assumed that the proposed iteration does converge, so that the incremental analysis can actually be carried out. We discuss this question in detail in Section 8.4. Furthermore, we assumed in the formulation that a static analysis is performed or a dynamic analysis is sought with an implicit time integration scheme (see Section 9.5.2). If a dynamic analysis is to be performed using an explicit time integration method, the governing continuum mechanics equations are, using the TL formulation,

$$\int_{{}^0V} {}^t_0S_{ij} \, \delta {}^t_0\epsilon_{ij} \, d^0V = {}^t\mathcal{R} \tag{6.86}$$

using the UL formulation,

$$\int_{{}^tV} {}^t\tau_{ij} \, \delta {}^te_{ij} \, d^tV = {}^t\mathcal{R} \tag{6.87}$$

and using the materially-nonlinear-only analysis,

$$\int_V {}^t\sigma_{ij} \, \delta e_{ij} \, dV = {}^t\mathcal{R} \tag{6.88}$$

where the stress and strain tensors are as defined previously and equilibrium is considered at time t. In these analyses the external virtual work must include the inertia forces corresponding to time t, and the incremental solution corresponds to a marching-forward algorithm without equilibrium iterations. For this reason, deformation-dependent loading can be directly included by simply updating the load intensity and using the new geometry in the evaluation of ${}^t\mathcal{R}$. The details of the actual step-by-step solution are discussed in Section 9.5.1.

6.2.4 Exercises

6.1. A four-node plane strain finite element undergoes the deformation shown. The element is originally square, the density ${}^0\rho$ of the element is 0.05, and $d^0\mathbf{x}$ and $d^0\hat{\mathbf{x}}$ are infinitesimal fibers. For the deformed configuration at time t:

(a) Calculate the displacements of the material points within the element as functions of ${}^0x_1$ and ${}^0x_2$.

(b) Calculate the deformation gradient ${}_0^t\mathbf{X}$, the right Cauchy-Green deformation tensor ${}_0^t\mathbf{C}$, and the mass density ${}^t\rho$ as a function of ${}^0x_1$ and ${}^0x_2$.

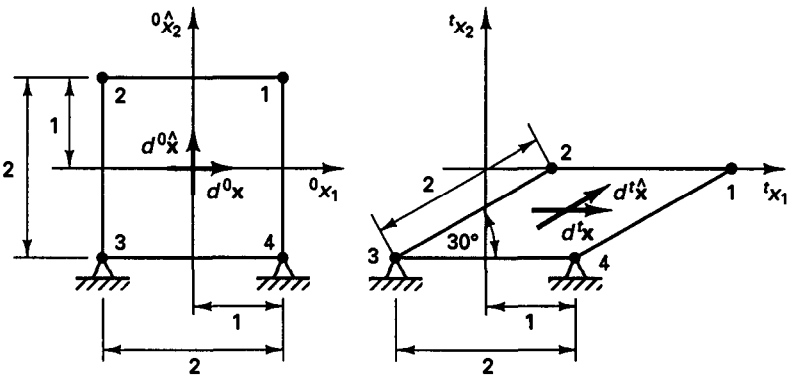

6.2. For the element in Exercise 6.1, calculate the stretches ${}^t\lambda$ and ${}^t\hat{\lambda}$ of the line segments $d^0\mathbf{x}$ and $d^0\hat{\mathbf{x}}$ and the angular distortion between these line segments.

6.3. Consider the four-node plane strain element shown. Calculate the deformation gradient for times Δt and $2\Delta t$. [*Hint:* Establish (by inspection) the matrices ${}_0^t\mathbf{R}$ and ${}_0^t\mathbf{U}$ such that ${}_0^t\mathbf{X} = {}_0^t\mathbf{R}\,{}_0^t\mathbf{U}$, where ${}_0^t\mathbf{R}$ is an orthogonal (rotation) matrix and ${}_0^t\mathbf{U}$ is a symmetric (stretch) matrix.]

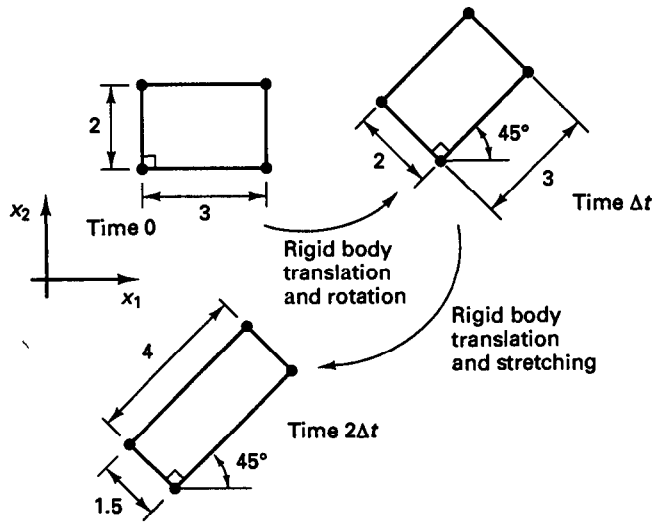

6.4. The four-node plane stress element of incompressible material shown is first stretched in the x_1 and x_2 directions and then rigidly rotated by 30 degrees.
(a) Calculate the deformation gradient ${}^{2\Delta t}_{0}\mathbf{X}$ of the material points in the element.
(b) Calculate the stretches of the line elements d^0s_1 and d^0s_2.

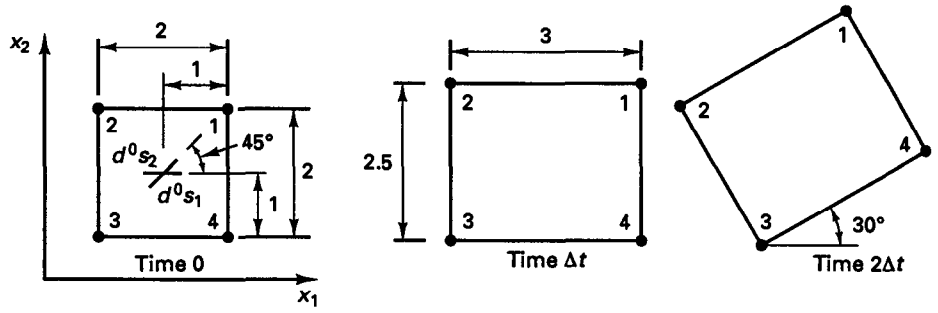

6.5. Consider the four-node element and its deformations to time Δt in Exercise 6.4. Assume that the deformation gradient at time Δt is now expressed in the coordinate axes $\bar{x}_1, \bar{x}_2$ shown. Calculate this deformation gradient ${}^{\Delta t}_{0}\bar{\mathbf{X}}$ and show that ${}^{\Delta t}_{0}\bar{\mathbf{X}}$ is not equal to ${}^{2\Delta t}_{0}\mathbf{X}$ calculated in Exercise 6.4. (In Exercise 6.4 the element was stretched *and* rotated, whereas here the element is *only* stretched.)

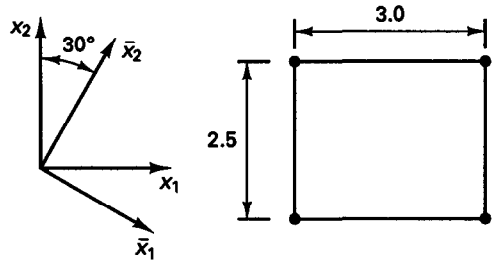

6.6. Consider the motions of two infinitesimal fibers in a two-dimensional continuum. At time 0, the fibers are

$$d^0\mathbf{x} = \frac{1}{\sqrt{2}}\begin{bmatrix}1\\1\end{bmatrix} d^0s; \qquad d^0\hat{\mathbf{x}} = \begin{bmatrix}0\\1\end{bmatrix} d^0\hat{s}$$

and at time t, the fibers are

$$d^t\mathbf{x} = \begin{bmatrix}2\\1\end{bmatrix} d^0s; \qquad d^t\hat{\mathbf{x}} = \begin{bmatrix}-1\\1\end{bmatrix} d^0\hat{s}$$

Both fibers emanate from the same material point.
(a) Calculate the deformation gradient ${}^{t}_{0}\mathbf{X}$ at that material point.
(b) Calculate the inverse deformation gradient ${}^{0}_{t}\mathbf{X}$ at that material point (i) by inverting ${}^{t}_{0}\mathbf{X}$ and (ii) without inverting ${}^{t}_{0}\mathbf{X}$.
(c) Calculate the mass density ratio ${}^t\rho/{}^0\rho$ at the material point.

6.7. Prove that a deformation gradient $\mathbf{X}$ can always be decomposed into the form $\mathbf{X} = \mathbf{VR}$ where $\mathbf{V}$ is a symmetric matrix and $\mathbf{R}$ is an orthogonal matrix. Establish $\mathbf{V}$ and $\mathbf{R}$ for the deformation in Exercise 6.4.

6.8. A four-node plane strain element is subjected to the following deformations:

from time 0 to time Δt: $\quad {}^{\Delta t}_{0}\mathbf{U} = \begin{bmatrix} 2 & 0.5 \\ 0.5 & 0.5 \end{bmatrix}$

from time Δt to time $2\Delta t$: $\quad {}^{2\Delta t}_{\Delta t}\mathbf{R} = \begin{bmatrix} \cos 30° & -\sin 30° \\ \sin 30° & \cos 30° \end{bmatrix}$

(a) Sketch the element and its motions and establish the deformation gradient ${}^{2\Delta t}_{0}\mathbf{X}$.
(b) Calculate the spectral decomposition of ${}^{\Delta t}_{0}\mathbf{U}$ as per (6.32).
(c) Calculate the elements of the decomposition of $\mathbf{X} = \mathbf{VR}$ and interpret this decomposition conceptually.

6.9. Consider the four-node axisymmetric element shown. Evaluate the deformation gradient and the right and left stretch tensors $\mathbf{U}$, $\mathbf{V}$.

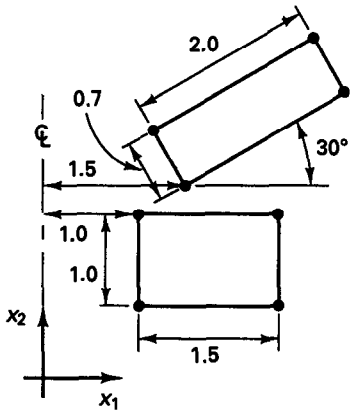

6.10. Consider the motion of the four-node finite element shown. Calculate for time t,
(a) The deformation gradient and the polar decompositions $\mathbf{X} = \mathbf{RU}$ and $\mathbf{X} = \mathbf{VR}$
(b) The spectral decompositions of $\mathbf{U}$ and $\mathbf{V}$ in (6.32) and (6.33)
(c) The velocity strain and spin tensors in (6.42) and (6.43).

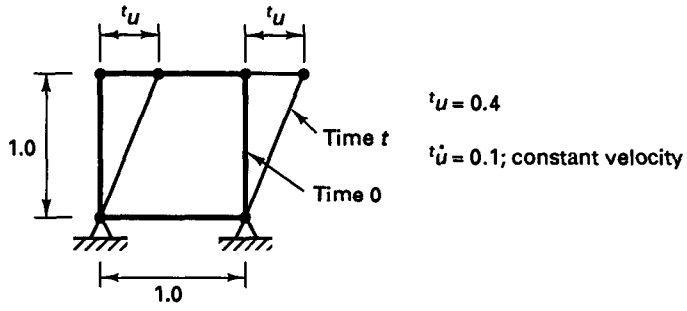

6.11. Prove the relations in (6.48) to (6.50).

6.12. Prove the relations in (6.56) to (6.61).

6.13. Consider the motion of the four-node element in Exercise 6.10. Calculate $[\dot{\Lambda}]_{\alpha\alpha}$, $[\Omega_L]_{\alpha\beta}$, and $[\Omega_E]_{\alpha\beta}$ using the relations (6.48) to (6.50). Verify that (6.46) and (6.47) hold.

6.14. Calculate the components of the Green-Lagrange strain tensors of the elements and their deformations in Exercises 6.1, 6.3, and 6.4. In each case establish the relations in (6.51) and (6.53) to (6.55).

6.15. Calculate the components of the Hencky strain tensor (6.52) for the elements and their deformations in Exercises 6.1, 6.3, and 6.4.

6.16. Consider the element and its motion in Exercise 6.10. For the Green-Lagrange strain and Hencky strain tensors, calculate $\dot{\mathbf{E}}_g$ in (6.57) by direct differentiation of (6.56). Also, establish $\dot{\mathbf{E}}_g$ using the detailed relations (6.59) to (6.61).

6.17. Consider the motion of a material fiber $d^0\mathbf{x}$ in a body.

(a) Prove that for the material fiber the following relation holds using the Green-Lagrange strain tensor

$$ {}_0^t\epsilon_{ij}\, d^0x_i\, d^0x_j = \tfrac{1}{2}[(d^ts)^2 - (d^0s)^2] $$

where $(d^ts)^2 = d^tx_i\, d^tx_i$, $(d^0s)^2 = d^0x_i\, d^0x_i$ and (6.22) is applicable.

(b) At point A in a deformed body the Green-Lagrange strain tensor is known to be

$$ {}_0^t\boldsymbol{\epsilon} = \begin{bmatrix} 0.6 & 0.2 \\ 0.2 & -0.3 \end{bmatrix} $$

Find the stretch ${}^t\lambda$ of the line element $d^0s = \| d^0\mathbf{x} \|_2$ shown. Can you calculate the rotation of the line element? Explain your answer.

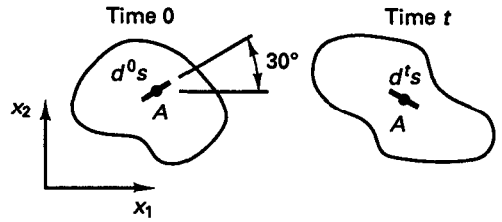

6.18. The nodal point velocities of a four-node element are as shown. Using the element interpolation functions, evaluate the components of the velocity strain tensor and spin tensor of the element. Physically explain why your answer is correct.

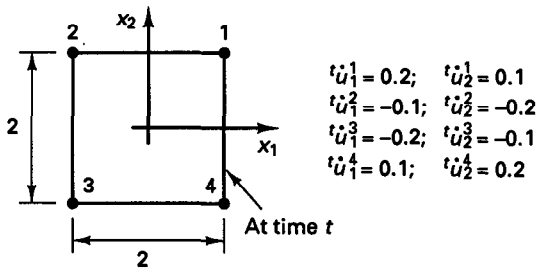

6.19. Consider the four-node plane strain element and its motion in Exercise 6.10. Evaluate the components ${}^tD_{mn}$ using the relation (6.64).

6.20. Consider the four-node plane strain element shown. Evaluate the components of the tensor $\delta_t e_{mn}$ corresponding to the virtual displacement $\delta u_1^1 = \Delta$ at node 1 as a function of ${}^0x_1$ and ${}^0x_2$. (All other $\delta u_j^k = 0$.)

Evaluate all matrix expressions required but do not necessarily perform the matrix multiplications.

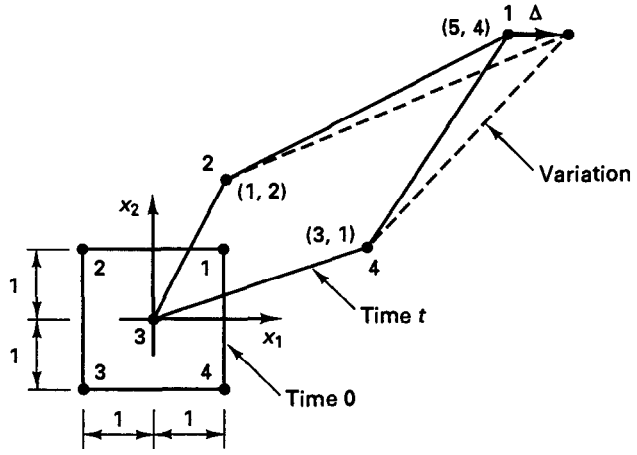

6.21. Consider the four-node element shown, subjected to an initial stress with components

$$\begin{matrix}\text{Initial stress} \\ \text{(stress at time 0)}\end{matrix} = {}_0^0\mathbf{S} \equiv {}^0\boldsymbol{\tau} = \begin{bmatrix} 200 & 100 \\ 100 & 300 \end{bmatrix}$$

The element is undeformed in its initial configuration. Assume that the element is subjected to a counterclockwise rigid body rotation of 30 degrees from time 0 to time Δt.

(a) Calculate the Cauchy stresses ${}^{\Delta t}\boldsymbol{\tau}$ corresponding to the stationary coordinate system x_1, x_2.

(b) Calculate the second Piola-Kirchhoff stresses ${}_0^{\Delta t}\mathbf{S}$ corresponding to x_1, x_2.

(c) Calculate the deformation gradient ${}_0^{\Delta t}\mathbf{X}$.

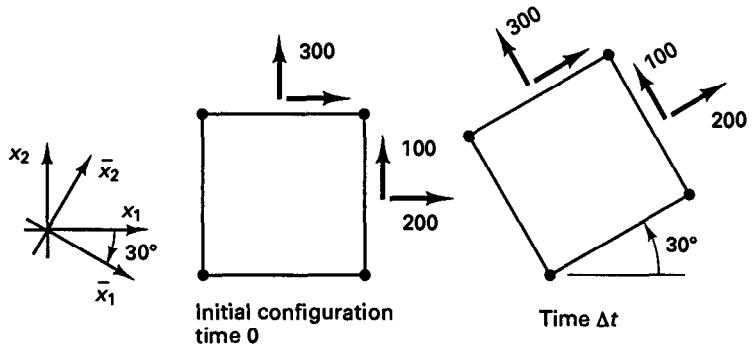

Next, assume that the element remains in its initial configuration but the coordinate system is rotated clockwise by 30 degrees.

(d) Calculate the Cauchy stresses ${}^0\bar{\boldsymbol{\tau}}$ corresponding to $\bar{x}_1, \bar{x}_2$.

(e) Calculate the second Piola-Kirchhoff stresses ${}_0^0\bar{\mathbf{S}}$ corresponding to $\bar{x}_1, \bar{x}_2$.

(f) Calculate the deformation gradient ${}_0^0\bar{\mathbf{X}}$ corresponding to $\bar{x}_1, \bar{x}_2$.

6.22. The four-node plane strain finite element shown carries at time t the second Piola-Kirchhoff stresses

$$ {}_0^t\mathbf{S} = \begin{bmatrix} 100 & 50 & 0 \\ 50 & 200 & 0 \\ 0 & 0 & 100 \end{bmatrix} $$

The deformation gradient at time t is

$$ {}_0^t\mathbf{X} = \begin{bmatrix} 2 & 1 & 0 \\ 0 & 2 & 0 \\ 0 & 0 & 1 \end{bmatrix} $$

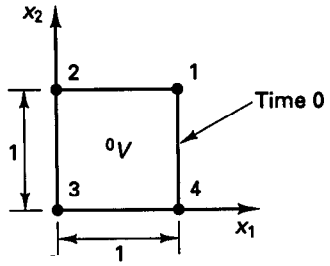

(a) Sketch the deformed configuration at time t.

(b) A rigid body rotation of 30 degrees counterclockwise is applied from time t to time $t + \Delta t$ to the element. Sketch the configuration at time $t + \Delta t$.

(c) Calculate corresponding to the stationary Cartesian coordinate system (i) the Cauchy stresses at time t, (ii) the Cauchy stresses at time $t + \Delta t$, and (iii) the second Piola-Kirchhoff stresses at time $t + \Delta t$.

6.23. The second Piola-Kirchhoff stresses ${}_0^t\mathbf{S}$ are for the plane strain four-node element as shown.

(a) Calculate the Cauchy stresses at time t.

(b) Obtain the second Piola-Kirchhoff stresses at time $t + \Delta t$, ${}_0^{t+\Delta t}\mathbf{S}$, and the Cauchy stresses at time $t + \Delta t$, ${}^{t+\Delta t}\boldsymbol{\tau}$.

All stress components are measured in the stationary coordinate system x_1, x_2.

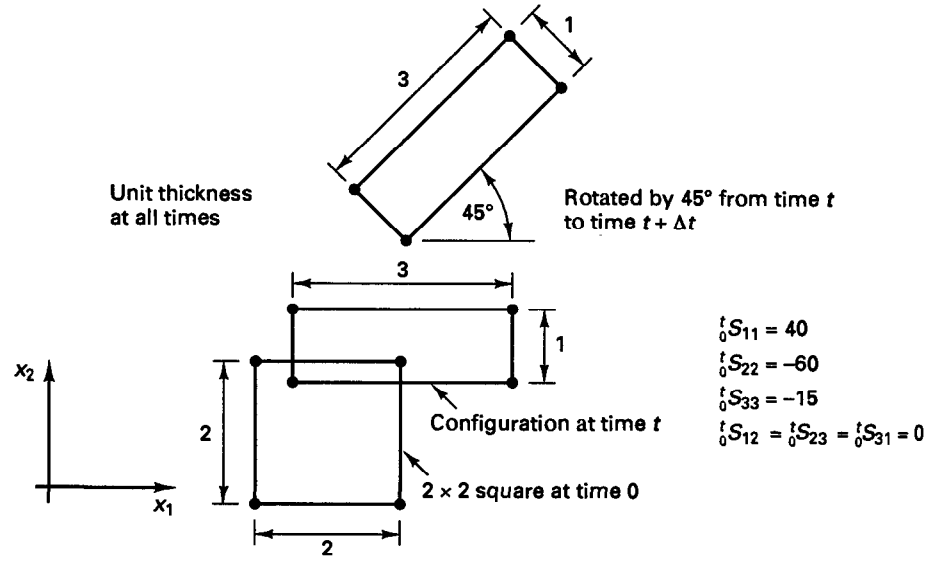

6.24. We have used a computer program to perform the following finite element analysis.

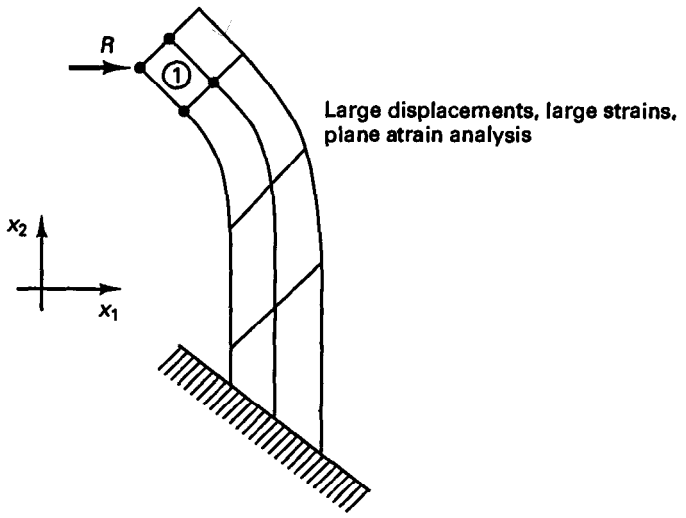

We would like to verify that the program is working properly. As part of this verification, we consider the displacements of element 1:

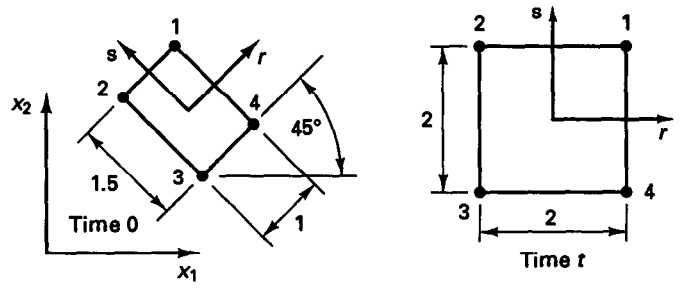

(a) Calculate the 2×2 deformation gradient ${}^t_0\mathbf{X}$ at the centroid of the element. (*Hint:* Remember that ${}^t_0\mathbf{X} = {}^0_t\mathbf{X}^{-1}$.)

(b) The program also prints out the Cauchy stresses at the centroid of the element:

$$\begin{bmatrix} {}^t\tau_{11} \\ {}^t\tau_{22} \\ {}^t\tau_{12} \end{bmatrix} = \begin{bmatrix} 20.50 \\ 20.50 \\ 12.50 \end{bmatrix}$$

The material law used in the analysis is given by

$$\begin{bmatrix} {}^t_0S_{11} \\ {}^t_0S_{22} \\ {}^t_0S_{12} \end{bmatrix} = \begin{bmatrix} 11 & 7 & 0 \\ 7 & 11 & 0 \\ 0 & 0 & 9 \end{bmatrix} \begin{bmatrix} {}^t_0\epsilon_{11} \\ {}^t_0\epsilon_{22} \\ {}^t_0\epsilon_{12} \end{bmatrix}$$

Show that the Cauchy stresses printed by the program are not correct and compute the correct Cauchy stresses based on the given element displacements.

Can you identify the program error?

6.25. Consider the sheet of material shown.

Here

$$^{t}u_1 = -\tfrac{1}{2}\,{}^{0}x_1 + 3; \qquad {}^{t}u_2 = \tfrac{1}{2}\,{}^{0}x_2 + 2.5$$

Also, the stresses are

$$^{t}\tau_{11} = -10 \text{ psi}$$

$$^{t}\tau_{22} = 20 \text{ psi}$$

$$^{t}\tau_{12} = 0$$

Identify six simple independent virtual displacement patterns and show that the principle of virtual work is satisfied for these patterns.

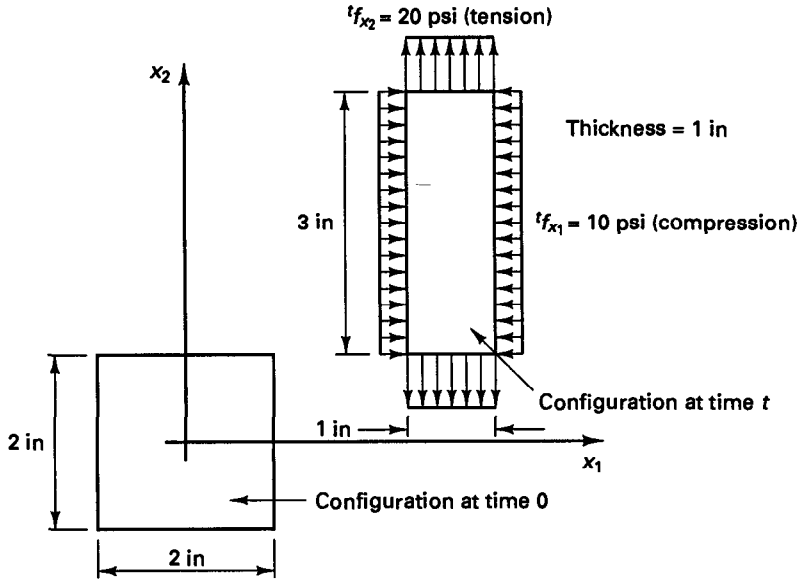

6.26. Consider the one-dimensional large strain analysis of the bar shown.

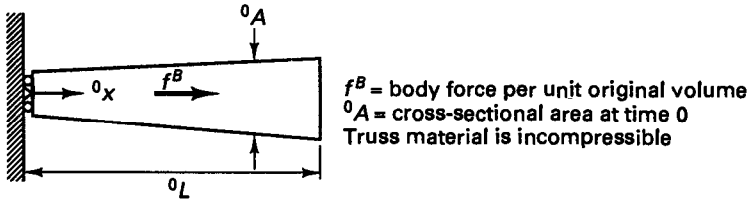

(a) For a cross section of the bar, derive an expression for the second Piola-Kirchhoff stress as a function of the Cauchy stress, the area ratio $^{t}A/{}^{0}A$, and the deformation gradient.

(b) Starting from the principle of virtual work, derive the governing differential equation of equilibrium in terms of quantities referred to the original configuration. Also, derive the boundary conditions.

(c) Now rewrite the governing differential equation in terms of quantities referred to the current configuration and compare this equation with the differential equation associated with small strain analysis.

6.27. Consider a thin disk spinning around its symmetry axis with constant angular velocity ω as shown. The disk is subjected to large displacements. Specialize the general equations of the principle of virtual work in Tables 6.2 and 6.3 to this case. In the analysis, only the displacements of the disk particles in the x_1 direction are considered.

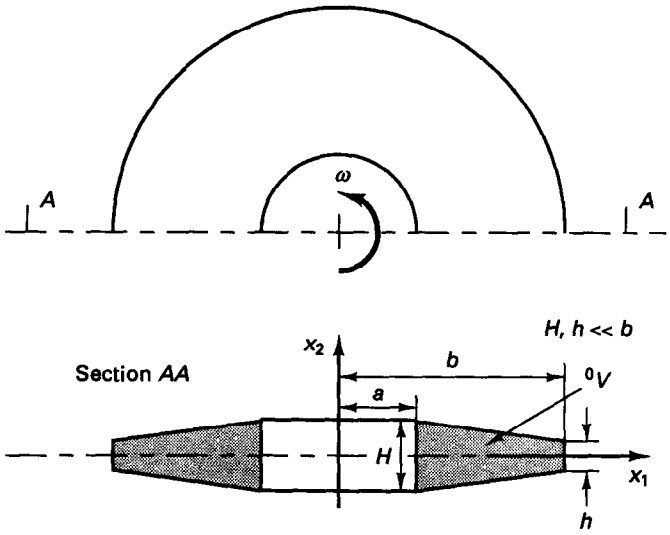

6.28. Consider the four-node plane strain element shown. The nodal point displacements at time t and time $t + \Delta t$ are shown. Calculate the incremental Green-Lagrange strain tensor components ${}_0\epsilon$ from time t to time $t + \Delta t$.

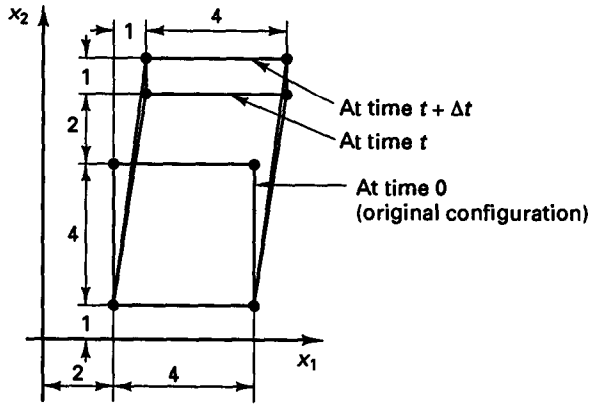

6.29. In the derivations in Section 6.2.3 we used

$$\int_{{}^0V} {}^{t+\Delta t}_0 S_{ij}\, \delta\, {}^{t+\Delta t}_0 \epsilon_{ij}\, d^0V = \int_{{}^0V} {}^{t+\Delta t}_0 S_{ij}\, \delta_0 \epsilon_{ij}\, d^0V$$

and hence, here $\delta\, {}^t_0\epsilon_{ij} = 0$. But we also used

$$\int_{{}^0V} {}^t_0 S_{ij}\, \delta_0 e_{ij}\, d^0V = \int_{{}^0V} {}^t_0 S_{ij}\, \delta\, {}^t_0 \epsilon_{ij}\, d^0V$$

and hence, here $\delta\, {}_0e_{ij} = \delta\, {}^t_0\epsilon_{ij}$ and clearly $\delta\, {}^t_0\epsilon_{ij} \neq 0$. Discuss briefly why all these equations are correct.

6.30. Establish the second Piola-Kirchhoff stresses ${}_0^tS_{ij}$ and the variations in the Green-Lagrange strains $\delta {}_0^t\epsilon_{ij}$ for the disk in Exercise 6.27 and show explicitly that for this case, $\int_{{}^tV} {}^t\tau_{ij}\, \delta {}_t e_{ij}\, d^tV = \int_{{}^0V} {}_0^tS_{ij}\, \delta {}_0^t\epsilon_{ij}\, d^0V$ is indeed true.

6.3 DISPLACEMENT-BASED ISOPARAMETRIC CONTINUUM FINITE ELEMENTS

In the previous section we developed the linearized principle of virtual displacements (linearized about the state at time t) in *continuum* form. The only variables in the equations are the displacements of the material particles.

If finite elements with only nodal point displacements as degrees of freedom are considered, then the governing finite element matrices corresponding to a full linearization of the principle of virtual displacements about the state at time t can be obtained directly by use of the equations given in the previous section. The key point to note is that in this case the element degrees of freedom, i.e., the element displacements, are exactly the variables with respect to which the general principle of virtual displacements has been linearized. Let us consider the following derivation to emphasize this point. This derivation will also show that if other than displacement degrees of freedom are used, such as rotations in structural elements or stresses in mixed formulations, the linearization with respect to such finite element degrees of freedom is more efficiently achieved by a direct Taylor series expansion with respect to such variables.

6.3.1 Linearization of the Principle of Virtual Work with Respect to Finite Element Variables

The principle of virtual displacements in the total Lagrangian formulation is given by

$$\int_{{}^0V} {}^{t+\Delta t}_0S_{ij}\, \delta {}^{t+\Delta t}_0\epsilon_{ij}\, d^0V = {}^{t+\Delta t}\mathcal{R} \tag{6.89}$$

Let us linearize this expression with respect to a general finite element nodal degree of freedom ${}^ta_k$, where ${}^ta_k$ may be a displacement or rotation. We assume that ${}^{t+\Delta t}\mathcal{R}$ is independent of the deformations. We then have, using a Taylor series expansion,

$${}^{t+\Delta t}_0S_{ij}\, \delta {}^{t+\Delta t}_0\epsilon_{ij} \doteq {}_0^tS_{ij}\, \delta {}_0^t\epsilon_{ij} + \frac{\partial}{\partial {}^ta_k}\left({}_0^tS_{ij}\, \delta {}_0^t\epsilon_{ij}\right) da_k \tag{6.90}$$

where da_k is a differential increment in ${}^ta_k$. We note that

$$\delta {}_0^t\epsilon_{ij} = \frac{\partial {}_0^t\epsilon_{ij}}{\partial {}^ta_l}\delta a_l \tag{6.91}$$

where δa_l is a variation in ${}^ta_l$, and hence the variation is taken with respect to the nodal parameter ${}^ta_l$ about the configuration at time t.

The second term in (6.90) may be chain-differentiated to obtain

$$\begin{aligned}\frac{\partial}{\partial {}^t a_k}({}_0^t S_{ij}\,\delta {}_0^t\epsilon_{ij})\,da_k &= \frac{\partial {}_0^t S_{ij}}{\partial {}^t a_k}\delta {}_0^t\epsilon_{ij}\,da_k + {}_0^t S_{ij}\frac{\partial}{\partial {}^t a_k}(\delta {}_0^t\epsilon_{ij})\,da_k \\ &= \left(\frac{\partial {}_0^t S_{ij}}{\partial {}_0^t\epsilon_{rs}}\frac{\partial {}_0^t\epsilon_{rs}}{\partial {}^t a_k}\right)\left(\frac{\partial {}_0^t\epsilon_{ij}}{\partial {}^t a_l}\delta a_l\right)da_k + {}_0^t S_{ij}\frac{\partial}{\partial {}^t a_k}\left(\frac{\partial {}_0^t\epsilon_{ij}}{\partial {}^t a_l}\delta a_l\right)da_k \qquad (6.92)\\ &= {}_0C_{ijrs}\frac{\partial {}_0^t\epsilon_{rs}}{\partial {}^t a_k}\frac{\partial {}_0^t\epsilon_{ij}}{\partial {}^t a_l}\delta a_l\,da_k + {}_0^t S_{ij}\frac{\partial^2 {}_0^t\epsilon_{ij}}{\partial {}^t a_k\,\partial {}^t a_l}\delta a_l\,da_k\end{aligned}$$

where in the last step we used

$$\frac{\partial {}_0^t S_{ij}}{\partial {}_0^t\epsilon_{rs}} = {}_0C_{ijrs} \qquad (6.93)$$

Using the definition of the Green-Lagrange strain, we further have

$$\frac{\partial {}_0^t\epsilon_{ij}}{\partial {}^t a_k} = \frac{1}{2}\left(\frac{\partial {}_0^t u_{i,j}}{\partial {}^t a_k} + \frac{\partial {}_0^t u_{j,i}}{\partial {}^t a_k} + {}_0^t u_{m,i}\frac{\partial {}_0^t u_{m,j}}{\partial {}^t a_k} + {}_0^t u_{m,j}\frac{\partial {}_0^t u_{m,i}}{\partial {}^t a_k}\right) \qquad (6.94)$$

and

$$\frac{\partial^2 {}_0^t\epsilon_{ij}}{\partial {}^t a_k\,\partial {}^t a_l} = \frac{1}{2}\left({}_0^t x_{m,i}\frac{\partial^2 {}_0^t u_{m,j}}{\partial {}^t a_k\,\partial {}^t a_l} + {}_0^t x_{m,j}\frac{\partial^2 {}_0^t u_{m,i}}{\partial {}^t a_k\,\partial {}^t a_l} + \frac{\partial {}_0^t u_{m,i}}{\partial {}^t a_k}\frac{\partial {}_0^t u_{m,j}}{\partial {}^t a_l} + \frac{\partial {}_0^t u_{m,i}}{\partial {}^t a_l}\frac{\partial {}_0^t u_{m,j}}{\partial {}^t a_k}\right) \qquad (6.95)$$

The substitution of (6.90) and (6.92) into the principle of virtual displacements (6.89) gives

$$\left\{\int_{{}_0V} {}_0C_{ijrs}\frac{\partial {}_0^t\epsilon_{rs}}{\partial {}^t a_k}\frac{\partial {}_0^t\epsilon_{ij}}{\partial {}^t a_l}\,d^0V + \int_{{}_0V} {}_0^t S_{ij}\frac{\partial^2 {}_0^t\epsilon_{ij}}{\partial {}^t a_k\,\partial {}^t a_l}\,d^0V\right\}da_k\,\delta a_l = {}^{t+\Delta t}\mathcal{R}_l - \left(\int_{{}_0V} {}_0^t S_{ij}\frac{\partial {}_0^t\epsilon_{ij}}{\partial {}^t a_l}\,d^0V\right)\delta a_l \qquad (6.96)$$

where ${}^{t+\Delta t}\mathcal{R}_l$ denotes the external virtual work corresponding to δa_l.

If we now compare the expression in (6.96) [and using (6.94) and (6.95)] with the linearized principle of virtual displacement expression in Table 6.2, we recognize that for isoparametric displacement-based continuum elements with nodal displacement degrees of freedom only, both expressions can directly, and easily, be employed to obtain the same finite element equations. However, for elements with rotational degrees of freedom, the expression in (6.96) may be more direct for the derivation of the fully linearized finite element equations. Namely, the second derivatives of the displacement gradients with respect to the nodal point variables appearing in (6.95) are then not zero, and their effect also needs to be included. Consequently, if the continuum linearizations in Tables 6.2 and 6.3 are used, it must be recognized that the terms ${}_0^t S_{ij}\,\delta_0 e_{ij}$ and ${}^t\tau_{ij}\,\delta_t e_{ij}$, on the right-hand side of the equations, still contribute terms to the stiffness matrix when ${}_0e_{ij}$ and ${}_te_{ij}$ are not a linear function of the nodal point variables (see Section 6.5).

If, in addition, other than displacement and rotational element degrees of freedom are used, then certainly the above approach of linearization is very effective (see Section 6.4 for the derivation of the displacement/pressure formulations).

Here we have considered only a total Lagrangian formulation but should recognize that the same procedure of linearization is also applicable to updated Lagrangian formulations, and to all these formulations with all different material descriptions. The same procedure can also be employed to linearize the external virtual work term in (6.89) in case the loading is deformation dependent.

6.3.2 General Matrix Equations of Displacement-Based Continuum Elements

Let us now consider in more detail the matrices of isoparametric continuum finite elements with displacement degrees of freedom only.

The basic steps in the derivation of the governing finite element equations are the same as those used in linear analysis: the selection of the interpolation functions and the interpolation of the element coordinates and displacements with these functions in the governing continuum mechanics equations. By invoking the linearized principle of virtual displacements for each of the nodal point displacements in turn, the governing finite element equations are obtained. As in linear analysis, we need to consider only a single element of a specific type in this derivation because the governing equilibrium equations of an assemblage of elements can be constructed using the direct stiffness procedure.

In considering the element coordinate and displacement interpolations, we should recognize that it is important to employ the same interpolations for the coordinates and displacements at any and all times during the motion of the element. Since the new element coordinates are obtained by adding the element displacements to the original coordinates, it follows that the use of the same interpolations for the displacements and coordinates represents a consistent solution approach, and means that the discussions on convergence requirements in Sections 4.3 and 5.3.3 are directly applicable to the incremental analysis. In particular, it is then ensured that an assemblage of elements that are displacement-compatible across element boundaries in the original configuration will preserve this compatibility in all subsequent configurations.

In Sections 6.2.3 and 6.3.1 we derived the basic incremental equations used in our finite element formulations. While in practice an iteration is necessary, we also recognized that the equations in Tables 6.2 and 6.3 and Section 6.3.1 are the basic relations that are used in such iterations. Hence, in the following presentation we only need to focus on the basic incremental equations derived in Tables 6.2 and 6.3 (with the discussion in Section 6.3.1) and summarized in (6.74) and (6.75).

Substituting now the element coordinate and displacement interpolations into these equations as we did in linear analysis, we obtain—for a single element or for an assemblage of elements—

in materially-nonlinear-only analysis:

static analysis:

$$^{t}\mathbf{K}\mathbf{U} = {}^{t+\Delta t}\mathbf{R} - {}^{t}\mathbf{F} \tag{6.97}$$

dynamic analysis, implicit time integration:

$$\mathbf{M}\,{}^{t+\Delta t}\ddot{\mathbf{U}} + {}^{t}\mathbf{K}\mathbf{U} = {}^{t+\Delta t}\mathbf{R} - {}^{t}\mathbf{F} \tag{6.98}$$

dynamic analysis, explicit time integration:

$$\mathbf{M}\,{}^{t}\ddot{\mathbf{U}} = {}^{t}\mathbf{R} - {}^{t}\mathbf{F} \tag{6.99}$$

using the TL formulation:

static analysis:

$$({}_{0}\mathbf{K}_{L} + {}_{0}\mathbf{K}_{NL})\mathbf{U} = {}^{t+\Delta t}\mathbf{R} - {}_{0}\mathbf{F} \tag{6.100}$$

dynamic analysis, implicit time integration:

$$\mathbf{M}\,{}^{t+\Delta t}\ddot{\mathbf{U}} + ({}_0^t\mathbf{K}_L + {}_0^t\mathbf{K}_{NL})\mathbf{U} = {}^{t+\Delta t}\mathbf{R} - {}_0^t\mathbf{F} \tag{6.101}$$

dynamic analysis, explicit time integration:

$$\mathbf{M}\,{}^t\ddot{\mathbf{U}} = {}^t\mathbf{R} - {}_0^t\mathbf{F} \tag{6.102}$$

and using the UL formulation:
static analysis:

$$({}_t^t\mathbf{K}_L + {}_t^t\mathbf{K}_{NL})\mathbf{U} = {}^{t+\Delta t}\mathbf{R} - {}_t^t\mathbf{F} \tag{6.103}$$

dynamic analysis, implicit time integration:

$$\mathbf{M}\,{}^{t+\Delta t}\ddot{\mathbf{U}} + ({}_t^t\mathbf{K}_L + {}_t^t\mathbf{K}_{NL})\mathbf{U} = {}^{t+\Delta t}\mathbf{R} - {}_t^t\mathbf{F} \tag{6.104}$$

dynamic analysis, explicit time integration:

$$\mathbf{M}\,{}^t\ddot{\mathbf{U}} = {}^t\mathbf{R} - {}_t^t\mathbf{F} \tag{6.105}$$

where $\mathbf{M}$ = time-independent mass matrix
$^t\mathbf{K}$ = linear strain incremental stiffness matrix, not including the initial displacement effect
${}_0^t\mathbf{K}_L$, ${}_t^t\mathbf{K}_L$ = linear strain incremental stiffness matrices
${}_0^t\mathbf{K}_{NL}$, ${}_t^t\mathbf{K}_{NL}$ = nonlinear strain (geometric or initial stress) incremental stiffness matrices
$^{t+\Delta t}\mathbf{R}$ = vector of externally applied nodal point loads at time $t + \Delta t$; this vector is also used at time t in explicit time integration
$^t\mathbf{F}$, ${}_0^t\mathbf{F}$, ${}_t^t\mathbf{F}$ = vectors of nodal point forces equivalent to the element stresses at time t
$\mathbf{U}$ = vector of increments in the nodal point displacements
$^t\ddot{\mathbf{U}}$, $^{t+\Delta t}\ddot{\mathbf{U}}$ = vectors of nodal point accelerations at times t and $t + \Delta t$

In the above finite element discretization we have assumed that damping effects are negligible or can be modeled in the nonlinear constitutive relationships (for example, by use of a strain-rate-dependent material law). We also assumed that the externally applied loads are deformation-independent, and thus the load vector corresponding to all load (or time) steps can be calculated prior to the incremental analysis. If the loads include deformation-dependent components, it is necessary to update and iterate on the load vector as briefly discussed in Section 6.2.3.

The above finite element matrices are evaluated as in linear analysis. Table 6.4 summarizes—for a single element—the basic integrals being considered and the corresponding matrix evaluations. The following notation is used for the calculation of the element matrices:

$\mathbf{H}^S$, $\mathbf{H}$ = surface- and volume-displacement interpolation matrices
${}^{t+\Delta t}_0\mathbf{f}^S$, ${}^{t+\Delta t}_0\mathbf{f}^B$ = vectors of surface and body forces defined per unit area and per unit volume of the element at time 0
$\mathbf{B}_L$, ${}_0^t\mathbf{B}_L$, ${}_t^t\mathbf{B}_L$ = linear strain-displacement transformation matrices; $\mathbf{B}_L$ is equal to ${}_0^t\mathbf{B}_L$ when the initial displacement effect is neglected
${}_0^t\mathbf{B}_{NL}$, ${}_t^t\mathbf{B}_{NL}$ = nonlinear strain-displacement transformation matrices
$\mathbf{C}$ = stress-strain material property matrix (incremental or total)
${}_0\mathbf{C}$, ${}_t\mathbf{C}$ = incremental stress-strain material property matrices
$^t\boldsymbol{\tau}$, $^t\hat{\boldsymbol{\tau}}$ = matrix and vector of Cauchy stresses
${}_0^t\mathbf{S}$, $^t\hat{\mathbf{S}}$ = matrix and vector of second Piola-Kirchhoff stresses
$^t\hat{\boldsymbol{\Sigma}}$ = vector of stresses in materially-nonlinear-only analysis

TABLE 6.4 *Finite element matrices*

Analysis type	Integral	Matrix evaluation
In all analyses	$\int_{{}^0V} {}^0\rho\, {}^{t+\Delta t}\ddot{u}_i\, \delta u_i\, d^0V$	$\mathbf{M}\, {}^{t+\Delta t}\ddot{\hat{\mathbf{u}}} = \left(\int_{{}^0V} {}^0\rho\, \mathbf{H}^T\mathbf{H}\, d^0V\right) {}^{t+\Delta t}\ddot{\hat{\mathbf{u}}}$
	${}^{t+\Delta t}\mathcal{R} = \int_{{}^0S_f} {}^{t+\Delta t}_{\ 0}f_i^S\, \delta u_i^S\, d^0S + \int_{{}^0V} {}^{t+\Delta t}_{\ 0}f_i^B\, \delta u_i\, d^0V$	${}^{t+\Delta t}\mathbf{R} = \int_{{}^0S_f} \mathbf{H}^{S^T}\, {}^{t+\Delta t}_{\ 0}\mathbf{f}^S\, d^0S + \int_{{}^0V} \mathbf{H}^T\, {}^{t+\Delta t}_{\ 0}\mathbf{f}^B\, d^0V$
Materially-nonlinear-only	$\int_V C_{ijrs}\, e_{rs}\, \delta e_{ij}\, dV$	${}^t\mathbf{K}\hat{\mathbf{u}} = \left(\int_V \mathbf{B}_L^T\mathbf{C}\mathbf{B}_L\, dV\right)\hat{\mathbf{u}}$
	$\int_V {}^t\sigma_{ij}\, \delta e_{ij}\, dV$	${}^t\mathbf{F} = \int_V \mathbf{B}_L^T\, {}^t\hat{\boldsymbol{\Sigma}}\, dV$
Total Lagrangian formulation	$\int_{{}^0V} {}_0C_{ijrs}\, {}_0e_{rs}\, \delta_0 e_{ij}\, d^0V$	${}_0^t\mathbf{K}_L\hat{\mathbf{u}} = \left(\int_{{}^0V} {}_0^t\mathbf{B}_L^T\, {}_0\mathbf{C}\, {}_0^t\mathbf{B}_L\, d^0V\right)\hat{\mathbf{u}}$
	$\int_{{}^0V} {}_0^tS_{ij}\, \delta_0\eta_{ij}\, d^0V$	${}_0^t\mathbf{K}_{NL}\hat{\mathbf{u}} = \left(\int_{{}^0V} {}_0^t\mathbf{B}_{NL}^T\, {}_0^t\mathbf{S}\, {}_0^t\mathbf{B}_{NL}\, d^0V\right)\hat{\mathbf{u}}$
	$\int_{{}^0V} {}_0^tS_{ij}\, \delta_0 e_{ij}\, d^0V$	${}_0^t\mathbf{F} = \int_{{}^0V} {}_0^t\mathbf{B}_L^T\, {}_0^t\hat{\mathbf{S}}\, d^0V$
Updated Lagrangian formulation	$\int_{{}^tV} {}_tC_{ijrs}\, {}_te_{rs}\, \delta_t e_{ij}\, d^tV$	${}_t^t\mathbf{K}_L\hat{\mathbf{u}} \left(\int_{{}^tV} {}_t^t\mathbf{B}_L^T\, {}_t\mathbf{C}\, {}_t^t\mathbf{B}_L\, d^tV\right)\hat{\mathbf{u}}$
	$\int_{{}^tV} {}^t\tau_{ij}\, \delta_t\eta_{ij}\, d^tV$	${}_t^t\mathbf{K}_{NL}\hat{\mathbf{u}} = \left(\int_{{}^tV} {}_t^t\mathbf{B}_{NL}^T\, {}^t\boldsymbol{\tau}\, {}_t^t\mathbf{B}_{NL}\, d^tV\right)\hat{\mathbf{u}}$
	$\int_{{}^tV} {}^t\tau_{ij}\, \delta_t e_{ij}\, d^tV$	${}_t^t\mathbf{F} = \int_{{}^tV} {}_t^t\mathbf{B}_L^T\, {}^t\hat{\boldsymbol{\tau}}\, d^tV$

These matrices depend on the specific element considered. The displacement interpolation matrices are simply assembled as in linear analysis from the displacement interpolation functions. In the following sections we discuss the calculation of the strain-displacement and stress matrices and vectors pertaining to the continuum elements that we considered earlier for linear analysis in Chapter 5. The discussion is abbreviated because the basic numerical procedures employed in the calculation of the nonlinear finite matrices are those that we have already covered. For example, we consider again variable-number-nodes elements whose interpolation functions were previously given. As before, the displacement interpolations and strain-displacement matrices are expressed in terms of the isoparametric coordinates. Thus, the integrations indicated in Table 6.4 are performed as explained in Section 5.5.

In the following discussion we consider only the UL and TL formulations because the matrices of the materially-nonlinear-only analysis can be directly obtained from these formulations, and we are only concerned with the required kinematic expressions. The evaluation of the stresses and stress-strain matrices of the elements depends on the material model used. These considerations are discussed in Section 6.6.

6.3.3 Truss and Cable Elements

As discussed previously in Section 4.2.3, a truss element is a structural member capable of transmitting stresses only in the direction normal to the cross section. It is assumed that this normal stress is constant over the cross-sectional area.

In the following we consider a truss element that has an arbitrary orientation in space. The element is described by two to four nodes, as shown in Fig. 6.3, and is subjected to large displacements and large strains. The global coordinates of the nodal points of the element are at time 0, ${}^0x_1^k$, ${}^0x_2^k$, ${}^0x_3^k$ and at time t, ${}^tx_1^k$, ${}^tx_2^k$, ${}^tx_3^k$, where $k = 1, \ldots, N$, with N equal to the number of nodes ($2 \leq N \leq 4$). These nodal point coordinates are assumed to determine the spatial configuration of the truss at time 0 and time t using

$$ {}^0x_1(r) = \sum_{k=1}^{N} h_k \, {}^0x_1^k; \qquad {}^0x_2(r) = \sum_{k=1}^{N} h_k \, {}^0x_2^k; \qquad {}^0x_3(r) = \sum_{k=1}^{N} h_k \, {}^0x_3^k \tag{6.106} $$

and

$$ {}^tx_1(r) = \sum_{k=1}^{N} h_k \, {}^tx_1^k; \qquad {}^tx_2(r) = \sum_{k=1}^{N} h_k \, {}^tx_2^k; \qquad {}^tx_3(r) = \sum_{k=1}^{N} h_k \, {}^tx_3^k \tag{6.107} $$

where the interpolation functions $h_k(r)$ have been defined in Fig. 5.3. Using (6.106) and (6.107), it follows that

$$ {}^tu_i(r) = \sum_{k=1}^{N} h_k \, {}^tu_i^k \tag{6.108} $$

and

$$ u_i(r) = \sum_{k=1}^{N} h_k u_i^k, \qquad i = 1, 2, 3 \tag{6.109} $$

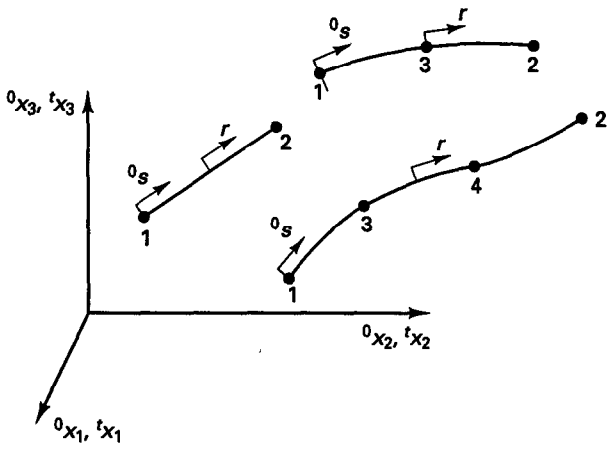

Figure 6.3 Two- to four-node truss element

Since for the truss element the only stress is the normal stress on its cross-sectional area, we consider only the corresponding longitudinal strain. Denoting the local element longitudinal strain by a curl, we have in the TL formulation,

$$ {}_0\tilde{\epsilon}_{11} = \frac{d^0x_i}{d^0s}\frac{d^tu_i}{d^0s} + \frac{1}{2}\frac{d^tu_i}{d^0s}\frac{d^tu_i}{d^0s} \tag{6.110} $$

where ${}^0s(r)$ is the arc length at time 0 of the material point ${}^0x_1(r)$, ${}^0x_2(r)$, ${}^0x_3(r)$ given by

$$ {}^0s(r) = \sum_{k=1}^{N} h_k \, {}^0s_k \tag{6.111} $$

The increment in the strain component ${}^t_0\tilde{\epsilon}_{11}$ is denoted as ${}_0\tilde{\epsilon}_{11}$, where ${}_0\tilde{\epsilon}_{11} = {}_0\tilde{e}_{11} + {}_0\tilde{\eta}_{11}$ and

$$ {}_0\tilde{e}_{11} = \frac{d^0x_i}{d^0s}\frac{du_i}{d^0s} + \frac{d^tu_i}{d^0s}\frac{du_i}{d^0s} \tag{6.112} $$

$$ {}_0\tilde{\eta}_{11} = \frac{1}{2}\frac{du_i}{d^0s}\frac{du_i}{d^0s} \tag{6.113} $$

For the strain-displacement matrices we define

$$ {}^0\hat{\mathbf{x}}^T = [{}^0x_1^1 \quad {}^0x_2^1 \quad {}^0x_3^1 \quad \cdots \quad {}^0x_1^N \quad {}^0x_2^N \quad {}^0x_3^N] \tag{6.114} $$

$$ {}^t\hat{\mathbf{u}}^T = [{}^tu_1^1 \quad {}^tu_2^1 \quad {}^tu_3^1 \quad \cdots \quad {}^tu_1^N \quad {}^tu_2^N \quad {}^tu_3^N] $$

$$ \hat{\mathbf{u}}^T = [u_1^1 \quad u_2^1 \quad u_3^1 \quad \cdots \quad u_1^N \quad u_2^N \quad u_3^N] \tag{6.115} $$

$$ \mathbf{H} = \begin{bmatrix} h_1\mathbf{I}_3 & \vdots & \cdots & \vdots & h_N\mathbf{I}_3 \end{bmatrix}; \qquad \mathbf{I}_3 = \begin{bmatrix} 1 & 0 & 0 \\ 0 & 1 & 0 \\ 0 & 0 & 1 \end{bmatrix} \tag{6.116} $$

and hence, using (6.112) and (6.113),

$$ {}^t_0\mathbf{B}_L = ({}^0J^{-1})^2 \, ({}^0\hat{\mathbf{x}}^T\mathbf{H}_{,r}^T\mathbf{H}_{,r} + {}^t\hat{\mathbf{u}}^T\mathbf{H}_{,r}^T\mathbf{H}_{,r}) \tag{6.117} $$

and

$$ {}^t_0\mathbf{B}_{NL} = {}^0J^{-1}\mathbf{H}_{,r} \tag{6.118} $$

where ${}^0J^{-1} = dr/d^0s$. We note that since ${}^t_0\mathbf{B}_{NL}$ is independent of the orientation of the element, the matrix ${}^t_0\mathbf{K}_{NL}$ is so as well.

The only nonzero stress component is ${}^t_0\tilde{S}_{11}$, which we assume to be given as a function of the Green-Lagrange strain ${}^t_0\tilde{\epsilon}_{11}$ at time t (see Section 6.6). The tangent stress-strain relationship is therefore

$$ {}_0\tilde{C}_{1111} = \frac{\partial {}^t_0\tilde{S}_{11}}{\partial {}^t_0\tilde{\epsilon}_{11}} \tag{6.119} $$

Using (6.114) to (6.119), the truss element matrices can be directly calculated as given in Table 6.4. Referring to Tables 6.2 to 6.4, the above relations can also be directly employed to develop the UL formulation, and of course the materially-nonlinear-only formulation. Consider the following examples.

EXAMPLE 6.16: For the two-node truss element shown in Fig. E6.16 develop the tangent stiffness matrix and force vector corresponding to the configuration at time t. Consider large displacement and large strain conditions.

We note that the element is straight and is at time 0 aligned with the ${}^0x_1$ axis. Hence, we need not use the curl on the stress and strain components, and the equations of the formulation are somewhat simpler than (6.110) to (6.119). In the following we use two formulation approaches to emphasize some important points.

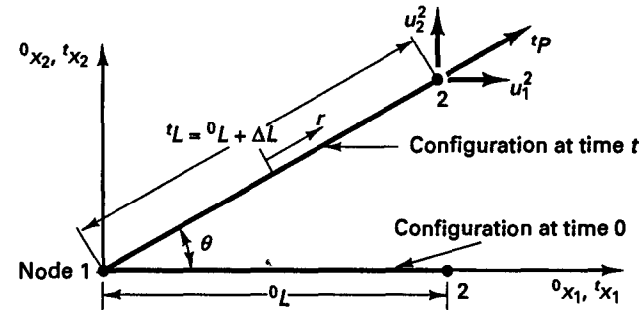

(a) Two-node element

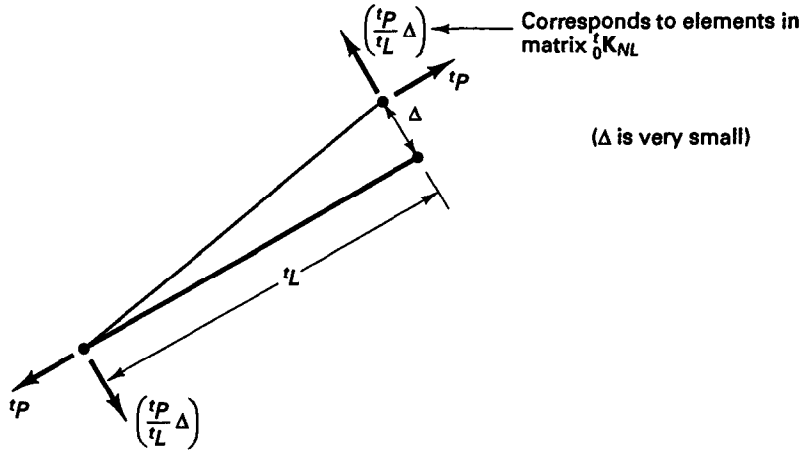

(b) Moment equilibrium of element

Figure E6.16 Formulation of two-node truss element

First Approach: Evaluation of Element Matrices Using Table 6.4: Using the TL formulation we need to express the strains ${}_0e_{11}$ and ${}_0\eta_{11}$ given in Table 6.2 [and (6.112) and (6.113)] in terms of the element displacement functions. Since the truss element undergoes displacements only in the $^0x_1$, $^0x_2$ plane, we have

$$ {}_0e_{11} = \frac{\partial u_1}{\partial {}^0x_1} + \frac{\partial {}^tu_1}{\partial {}^0x_1}\frac{\partial u_1}{\partial {}^0x_1} + \frac{\partial {}^tu_2}{\partial {}^0x_1}\frac{\partial u_2}{\partial {}^0x_1} $$

$$ {}_0\eta_{11} = \frac{1}{2}\left[\left(\frac{\partial u_1}{\partial {}^0x_1}\right)^2 + \left(\frac{\partial u_2}{\partial {}^0x_1}\right)^2\right] $$

But by geometry, or using ${}^tu_i = \Sigma_{k=1}^2 h_k\, {}^tu_i^k$ with ${}^tu_1^1 = 0$, ${}^tu_2^1 = 0$, ${}^tu_1^2 = ({}^0L + \Delta L)\cos\theta - {}^0L$, ${}^tu_2^2 = ({}^0L + \Delta L)\sin\theta$, ${}^0J = {}^0L/2$ and the interpolation functions given in Fig. 5.3, we obtain

$$ \frac{\partial {}^tu_1}{\partial {}^0x_1} = \frac{({}^0L + \Delta L)\cos\theta}{{}^0L} - 1; \qquad \frac{\partial {}^tu_2}{\partial {}^0x_1} = \frac{({}^0L + \Delta L)\sin\theta}{{}^0L} $$

We therefore have

$$
\begin{aligned}
{}_0e_{11} &= \frac{1}{{}^0L}\left\{[-1 \quad 0 \quad 1 \quad 0] + \left(\frac{{}^0L + \Delta L}{{}^0L}\cos\theta - 1\right)[-1 \quad 0 \quad 1 \quad 0]\right. \\
&\quad \left. + \left(\frac{{}^0L + \Delta L}{{}^0L}\sin\theta\right)[0 \quad -1 \quad 0 \quad 1]\right\}\begin{bmatrix} u_1^1 \\ u_2^1 \\ u_1^2 \\ u_2^2 \end{bmatrix} \\
&= \frac{{}^0L + \Delta L}{({}^0L)^2}[-\cos\theta \quad -\sin\theta \quad \cos\theta \quad \sin\theta]\begin{bmatrix} u_1^1 \\ u_2^1 \\ u_1^2 \\ u_2^2 \end{bmatrix}
\end{aligned}
$$

and hence,

$$
{}_0^t\mathbf{B}_L = \frac{{}^0L + \Delta L}{({}^0L)^2}[-\cos\theta \quad -\sin\theta \quad \cos\theta \quad \sin\theta]
$$

Of course, the same result for ${}_0^t\mathbf{B}_L$ is obtained using (6.117). The nonlinear strain displacement matrix is [from (6.118)]

$$
{}_0^t\mathbf{B}_{NL} = \frac{1}{{}^0L}\begin{bmatrix} -1 & 0 & 1 & 0 \\ 0 & -1 & 0 & 1 \end{bmatrix}
$$

In the total Lagrangian formulation we assume that ${}_0^tS_{11}$ is given in terms of ${}_0^t\epsilon_{11}$, and we have

$$
{}_0C_{1111} = \frac{\partial {}_0^tS_{11}}{\partial {}_0^t\epsilon_{11}}
$$

If we use ${}_0^tS_{11} = E\,{}_0^t\epsilon_{11}$, we have of course ${}_0C_{1111} = E$. The tangent stiffness matrix and force vector are therefore (see Table 6.4)

$$
\begin{aligned}
{}_0^t\mathbf{K} &= {}_0C_{1111}\frac{({}^0L + \Delta L)^2}{({}^0L)^3}{}^0A\begin{bmatrix} \cos^2\theta & \cos\theta\sin\theta & -\cos^2\theta & -\cos\theta\sin\theta \\ & \sin^2\theta & -\sin\theta\cos\theta & -\sin^2\theta \\ & & \cos^2\theta & \sin\theta\cos\theta \\ \text{Symmetric} & & & \sin^2\theta \end{bmatrix} \\
&\quad + \frac{{}^tP}{{}^0L + \Delta L}\begin{bmatrix} 1 & 0 & -1 & 0 \\ 0 & 1 & 0 & -1 \\ -1 & 0 & 1 & 0 \\ 0 & -1 & 0 & 1 \end{bmatrix} \qquad \text{(a)} \\
{}_0^t\mathbf{F} &= {}^tP\begin{bmatrix} -\cos\theta \\ -\sin\theta \\ \cos\theta \\ \sin\theta \end{bmatrix}
\end{aligned}
$$

where ${}^tP$ is the current force carried in the truss element. Here we have used, with the Cauchy stress equal to ${}^tP/{}^tA$,

$$
\begin{aligned}
{}^t_0S_{11} &= \frac{{}^0\rho}{{}^t\rho}\left(\frac{{}^0L}{{}^0L+\Delta L}\right)^2 \frac{{}^tP}{{}^tA}; \qquad {}^t_0\epsilon_{11} = \frac{\Delta L}{{}^0L} + \frac{1}{2}\left(\frac{\Delta L}{{}^0L}\right)^2 \\
{}^0\rho\,{}^0L\,{}^0A &= {}^t\rho({}^0L+\Delta L)\,{}^tA; \qquad {}^t_0S_{11} = \frac{{}^0L}{{}^0L+\Delta L}\frac{{}^tP}{{}^0A} \qquad \text{(b)} \\
{}^tP &= {}^t_0S_{11}\,{}^0A\frac{{}^0L+\Delta L}{{}^0L}
\end{aligned}
$$

The first term in (a) represents the linear strain stiffness matrix, and the second term is the nonlinear strain stiffness matrix, which, as noted earlier, is independent of the angle θ.

Second Approach: Taking the Derivative of the Force Vector ${}^t_0\mathbf{F}$: The tangent stiffness matrix of any element can be obtained by direct differentiation of the force vector ${}^t_0\mathbf{F}$ (see Section 6.3.1); that is,

$$
{}^t_0\mathbf{K} = \frac{\partial {}^t_0\mathbf{F}}{\partial {}^t\hat{\mathbf{u}}} \qquad \text{(c)}
$$

where ${}^t\hat{\mathbf{u}}$ is the vector of nodal point displacements corresponding to time t. Here we have for the general truss element formulation in (6.106) to (6.119), ${}^t_0\mathbf{F} = \int_{{}^0V} {}^t_0\mathbf{B}_L^T\,{}^t_0\tilde{S}_{11}\,d^0V$, so that

$$
\frac{\partial {}^t_0\mathbf{F}}{\partial {}^t\hat{\mathbf{u}}} = \int_{{}^0V} {}^t_0\mathbf{B}_L^T \frac{\partial {}^t_0\tilde{S}_{11}}{\partial {}^t_0\tilde{\epsilon}_{11}} \frac{\partial {}^t_0\tilde{\epsilon}_{11}}{\partial {}^t\hat{\mathbf{u}}}\,d^0V + \int_{{}^0V} \frac{\partial {}^t_0\mathbf{B}_L^T}{\partial {}^t\hat{\mathbf{u}}}\,{}^t_0\tilde{S}_{11}\,d^0V \qquad \text{(d)}
$$

Using (6.117) and (6.118), we have

$$
\frac{\partial {}^t_0\mathbf{B}_L^T}{\partial {}^t\hat{\mathbf{u}}} = ({}^0J^{-1})^2\,\mathbf{H}_{,r}^T\,\mathbf{H}_{,r} = {}^t_0\mathbf{B}_{NL}^T\,{}^t_0\mathbf{B}_{NL}
$$

so that the second term in (d) gives the ${}^t_0\mathbf{K}_{NL}$ matrix. Also, using (6.110) and (6.117), we directly see that

$$
\frac{\partial {}^t_0\tilde{\epsilon}_{11}}{\partial {}^t\hat{\mathbf{u}}} = {}^t_0\mathbf{B}_L
$$

and hence, the first term in (d) gives the ${}^t_0\mathbf{K}_L$ matrix.

However, to gain more insight, let us consider the derivation of ${}^t_0\mathbf{K}$ in (c) specifically for the two-node truss element in Fig. E6.16 using the following details.

For the two-node element, ${}^t_0\mathbf{F}$ is given by simple equilibrium

$$
{}^t_0\mathbf{F} = {}^tP\begin{bmatrix} -\cos\theta \\ -\sin\theta \\ \cos\theta \\ \sin\theta \end{bmatrix}
$$

where ${}^tP$ is the current force (positive when a tensile force) carried by the element, and we have

$${}^t\hat{\mathbf{u}}^T = \begin{bmatrix} {}^tu_1^1 & {}^tu_2^1 & {}^tu_1^2 & {}^tu_2^2 \end{bmatrix}$$

Let us consider the third and fourth columns of the stiffness matrix (from which the first and second columns can be derived). We have

$$ {}^{t}u_1^2 = ({}^{0}L + \Delta L)\cos\theta - {}^{0}L $$

$$ {}^{t}u_2^2 = ({}^{0}L + \Delta L)\sin\theta $$

and hence,

$$ \begin{bmatrix} \dfrac{\partial}{\partial(\Delta L)} \\ \dfrac{\partial}{\partial\theta} \end{bmatrix} = \begin{bmatrix} \cos\theta & \sin\theta \\ -({}^{0}L + \Delta L)\sin\theta & ({}^{0}L + \Delta L)\cos\theta \end{bmatrix} \begin{bmatrix} \dfrac{\partial}{\partial\, {}^{t}u_1^2} \\ \dfrac{\partial}{\partial\, {}^{t}u_2^2} \end{bmatrix} $$

from which

$$ \begin{bmatrix} \dfrac{\partial}{\partial\, {}^{t}u_1^2} \\ \dfrac{\partial}{\partial\, {}^{t}u_2^2} \end{bmatrix} = \begin{bmatrix} \cos\theta & -\dfrac{\sin\theta}{{}^{0}L + \Delta L} \\ \sin\theta & \dfrac{\cos\theta}{{}^{0}L + \Delta L} \end{bmatrix} \begin{bmatrix} \dfrac{\partial}{\partial(\Delta L)} \\ \dfrac{\partial}{\partial\theta} \end{bmatrix} $$

Therefore, the third column of ${}_{0}^{t}\mathbf{K}$ is given by[7]

$$ \frac{\partial\, {}_{0}^{t}\mathbf{F}}{\partial\, {}^{t}u_1^2} = \frac{\partial\, {}_{0}^{t}\mathbf{F}}{\partial(\Delta L)}\frac{\partial(\Delta L)}{\partial\, {}^{t}u_1^2} + \frac{\partial\, {}_{0}^{t}\mathbf{F}}{\partial\theta}\frac{\partial\theta}{\partial\, {}^{t}u_1^2} $$

$$ = \frac{\partial\, {}^{t}P}{\partial(\Delta L)}\begin{bmatrix} -\cos\theta \\ -\sin\theta \\ \cos\theta \\ \sin\theta \end{bmatrix}\cos\theta + {}^{t}P\begin{bmatrix} \sin\theta \\ -\cos\theta \\ -\sin\theta \\ \cos\theta \end{bmatrix}\left(\frac{-\sin\theta}{{}^{0}L + \Delta L}\right) \tag{e} $$

$$ = \frac{\partial\left(\dfrac{{}^{t}P}{{}^{0}L + \Delta L}\right)}{\partial(\Delta L)}({}^{0}L + \Delta L)\begin{bmatrix} -\cos^2\theta \\ -\sin\theta\cos\theta \\ \cos^2\theta \\ \sin\theta\cos\theta \end{bmatrix} + \frac{{}^{t}P}{{}^{0}L + \Delta L}\begin{bmatrix} -1 \\ 0 \\ 1 \\ 0 \end{bmatrix} $$

Similarly, for the fourth column of ${}_{0}^{t}\mathbf{K}$,

$$ \frac{\partial\, {}_{0}^{t}\mathbf{F}}{\partial\, {}^{t}u_2^2} = \frac{\partial\, {}_{0}^{t}\mathbf{F}}{\partial(\Delta L)}\frac{\partial(\Delta L)}{\partial\, {}^{t}u_2^2} + \frac{\partial\, {}_{0}^{t}\mathbf{F}}{\partial\theta}\frac{\partial\theta}{\partial\, {}^{t}u_2^2} $$

$$ = \frac{\partial\left(\dfrac{{}^{t}P}{{}^{0}L + \Delta L}\right)}{\partial(\Delta L)}({}^{0}L + \Delta L)\begin{bmatrix} -\cos\theta\sin\theta \\ -\sin^2\theta \\ \sin\theta\cos\theta \\ \sin^2\theta \end{bmatrix} + \frac{{}^{t}P}{{}^{0}L + \Delta L}\begin{bmatrix} 0 \\ -1 \\ 0 \\ 1 \end{bmatrix} \tag{f} $$

However, using (b),

$$ \frac{\partial\left(\dfrac{{}^{t}P}{{}^{0}L + \Delta L}\right)}{\partial(\Delta L)}({}^{0}L + \Delta L) = \frac{\partial\, {}_{0}^{t}S_{11}}{\partial(\Delta L)}\frac{{}^{0}L + \Delta L}{{}^{0}L}{}^{0}A $$

$$ = \frac{\partial\, {}_{0}^{t}S_{11}}{\partial\, {}_{0}^{t}\epsilon_{11}}\frac{\partial\, {}_{0}^{t}\epsilon_{11}}{\partial(\Delta L)}\frac{{}^{0}L + \Delta L}{{}^{0}L}{}^{0}A = \frac{\partial\, {}_{0}^{t}S_{11}}{\partial\, {}_{0}^{t}\epsilon_{11}}\frac{({}^{0}L + \Delta L)^2}{{}^{0}L^3}{}^{0}A $$

$$ = {}_{0}C_{1111}\frac{({}^{0}L + \Delta L)^2}{{}^{0}L^3}{}^{0}A $$

[7] Note that if the material stress-strain relationship is such that ${}^{t}P$ is constant with changes in ΔL, only the second term in the second line of this equation is nonzero.

Hence, the results in (e) and (f) are those already given in (a).

We note that the entries in the nonlinear strain stiffness matrix can also be directly obtained from equilibrium considerations as shown in Fig. E6.16(b).

Also, the updated Lagrangian formulation could be obtained from the result in (a) by using the relation (see Example 6.23)

$$ {}_0C_{1111} = \frac{{}^0\rho}{{}^t\rho}\left(\frac{{}^0L}{{}^0L + \Delta L}\right)^4 {}_tC_{1111} $$

so that in (a)

$$ {}_0C_{1111}\frac{({}^0L + \Delta L)^2}{({}^0L)^3}\,{}^0A = {}_tC_{1111}\frac{{}^tA}{{}^0L + \Delta L} \tag{g} $$

If we also note that for infinitesimally small displacements the linear strain stiffness matrix reduces to the well-known truss element matrix (see Example 4.1), we recognize that with the result of (g) substituted in (a), the updated Lagrangian stiffness matrix is in fact what we would expect it to be from physical considerations.

EXAMPLE 6.17: Establish the equilibrium equations used in the nonlinear analysis of the simple arch structure considered in Example 6.3 when the modified Newton-Raphson iteration is used for solution.

In the modified Newton-Raphson iteration, we use (6.11) and (6.12) but evaluate new tangent stiffness matrices only at the beginning of each step.

As in Example 6.3, we idealize the structure using one truss element [see Fig. E6.3(b)]. Since the displacements at node 1 are zero, we need to consider only the displacements at node 2. Using the derivations given in Example 6.16, with $\theta = {}^t\beta$ we have

$$ {}^t_0\mathbf{K}_L = \frac{EA}{L}\begin{bmatrix} (\cos {}^t\beta)^2 & \sin {}^t\beta \cos {}^t\beta \\ \sin {}^t\beta \cos {}^t\beta & (\sin {}^t\beta)^2 \end{bmatrix} $$

$$ {}^t_0\mathbf{K}_{NL} = \frac{{}^tP}{L}\begin{bmatrix} 1 & 0 \\ 0 & 1 \end{bmatrix} $$

$$ {}^t_0\mathbf{F} = {}^tP\begin{bmatrix} \cos {}^t\beta \\ \sin {}^t\beta \end{bmatrix} $$

where we assumed in the stiffness expressions that L and EA/L are constant throughout the response.

The matrices correspond to the global displacements ${}^tu_1^2$ and ${}^tu_2^2$ at node 2. However, ${}^tu_1^2$ is zero, hence the governing equilibrium equation is

$$ \left[\frac{EA}{L}(\sin {}^t\beta)^2 + \frac{{}^tP}{L}\right]\Delta u_2^{2(i)} = -\frac{{}^{t+\Delta t}R}{2} - {}^{t+\Delta t}P^{(i-1)} \sin ({}^{t+\Delta t}\beta^{(i-1)}) $$

where ${}^{t+\Delta t}R/2$ is positive as shown in Fig. E6.3(b) and ${}^{t+\Delta t}P^{(i-1)}$ is the force in the bar (tensile force being positive) corresponding to the displacements at time $t + \Delta t$ and end of iteration $(i - 1)$.

6.3.4 Two-Dimensional Axisymmetric, Plane Strain, and Plane Stress Elements

For the derivation of the required matrices and vectors, we consider a typical two-dimensional element in its configuration at time 0 and at time t, as illustrated for a nine-node element in Fig. 6.4. The global coordinates of the nodal points of the element are

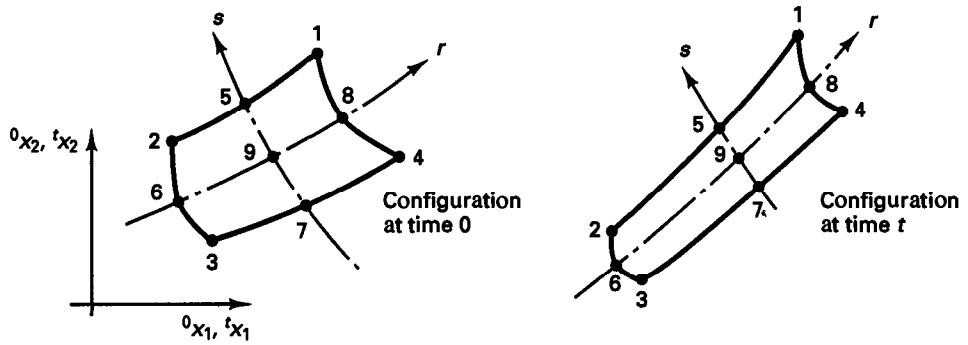

Figure 6.4 Two-dimensional element shown in the global ${}^tx_1, {}^tx_2$ plane

at time 0, ${}^0x_1^k$, ${}^0x_2^k$, and at time t, ${}^tx_1^k$, ${}^tx_2^k$, where $k = 1, 2, \ldots, N$, and N denotes the total number of element nodes.

Using the interpolation concepts discussed in Section 5.3, we have at time 0,

$$^0x_1 = \sum_{k=1}^{N} h_k \, {}^0x_1^k; \qquad {}^0x_2 = \sum_{k=1}^{N} h_k \, {}^0x_2^k \tag{6.120}$$

and at time t

$$^tx_1 = \sum_{k=1}^{N} h_k \, {}^tx_1^k; \qquad {}^tx_2 = \sum_{k=1}^{N} h_k \, {}^tx_2^k \tag{6.121}$$

where the h_k are the interpolation functions presented in Fig. 5.4.

Since we use the isoparametric finite element discretization, the element displacements are interpolated in the same way as the geometry; i.e.,

$$^tu_1 = \sum_{k=1}^{N} h_k \, {}^tu_1^k; \qquad {}^tu_2 = \sum_{k=1}^{N} h_k \, {}^tu_2^k \tag{6.122}$$

$$u_1 = \sum_{k=1}^{N} h_k \, u_1^k; \qquad u_2 = \sum_{k=1}^{N} h_k \, u_2^k \tag{6.123}$$

The evaluation of strains requires the following derivatives:

$$\frac{\partial {}^tu_i}{\partial {}^0x_j} = \sum_{k=1}^{N} \left(\frac{\partial h_k}{\partial {}^0x_j}\right) {}^tu_i^k \tag{6.124}$$

$$\frac{\partial u_i}{\partial {}^0x_j} = \sum_{k=1}^{N} \left(\frac{\partial h_k}{\partial {}^0x_j}\right) u_i^k \qquad \begin{matrix} i = 1, 2 \\ j = 1, 2 \end{matrix} \tag{6.125}$$

$$\frac{\partial u_i}{\partial {}^tx_j} = \sum_{k=1}^{N} \left(\frac{\partial h_k}{\partial {}^tx_j}\right) u_i^k \tag{6.126}$$

These derivatives are calculated in the same way as in linear analysis, i.e., using a Jacobian transformation. As an example, consider briefly the evaluation of the derivatives in (6.126). The other derivatives are obtained in an analogous manner.

The chain rule relating ${}^t x_1$, ${}^t x_2$, to r, s derivatives is written as

$$\begin{bmatrix} \frac{\partial}{\partial r} \\ \frac{\partial}{\partial s} \end{bmatrix} = {}^t\mathbf{J} \begin{bmatrix} \frac{\partial}{\partial {}^t x_1} \\ \frac{\partial}{\partial {}^t x_2} \end{bmatrix}$$

in which

$${}^t\mathbf{J} = \begin{bmatrix} \frac{\partial {}^t x_1}{\partial r} & \frac{\partial {}^t x_2}{\partial r} \\ \frac{\partial {}^t x_1}{\partial s} & \frac{\partial {}^t x_2}{\partial s} \end{bmatrix}$$

Inverting the Jacobian operator $\mathbf{J}$, we obtain

$$\begin{bmatrix} \frac{\partial}{\partial {}^t x_1} \\ \frac{\partial}{\partial {}^t x_2} \end{bmatrix} = \frac{1}{\det {}^t\mathbf{J}} \begin{bmatrix} \frac{\partial {}^t x_2}{\partial s} & -\frac{\partial {}^t x_2}{\partial r} \\ -\frac{\partial {}^t x_1}{\partial s} & \frac{\partial {}^t x_1}{\partial r} \end{bmatrix} \begin{bmatrix} \frac{\partial}{\partial r} \\ \frac{\partial}{\partial s} \end{bmatrix}$$

where the Jacobian determinant is

$$\det {}^t\mathbf{J} = \frac{\partial {}^t x_1}{\partial r}\frac{\partial {}^t x_2}{\partial s} - \frac{\partial {}^t x_1}{\partial s}\frac{\partial {}^t x_2}{\partial r}$$

and the derivatives of the coordinates with respect to r and s are obtained as usual using (6.121); e.g.,

$$\frac{\partial {}^t x_1}{\partial r} = \sum_{k=1}^{N} \frac{\partial h_k}{\partial r} {}^t x_1^k$$

With all required derivatives defined, it is now possible to establish the strain-displacement transformation matrices for the elements. Table 6.5 gives the required matrices for the UL and TL formulations. In the numerical integration these matrices are evaluated at the Gauss integration points (see Section 5.5).

As we pointed out earlier, the choice between the TL and UL formulations essentially depends on their relative numerical effectiveness. Table 6.5 shows that all matrices of the two formulations have corresponding patterns of zero elements, except that ${}_0^t\mathbf{B}_L$ is a full matrix whereas ${}_t^t\mathbf{B}_L$ is sparse. The strain-displacement transformation matrix ${}_0^t\mathbf{B}_L$ is full because of the initial displacement effect in the linear strain terms (see Tables 6.2 and 6.3). Therefore, the calculation of the matrix product ${}_t^t\mathbf{B}_L^T {}_t\mathbf{C} {}_t^t\mathbf{B}_L$ in the UL formulation requires less time than the calculation of the matrix product ${}_0^t\mathbf{B}_L^T {}_0\mathbf{C} {}_0^t\mathbf{B}_L$ in the TL formulation.

The second numerical difference between the two formulations is that in the TL formulation all derivatives of interpolation functions are with respect to the initial coordinates, whereas in the UL formulation all derivatives are with respect to the coordinates at time t. Therefore, in the TL formulation the derivatives could be calculated only once in the first load step and stored on back-up storage for use in all subsequent load steps. However, in practice, such storage can be expensive and in a computer implementation the derivatives of the interpolation functions are in general best recalculated in each time step.

TABLE 6.5 *Matrices used in the two-dimensional element formulation*

A. *Total Lagrangian formulation*

1. *Incremental strains*

$$ {}_0\epsilon_{11} = {}_0u_{1,1} + {}_0^t u_{1,1}\,{}_0u_{1,1} + {}_0^t u_{2,1}\,{}_0u_{2,1} + \tfrac{1}{2}(({}_0u_{1,1})^2 + ({}_0u_{2,1})^2) $$

$$ {}_0\epsilon_{22} = {}_0u_{2,2} + {}_0^t u_{1,2}\,{}_0u_{1,2} + {}_0^t u_{2,2}\,{}_0u_{2,2} + \tfrac{1}{2}(({}_0u_{1,2})^2 + ({}_0u_{2,2})^2) $$

$$ {}_0\epsilon_{12} = \tfrac{1}{2}({}_0u_{1,2} + {}_0u_{2,1}) + \tfrac{1}{2}({}_0^t u_{1,1}\,{}_0u_{1,2} + {}_0^t u_{2,1}\,{}_0u_{2,2} + {}_0^t u_{1,2}\,{}_0u_{1,1} + {}_0^t u_{2,2}\,{}_0u_{2,1}) + \tfrac{1}{2}({}_0u_{1,1}\,{}_0u_{1,2} + {}_0u_{2,1}\,{}_0u_{2,2}) $$

$$ {}_0\epsilon_{33} = \frac{u_1}{{}_0x_1} + \frac{{}^t u_1 u_1}{({}_0x_1)^2} + \frac{1}{2}\left(\frac{u_1}{{}_0x_1}\right)^2 \qquad \text{for axisymmetric analysis} $$

where $ {}_0u_{i,j} = \dfrac{\partial u_i}{\partial {}_0x_j}; \qquad {}_0^t u_{i,j} = \dfrac{\partial {}^t u_i}{\partial {}_0x_j} $

2. *Linear strain-displacement transformation matrix*

Using $ {}_0\mathbf{e} = {}_0^t\mathbf{B}_L\hat{\mathbf{u}} $

where $ {}_0\mathbf{e}^T = [{}_0\epsilon_{11} \;\; {}_0\epsilon_{22} \;\; 2{}_0\epsilon_{12} \;\; {}_0\epsilon_{33}]; \qquad \hat{\mathbf{u}}^T = [u_1^1 \;\; u_2^1 \;\; u_1^2 \;\; u_2^2 \cdots u_1^N \;\; u_2^N] $

and $ {}_0^t\mathbf{B}_L = {}_0^t\mathbf{B}_{L0} + {}_0^t\mathbf{B}_{L1} $

$$ {}_0^t\mathbf{B}_{L0} = \begin{bmatrix} {}_0h_{1,1} & 0 & {}_0h_{2,1} & 0 & {}_0h_{3,1} & 0 & \cdots & {}_0h_{N,1} & 0 \\ 0 & {}_0h_{1,2} & 0 & {}_0h_{2,2} & 0 & {}_0h_{3,2} & \cdots & 0 & {}_0h_{N,2} \\ {}_0h_{1,2} & {}_0h_{1,1} & {}_0h_{2,2} & {}_0h_{2,1} & {}_0h_{3,2} & {}_0h_{3,1} & \cdots & {}_0h_{N,2} & {}_0h_{N,1} \\ \dfrac{h_1}{{}_0\bar{x}_1} & 0 & \dfrac{h_2}{{}_0\bar{x}_1} & 0 & \dfrac{h_3}{{}_0\bar{x}_1} & 0 & \cdots & \dfrac{h_N}{{}_0\bar{x}_1} & 0 \end{bmatrix} $$

where $ {}_0h_{k,j} = \dfrac{\partial h_k}{\partial {}_0x_j}; \qquad u_j^k = {}^{t+\Delta t}u_j^k - {}^t u_j^k; \qquad {}_0\bar{x}_1 = \sum_{k=1}^{N} h_k\,{}_0x_1^k; \qquad N = \text{number of nodes} $

and

$$ {}_0^t\mathbf{B}_{L1} = \begin{bmatrix} l_{11}\,{}_0h_{1,1} & l_{21}\,{}_0h_{1,1} & l_{11}\,{}_0h_{2,1} & l_{21}\,{}_0h_{2,1} & \cdots & l_{11}\,{}_0h_{N,1} & l_{21}\,{}_0h_{N,1} \\ l_{12}\,{}_0h_{1,2} & l_{22}\,{}_0h_{1,2} & l_{12}\,{}_0h_{2,2} & l_{22}\,{}_0h_{2,2} & \cdots & l_{12}\,{}_0h_{N,2} & l_{22}\,{}_0h_{N,2} \\ (l_{11}\,{}_0h_{1,2} + l_{12}\,{}_0h_{1,1}) & (l_{21}\,{}_0h_{1,2} + l_{22}\,{}_0h_{1,1}) & (l_{11}\,{}_0h_{2,2} + l_{12}\,{}_0h_{2,1}) & (l_{21}\,{}_0h_{2,2} + l_{22}\,{}_0h_{2,1}) & \cdots & (l_{11}\,{}_0h_{N,2} + l_{12}\,{}_0h_{N,1}) & (l_{21}\,{}_0h_{N,2} + l_{22}\,{}_0h_{N,1}) \\ l_{33}\dfrac{h_1}{{}_0\bar{x}_1} & 0 & l_{33}\dfrac{h_2}{{}_0\bar{x}_1} & 0 & \cdots & l_{33}\dfrac{h_N}{{}_0\bar{x}_1} & 0 \end{bmatrix} $$

where $ l_{11} = \sum_{k=1}^{N} {}_0h_{k,1}\,{}^t u_1^k; \qquad l_{22} = \sum_{k=1}^{N} {}_0h_{k,2}\,{}^t u_2^k; \qquad l_{21} = \sum_{k=1}^{N} {}_0h_{k,1}\,{}^t u_2^k; \qquad l_{12} = \sum_{k=1}^{N} {}_0h_{k,2}\,{}^t u_1^k; $

$ l_{33} = \dfrac{\sum_{k=1}^{N} h_k\,{}^t u_1^k}{{}_0\bar{x}_1} $

3. *Nonlinear strain-displacement transformation matrix*

$$ {}_0^t\mathbf{B}_{NL} = \begin{bmatrix} {}_0h_{1,1} & 0 & {}_0h_{2,1} & 0 & {}_0h_{3,1} & 0 & \cdots & {}_0h_{N,1} & 0 \\ {}_0h_{1,2} & 0 & {}_0h_{2,2} & 0 & {}_0h_{3,2} & 0 & \cdots & {}_0h_{N,2} & 0 \\ 0 & {}_0h_{1,1} & 0 & {}_0h_{2,1} & 0 & {}_0h_{3,1} & \cdots & 0 & {}_0h_{N,1} \\ 0 & {}_0h_{1,2} & 0 & {}_0h_{2,2} & 0 & {}_0h_{3,2} & \cdots & 0 & {}_0h_{N,2} \\ \dfrac{h_1}{{}_0\bar{x}_1} & 0 & \dfrac{h_2}{{}_0\bar{x}_1} & 0 & \dfrac{h_3}{{}_0\bar{x}_1} & 0 & \cdots & \dfrac{h_N}{{}_0\bar{x}_1} & 0 \end{bmatrix} $$

TABLE 6.5 (*cont.*)

4. *Second Piola-Kirchhoff stress matrix and vector*

$$ {}_0^t\mathbf{S} = \begin{bmatrix} {}_0^tS_{11} & {}_0^tS_{12} & 0 & 0 & 0 \\ {}_0^tS_{21} & {}_0^tS_{22} & 0 & 0 & 0 \\ 0 & 0 & {}_0^tS_{11} & {}_0^tS_{12} & 0 \\ 0 & 0 & {}_0^tS_{21} & {}_0^tS_{22} & 0 \\ 0 & 0 & 0 & 0 & {}_0^tS_{33} \end{bmatrix}; \qquad {}_0^t\hat{\mathbf{S}} = \begin{bmatrix} {}_0^tS_{11} \\ {}_0^tS_{22} \\ {}_0^tS_{12} \\ {}_0^tS_{33} \end{bmatrix} $$

B. *Updated Lagrangian formulation*

1. *Incremental strains*

$$ {}_t\epsilon_{11} = {}_tu_{1,1} + \tfrac{1}{2}(({}_tu_{1,1})^2 + ({}_tu_{2,1})^2) $$
$$ {}_t\epsilon_{22} = {}_tu_{2,2} + \tfrac{1}{2}(({}_tu_{1,2})^2 + ({}_tu_{2,2})^2) $$
$$ {}_t\epsilon_{12} = \tfrac{1}{2}({}_tu_{1,2} + {}_tu_{2,1}) + \tfrac{1}{2}({}_tu_{1,1}\,{}_tu_{1,2} + {}_tu_{2,1}\,{}_tu_{2,2}) $$
$$ {}_t\epsilon_{33} = \frac{u_1}{{}^tx_1} + \frac{1}{2}\left(\frac{u_1}{{}^tx_1}\right)^2 \qquad \text{for axisymmetric analysis} $$

where ${}_tu_{i,j} = \dfrac{\partial u_i}{\partial {}^tx_j}$

2. *Linear strain-displacement transformation matrix*

Using ${}_t\mathbf{e} = {}_t^t\mathbf{B}_L\hat{\mathbf{u}}$

where ${}_t\mathbf{e}^T = [{}_te_{11} \quad {}_te_{22} \quad 2{}_te_{12} \quad {}_te_{33}]$; $\quad \hat{\mathbf{u}}^T = [u_1^1 \quad u_2^1 \quad u_1^2 \quad u_2^2 \quad \cdots \quad u_1^N \quad u_2^N]$

$$ {}_t^t\mathbf{B}_L = \begin{bmatrix} {}_th_{1,1} & 0 & {}_th_{2,1} & 0 & {}_th_{3,1} & 0 & \cdots & {}_th_{N,1} & 0 \\ 0 & {}_th_{1,2} & 0 & {}_th_{2,2} & 0 & {}_th_{3,2} & \cdots & 0 & {}_th_{N,2} \\ {}_th_{1,2} & {}_th_{1,1} & {}_th_{2,2} & {}_th_{2,1} & {}_th_{3,2} & {}_th_{3,1} & \cdots & {}_th_{N,2} & {}_th_{N,1} \\ \dfrac{h_1}{{}^t\bar{x}_1} & 0 & \dfrac{h_2}{{}^t\bar{x}_1} & 0 & \dfrac{h_3}{{}^t\bar{x}_1} & 0 & \cdots & \dfrac{h_N}{{}^t\bar{x}_1} & 0 \end{bmatrix} $$

where ${}_th_{k,j} = \dfrac{\partial h_k}{\partial {}^tx_j}$; $\quad u_j^k = {}^{t+\Delta t}u_j^k - {}^tu_j^k$; $\quad {}^t\bar{x}_1 = \sum_{k=1}^{N} h_k\,{}^tx_1^k$; $\quad N =$ number of nodes

3. *Nonlinear strain-displacement transformation matrix*

$$ {}_t^t\mathbf{B}_{NL} = \begin{bmatrix} {}_th_{1,1} & 0 & {}_th_{2,1} & 0 & {}_th_{3,1} & 0 & \cdots & {}_th_{N,1} & 0 \\ {}_th_{1,2} & 0 & {}_th_{2,2} & 0 & {}_th_{3,2} & 0 & \cdots & {}_th_{N,2} & 0 \\ 0 & {}_th_{1,1} & 0 & {}_th_{2,1} & 0 & {}_th_{3,1} & \cdots & 0 & {}_th_{N,1} \\ 0 & {}_th_{1,2} & 0 & {}_th_{2,2} & 0 & {}_th_{3,2} & \cdots & 0 & {}_th_{N,2} \\ \dfrac{h_1}{{}^t\bar{x}_1} & 0 & \dfrac{h_2}{{}^t\bar{x}_1} & 0 & \dfrac{h_3}{{}^t\bar{x}_1} & 0 & \cdots & \dfrac{h_N}{{}^t\bar{x}_1} & 0 \end{bmatrix}. $$

4. *Cauchy stress matrix and stress vector*

$$ {}^t\boldsymbol{\tau} = \begin{bmatrix} {}^t\tau_{11} & {}^t\tau_{12} & 0 & 0 & 0 \\ {}^t\tau_{21} & {}^t\tau_{22} & 0 & 0 & 0 \\ 0 & 0 & {}^t\tau_{11} & {}^t\tau_{12} & 0 \\ 0 & 0 & {}^t\tau_{21} & {}^t\tau_{22} & 0 \\ 0 & 0 & 0 & 0 & {}^t\tau_{33} \end{bmatrix}; \qquad {}^t\hat{\boldsymbol{\tau}} = \begin{bmatrix} {}^t\tau_{11} \\ {}^t\tau_{22} \\ {}^t\tau_{12} \\ {}^t\tau_{33} \end{bmatrix} $$

EXAMPLE 6.18: Establish the matrices ${}^t_0\mathbf{B}_{L0}$, ${}^t_0\mathbf{B}_{L1}$, and ${}^t_0\mathbf{B}_{NL}$ corresponding to the TL formulation for the two-dimensional plane strain element shown in Fig. E6.18.

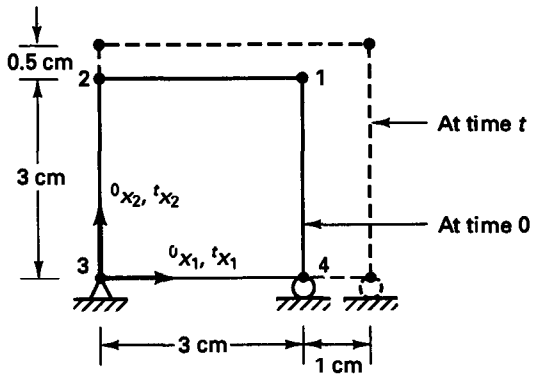

Figure E6.18 Four-node plane strain element in large displacement/large strain conditions

In this case we can directly use the information given in Table 6.5 with

$$
\begin{aligned}
{}^tu_1^1 &= 1; & {}^tu_2^1 &= 0.5 \\
{}^tu_1^2 &= 0; & {}^tu_2^2 &= 0.5 \\
{}^tu_1^3 &= 0; & {}^tu_2^3 &= 0 \\
{}^tu_1^4 &= 1; & {}^tu_2^4 &= 0
\end{aligned}
\qquad
{}^0\mathbf{J} = \begin{bmatrix} \frac{3}{2} & 0 \\ 0 & \frac{3}{2} \end{bmatrix}
$$

The interpolation functions of the four-node element are given in Fig. 5.4 (and the required derivatives have been given in Example 5.5), so that we obtain

$$
{}^t_0\mathbf{B}_{L0} = \frac{1}{6}\begin{bmatrix}
(1+s) & 0 & -(1+s) & 0 & -(1-s) & 0 & (1-s) & 0 \\
0 & (1+r) & 0 & (1-r) & 0 & -(1-r) & 0 & -(1+r) \\
(1+r) & (1+s) & (1-r) & -(1+s) & -(1-r) & -(1-s) & -(1+r) & (1-s)
\end{bmatrix}
$$

To evaluate ${}^t_0\mathbf{B}_{L1}$ we also need the l_{ij} values, where

$$
\begin{aligned}
l_{11} &= \sum_{k=1}^{4} {}_0h_{k,1}\,{}^tu_1^k = \tfrac{2}{3}\{h_{1,r}\,{}^tu_1^1 + h_{4,r}\,{}^tu_1^4\} = \tfrac{1}{3} \\
l_{12} &= \sum_{k=1}^{4} {}_0h_{k,2}\,{}^tu_1^k = \tfrac{2}{3}\{h_{1,s}\,{}^tu_1^1 + h_{4,s}\,{}^tu_1^4\} = 0 \\
l_{21} &= \sum_{k=1}^{4} {}_0h_{k,1}\,{}^tu_2^k = \tfrac{2}{3}\{h_{1,r}\,{}^tu_2^1 + h_{2,r}\,{}^tu_2^2\} = 0 \\
l_{22} &= \sum_{k=1}^{4} {}_0h_{k,2}\,{}^tu_2^k = \tfrac{2}{3}\{h_{1,s}\,{}^tu_2^1 + h_{2,s}\,{}^tu_2^2\} = \tfrac{1}{6}
\end{aligned}
$$

Hence, we have

$$
{}^t_0\mathbf{B}_{L1} = \frac{1}{36}\begin{bmatrix}
2(1+s) & 0 & -2(1+s) & 0 & -2(1-s) & 0 & 2(1-s) & 0 \\
0 & (1+r) & 0 & (1-r) & 0 & -(1-r) & 0 & -(1+r) \\
2(1+r) & (1+s) & 2(1-r) & -(1+s) & -2(1-r) & -(1-s) & -2(1+r) & (1-s)
\end{bmatrix}
$$

The nonlinear strain-displacement matrix can also directly be constructed using the derivatives of the interpolation functions and the Jacobian matrix:

$$
{}^{t}_{0}\mathbf{B}_{NL} = \frac{1}{6}\begin{bmatrix}
(1+s) & 0 & -(1+s) & 0 & -(1-s) & 0 & (1-s) & 0 \\
(1+r) & 0 & (1-r) & 0 & -(1-r) & 0 & -(1+r) & 0 \\
0 & (1+s) & 0 & -(1+s) & 0 & -(1-s) & 0 & (1-s) \\
0 & (1+r) & 0 & (1-r) & 0 & -(1-r) & 0 & -(1+r)
\end{bmatrix}
$$

6.3.5 Three-Dimensional Solid Elements

The evaluation of the matrices required in three-dimensional isoparametric finite element analysis is accomplished using the same procedures as in two-dimensional analysis. Thus, referring to Section 6.3.4, we simply note that for a typical element we now use the coordinate and displacement interpolations,

$$
{}^{0}x_i = \sum_{k=1}^{N} h_k\, {}^{0}x_i^k; \qquad {}^{t}x_i = \sum_{k=1}^{N} h_k\, {}^{t}x_i^k; \qquad i = 1, 2, 3 \tag{6.127}
$$

$$
{}^{t}u_i = \sum_{k=1}^{N} h_k\, {}^{t}u_i^k; \qquad u_i = \sum_{k=1}^{N} h_k\, u_i^k; \qquad i = 1, 2, 3 \tag{6.128}
$$

where the element interpolation functions h_k have been given in Fig. 5.5. Using (6.127) and (6.128) in the same way as in two-dimensional analysis, we can develop the relevant element matrices used in the TL and UL formulations for three-dimensional analysis (see Table 6.6).

TABLE 6.6 *Matrices used in the three-dimensional element formulation*

A. *Total Lagrangian formulation*

1. *Incremental strains*

$$
{}_{0}\epsilon_{ij} = \tfrac{1}{2}({}_{0}u_{i,j} + {}_{0}u_{j,i}) + \tfrac{1}{2}({}^{t}_{0}u_{k,i}\,{}_{0}u_{k,j} + {}_{0}u_{k,i}\,{}^{t}_{0}u_{k,j}) + \tfrac{1}{2}({}_{0}u_{k,i}\,{}_{0}u_{k,j}) \qquad i = 1, 2, 3;\ j = 1, 2, 3;\ k = 1, 2, 3
$$

where ${}_{0}u_{i,j} = \dfrac{\partial u_i}{\partial {}^{0}x_j}$

2. *Linear strain-displacement transformation matrix*

Using ${}_{0}\mathbf{e} = {}^{t}_{0}\mathbf{B}_L\hat{\mathbf{u}}$

where ${}_{0}\mathbf{e}^T = [{}_{0}e_{11}\ \ {}_{0}e_{22}\ \ {}_{0}e_{33}\ \ 2{}_{0}e_{12}\ \ 2{}_{0}e_{23}\ \ 2{}_{0}e_{31}]$;

$\hat{\mathbf{u}}^T = [u_1^1\ u_2^1\ u_3^1\ u_1^2\ u_2^2\ u_3^2\ \cdots\ u_1^N\ u_2^N\ u_3^N]$

$$
{}^{t}_{0}\mathbf{B}_L = {}^{t}_{0}\mathbf{B}_{L0} + {}^{t}_{0}\mathbf{B}_{L1}
$$

$$
{}^{t}_{0}\mathbf{B}_{L0} = \begin{bmatrix}
{}_{0}h_{1,1} & 0 & 0 & {}_{0}h_{2,1} & \cdots & 0 \\
0 & {}_{0}h_{1,2} & 0 & 0 & \cdots & 0 \\
0 & 0 & {}_{0}h_{1,3} & 0 & \cdots & {}_{0}h_{N,3} \\
{}_{0}h_{1,2} & {}_{0}h_{1,1} & 0 & {}_{0}h_{2,2} & \cdots & 0 \\
0 & {}_{0}h_{1,3} & {}_{0}h_{1,2} & 0 & \cdots & {}_{0}h_{N,2} \\
{}_{0}h_{1,3} & 0 & {}_{0}h_{1,1} & {}_{0}h_{2,3} & \cdots & {}_{0}h_{N,1}
\end{bmatrix}
$$

where ${}_{0}h_{k,j} = \dfrac{\partial h_k}{\partial {}^{0}x_j}$; $\qquad u_j^k = {}^{t+\Delta t}u_j^k - {}^{t}u_j^k$

TABLE 6.6 (*cont.*)

$$
{}_0^t\mathbf{B}_{L1} = \begin{bmatrix}
l_{11}\,{}_0h_{1,1} & l_{21}\,{}_0h_{1,1} & l_{31}\,{}_0h_{1,1} & l_{11}\,{}_0h_{2,1} & \cdots & l_{31}\,{}_0h_{N,1} \\
l_{12}\,{}_0h_{1,2} & l_{22}\,{}_0h_{1,2} & l_{32}\,{}_0h_{1,2} & l_{12}\,{}_0h_{2,2} & \cdots & l_{32}\,{}_0h_{N,2} \\
l_{13}\,{}_0h_{1,3} & l_{23}\,{}_0h_{1,3} & l_{33}\,{}_0h_{1,3} & l_{13}\,{}_0h_{2,3} & \cdots & l_{33}\,{}_0h_{N,3} \\
(l_{11}\,{}_0h_{1,2} + l_{12}\,{}_0h_{1,1}) & (l_{21}\,{}_0h_{1,2} + l_{22}\,{}_0h_{1,1}) & (l_{31}\,{}_0h_{1,2} + l_{32}\,{}_0h_{1,1}) & (l_{11}\,{}_0h_{2,2} + l_{12}\,{}_0h_{2,1}) & \cdots & (l_{31}\,{}_0h_{N,2} + l_{32}\,{}_0h_{N,1}) \\
(l_{12}\,{}_0h_{1,3} + l_{13}\,{}_0h_{1,2}) & (l_{22}\,{}_0h_{1,3} + l_{23}\,{}_0h_{1,2}) & (l_{32}\,{}_0h_{1,3} + l_{33}\,{}_0h_{1,2}) & (l_{12}\,{}_0h_{2,3} + l_{13}\,{}_0h_{2,2}) & \cdots & (l_{32}\,{}_0h_{N,3} + l_{33}\,{}_0h_{N,2}) \\
(l_{11}\,{}_0h_{1,3} + l_{13}\,{}_0h_{1,1}) & (l_{21}\,{}_0h_{1,3} + l_{23}\,{}_0h_{1,1}) & (l_{31}\,{}_0h_{1,3} + l_{33}\,{}_0h_{1,1}) & (l_{11}\,{}_0h_{2,3} + l_{13}\,{}_0h_{2,1}) & \cdots & (l_{31}\,{}_0h_{N,3} + l_{33}\,{}_0h_{N,1})
\end{bmatrix}
$$

where $l_{ij} = \sum_{k=1}^{N} {}_0h_{k,j}\,{}^tu_i^k$

3. *Nonlinear strain-displacement transformation matrix*

$$
{}_0^t\mathbf{B}_{NL} = \begin{bmatrix} {}_0^t\tilde{\mathbf{B}}_{NL} & \tilde{\mathbf{0}} & \tilde{\mathbf{0}} \\ \tilde{\mathbf{0}} & {}_0^t\tilde{\mathbf{B}}_{NL} & \tilde{\mathbf{0}} \\ \tilde{\mathbf{0}} & \tilde{\mathbf{0}} & {}_0^t\tilde{\mathbf{B}}_{NL} \end{bmatrix}; \qquad \tilde{\mathbf{0}} = \begin{bmatrix} 0 \\ 0 \\ 0 \end{bmatrix}
$$

where

$$
{}_0^t\tilde{\mathbf{B}}_{NL} = \begin{bmatrix} {}_0h_{1,1} & 0 & 0 & {}_0h_{2,1} & \cdots & {}_0h_{N,1} \\ {}_0h_{1,2} & 0 & 0 & {}_0h_{2,2} & \cdots & {}_0h_{N,2} \\ {}_0h_{1,3} & 0 & 0 & {}_0h_{2,3} & \cdots & {}_0h_{N,3} \end{bmatrix}
$$

4. *Second Piola-Kirchhoff stress matrix and vector*

$$
{}_0^t\mathbf{S} = \begin{bmatrix} {}_0^t\tilde{\mathbf{S}} & \bar{\mathbf{0}} & \bar{\mathbf{0}} \\ \bar{\mathbf{0}} & {}_0^t\tilde{\mathbf{S}} & \bar{\mathbf{0}} \\ \bar{\mathbf{0}} & \bar{\mathbf{0}} & {}_0^t\tilde{\mathbf{S}} \end{bmatrix}; \qquad \bar{\mathbf{0}} = \begin{bmatrix} 0 & 0 & 0 \\ 0 & 0 & 0 \\ 0 & 0 & 0 \end{bmatrix}
$$

$$
{}_0^t\hat{\mathbf{S}}^T = \begin{bmatrix} {}_0^tS_{11} & {}_0^tS_{22} & {}_0^tS_{33} & {}_0^tS_{12} & {}_0^tS_{23} & {}_0^tS_{31} \end{bmatrix}
$$

where

$$
{}_0^t\tilde{\mathbf{S}} = \begin{bmatrix} {}_0^tS_{11} & {}_0^tS_{12} & {}_0^tS_{13} \\ {}_0^tS_{21} & {}_0^tS_{22} & {}_0^tS_{23} \\ {}_0^tS_{31} & {}_0^tS_{32} & {}_0^tS_{33} \end{bmatrix}
$$

B. *Updated Lagrangian formulation*

1. *Incremental strains*

$$
{}_t\epsilon_{ij} = \tfrac{1}{2}({}_tu_{i,j} + {}_tu_{j,i}) + \tfrac{1}{2}({}_tu_{k,i}\,{}_tu_{k,j}) \qquad i = 1, 2, 3;\ j = 1, 2, 3;\ k = 1, 2, 3
$$

where ${}_tu_{i,j} = \dfrac{\partial u_i}{\partial {}^tx_j}$

2. *Linear strain-displacement transformation matrix*

Using ${}_t\mathbf{e} = {}_t^t\mathbf{B}_L\hat{\mathbf{u}}$

where ${}_t\mathbf{e}^T = \begin{bmatrix} {}_te_{11} & {}_te_{22} & {}_te_{33} & 2{}_te_{12} & 2{}_te_{23} & 2{}_te_{31} \end{bmatrix}$

$$
\hat{\mathbf{u}}^T = \begin{bmatrix} u & u_2^1 & u_3^1 & u_1^2 & u_2^2 & u_3^2 & \cdots & u_1^N & u_2^N & u_3^N \end{bmatrix}
$$

$$
{}_t^t\mathbf{B}_L = \begin{bmatrix}
{}_th_{1,1} & 0 & 0 & {}_th_{2,1} & \cdots & 0 \\
0 & {}_th_{1,2} & 0 & 0 & \cdots & 0 \\
0 & 0 & {}_th_{1,3} & 0 & \cdots & {}_th_{N,3} \\
{}_th_{1,2} & {}_th_{1,1} & 0 & {}_th_{2,2} & \cdots & 0 \\
0 & {}_th_{1,3} & {}_th_{1,2} & 0 & \cdots & {}_th_{N,2} \\
{}_th_{1,3} & 0 & {}_th_{1,1} & {}_th_{2,3} & \cdots & {}_th_{N,1}
\end{bmatrix}
$$

where ${}_th_{k,j} = \dfrac{\partial h_k}{\partial {}^tx_j}$; $\qquad u_j^k = {}^{t+\Delta t}u_j^k - {}^tu_j^k$; $\qquad N$ = number of nodes

3. *Nonlinear strain-displacement transformation matrix*

$$
{}_t^t\mathbf{B}_{NL} = \begin{bmatrix} {}_t^t\tilde{\mathbf{B}}_{NL} & \tilde{\mathbf{0}} & \tilde{\mathbf{0}} \\ \tilde{\mathbf{0}} & {}_t^t\tilde{\mathbf{B}}_{NL} & \tilde{\mathbf{0}} \\ \tilde{\mathbf{0}} & \tilde{\mathbf{0}} & {}_t^t\tilde{\mathbf{B}}_{NL} \end{bmatrix}; \qquad \tilde{\mathbf{0}} = \begin{bmatrix} 0 \\ 0 \\ 0 \end{bmatrix}
$$

TABLE 6.6 (*cont.*)

where $${}_t^{}\tilde{\mathbf{B}}_{NL} = \begin{bmatrix} {}_th_{1,1} & 0 & 0 & {}_th_{2,1} & \cdots & {}_th_{N,1} \\ {}_th_{1,2} & 0 & 0 & {}_th_{2,2} & \cdots & {}_th_{N,2} \\ {}_th_{1,3} & 0 & 0 & {}_th_{2,3} & \cdots & {}_th_{N,3} \end{bmatrix}$$

4. *Cauchy stress matrix and stress vector*

$${}_t\boldsymbol{\tau} = \begin{bmatrix} {}_t\tilde{\boldsymbol{\tau}} & \bar{\mathbf{0}} & \bar{\mathbf{0}} \\ \bar{\mathbf{0}} & {}_t\tilde{\boldsymbol{\tau}} & \bar{\mathbf{0}} \\ \bar{\mathbf{0}} & \bar{\mathbf{0}} & {}_t\tilde{\boldsymbol{\tau}} \end{bmatrix}; \qquad {}_t\hat{\boldsymbol{\tau}} = \begin{bmatrix} {}_t\tau_{11} \\ {}_t\tau_{22} \\ {}_t\tau_{33} \\ {}_t\tau_{12} \\ {}_t\tau_{23} \\ {}_t\tau_{31} \end{bmatrix} \qquad \bar{\mathbf{0}} = \begin{bmatrix} 0 & 0 & 0 \\ 0 & 0 & 0 \\ 0 & 0 & 0 \end{bmatrix}$$

where $${}_t\tilde{\boldsymbol{\tau}} = \begin{bmatrix} {}_t\tau_{11} & {}_t\tau_{12} & {}_t\tau_{13} \\ {}_t\tau_{21} & {}_t\tau_{22} & {}_t\tau_{23} \\ {}_t\tau_{31} & {}_t\tau_{32} & {}_t\tau_{33} \end{bmatrix}$$

6.3.6 Exercises

6.31. Consider the problem shown and evaluate the following quantities in terms of the given data: ${}_0e_{ij}$, ${}_0\eta_{ij}$, ${}_0^t u_{k,i}$, ${}_0u_{k,j}$, ${}_0^t x_{i,k}$.

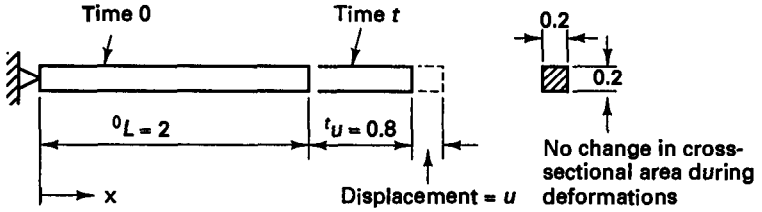

6.32. Consider the truss element shown. The truss has a cross-sectional area A and a Young's modulus E. We assume small strain conditions, i.e., $\Delta/{}^0L \ll 1$.

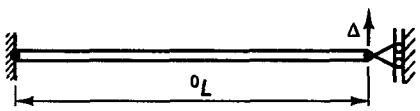

(a) Evaluate the total stiffness matrix as a function of Δ and plot the linear strain stiffness matrix element ${}_0^t\mathbf{K}_L$ and nonlinear strain stiffness matrix element ${}_0^t\mathbf{K}_{NL}$ as a function of Δ.

(b) Let R be the external load applied to obtain the displacement Δ. Plot the force R as a function of Δ.

6.33. Consider the snap-action toggle shown in its initial configuration.
Assume small strain conditions and that each element has a cross-sectional area A and Young's modulus E.

(a) For each element, calculate the linear and nonlinear strain stiffness matrices ${}^{t}_{0}\mathbf{K}_L$ and ${}^{t}_{0}\mathbf{K}_{NL}$ and the force vector ${}^{t}_{0}\mathbf{F}$.

(b) Calculate the linear and nonlinear strain stiffness matrices ${}^{t}_{0}\mathbf{K}_L$ and ${}^{t}_{0}\mathbf{K}_{NL}$ and the force vector ${}^{t}_{0}\mathbf{F}$ of the complete toggle.

Eliminate prescribed degrees of freedom.

(c) Using your results from part (b), establish the force-deflection curve P versus Δ.

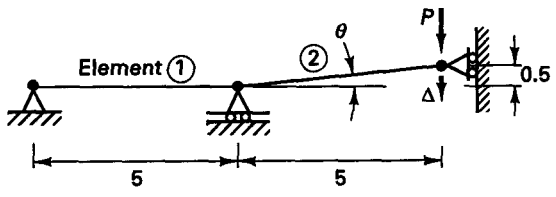

Initial stress-free configuration

6.34. Consider the three-element truss structure shown. Derive the tangent stiffness matrix ${}^{t}_{0}\mathbf{K}$ and force vector ${}^{t}_{0}\mathbf{F}$ corresponding to the configuration at time t allowing for large displacements, large rotations, and large strains. Assume that the constitutive relationship is ${}^{t}_{0}S_{11} = C\,{}^{t}_{0}\epsilon_{11}$, with C given as some function of the strain.

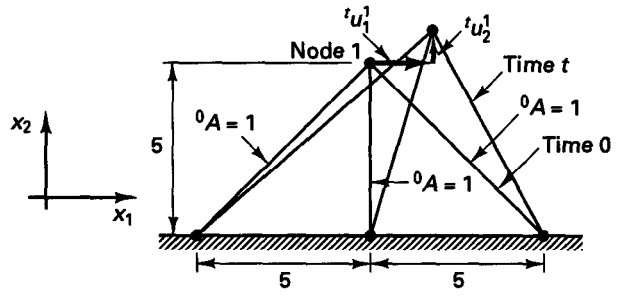

6.35. Consider the evaluation of the stiffness matrix of the four-node element shown when calculated with the information given in Table 6.5. Let the two-dimensional element be loaded with a deformation-dependent pressure between nodes 1 and 2. Establish the terms that should be added to the stiffness matrix if the effect of the pressure is included in the linearization to obtain the exact tangent stiffness matrix. Consider plane stress, plane strain, and axisymmetric conditions.

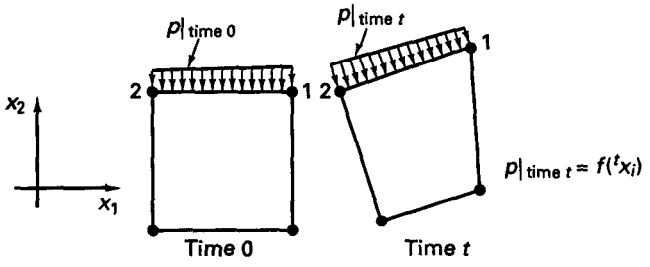

6.36. The initial configuration and configuration at time t of a four-node plane strain element are as shown. The material law is linear, ${}_0^tS_{ij} = {}_0^tC_{ijrs}\,{}_0^t\epsilon_{rs}$, with $E = 20{,}000$ N/m^2 and $\nu = 0.3$.

(a) Calculate the nodal point forces required to hold the element in equilibrium at time t. Use an appropriate finite element formulation.

(b) If the element now rotates rigidly from time t to time $t + \Delta t$ by an angle of 90 degrees counterclockwise, calculate the new nodal point forces corresponding to the configuration at time $t + \Delta t$.

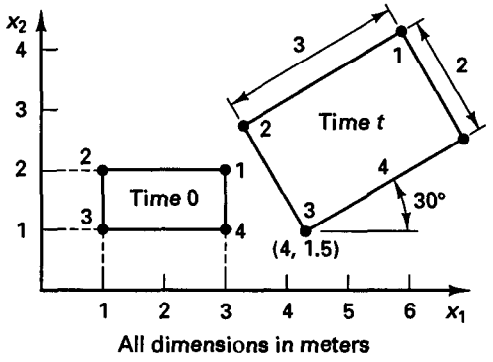

6.37. During a TL analysis, we find that a plane strain element is deformed as shown.

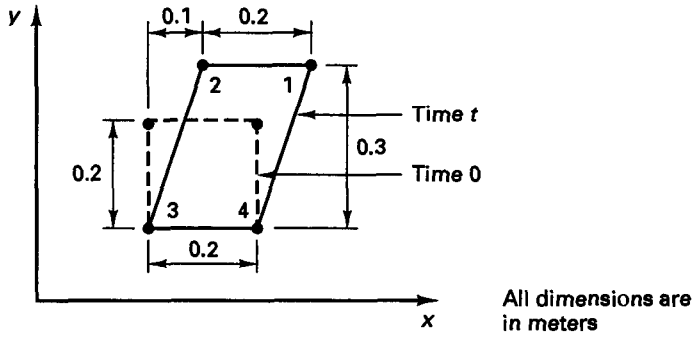

The stress state, not including ${}^t\tau_{zz}$, is

$${}^t\boldsymbol{\tau} = \begin{bmatrix} 5.849 \times 10^7 & 6.971 \times 10^7 \\ 6.971 \times 10^7 & 1.514 \times 10^8 \end{bmatrix} \text{Pa}$$

The Poisson's ratio $\nu = 0.3$ and the tangent Young's modulus is E. Compute ${}_0^tK_{11}$.

6.38. The two-dimensional four-node isoparametric finite element shown is used in an axisymmetric analysis. Evaluate the last row in the ${}_0\mathbf{B}_L$, ${}_0\mathbf{B}_{NL}$ and ${}_t\mathbf{B}_L$, ${}_t\mathbf{B}_{NL}$ matrices at the material particle P corresponding to the TL and UL formulations. The last row in the strain-displacement matrices corresponds to the circumferential strain.

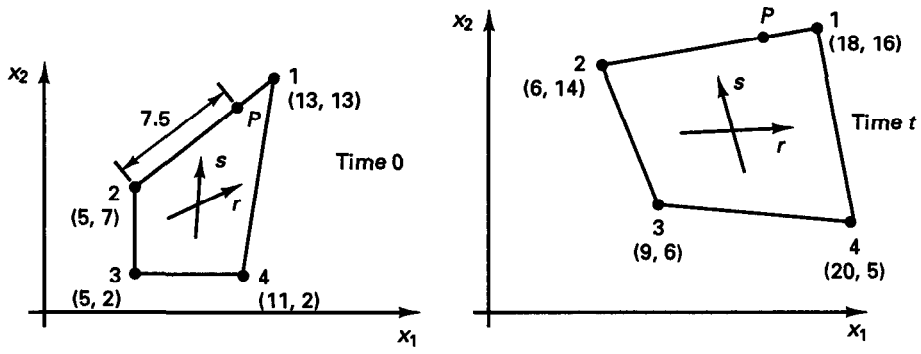

6.39. Consider the four-node plane stress element shown. Using the total Lagrangian formulation calculate the following.

(a) The element of the tangent stiffness matrix corresponding to the incremental displacement u_1^1; i.e., evaluate element (1, 1) of the matrix $({}_0\mathbf{K}_L + {}_0\mathbf{K}_{NL})$.

(b) The element of the force vector ${}_0\mathbf{F}$ corresponding to u_1^1; i.e., evaluate element (1) of ${}_0\mathbf{F}$, where ${}_0\mathbf{F}$ is the force vector corresponding to the current element stresses.

Assume that Young's modulus E and Poisson's ratio $\nu = 0.3$ relate the incremental second Piola-Kirchhoff stresses to the incremental Green-Lagrange strains and assume thickness h at time 0.

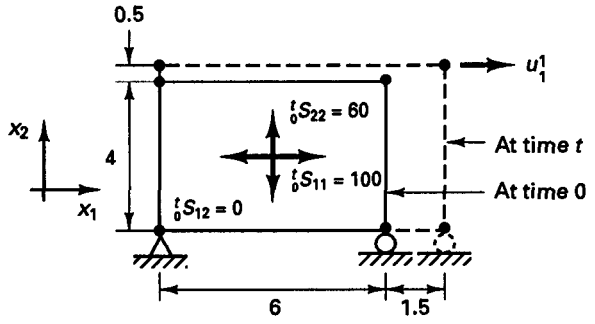

Constant stresses ${}_0^tS_{11}$ and ${}_0^tS_{22}$ and all other stresses are zero

6.40. A two-node finite element for modeling large strain torsion problems is to be constructed. The element has a circular cross section and is straight, and all cross sections are parallel to the x_1, x_2 plane as shown.

The kinematic assumption to be employed in the element is that each cross section rotates rigidly about its center. This is illustrated in the figure. Notice that the total rotation of fiber AA is fully described by ${}^t\theta_3$ and that the fiber rotation can be large. Also, note that the fiber AA does not stretch or shrink and that the center of the fiber (point C) remains fixed.

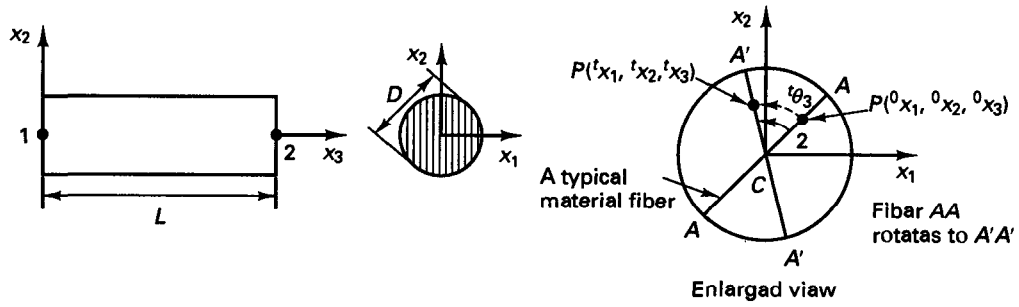

(a) Calculate the deformation gradient ${}_0^t\mathbf{X}$ in terms of the initial coordinates and ${}^t\theta_3$.
(b) Calculate the Green-Lagrange strain tensor ${}_0^t\boldsymbol{\epsilon}$. Clearly identify any terms that are associated with large strain effects.
(c) Calculate the mass density ratio ${}^t\rho/{}^0\rho$ in terms of the initial coordinates and ${}^t\theta_3$.
(d) Establish the strain-displacement matrix of the element.

6.4 DISPLACEMENT/PRESSURE FORMULATIONS FOR LARGE DEFORMATIONS

As discussed in Section 4.4.3, for (almost) incompressible analysis, a pure displacement-based procedure is, in general, not effective and instead, a displacement/pressure formulation is attractive. Materials in large deformations frequently behave as almost incompressible, and it is therefore important to extend the total and updated Lagrangian formulations of the previous sections to incompressible analysis. Typical applications are in the large strain analysis of rubberlike materials and in the large strain inelastic analysis of metals.

The formulations we present here are a direct and natural extension of the pure displacement-based large deformation formulations given in the previous section and of the pressure/displacement formulations that we discussed for linear analysis in Sections 4.4.3 and 5.3.5.

6.4.1 Total Lagrangian Formulation

We make the fundamental assumption that the material description used has an incremental potential $d_0^t\overline{W}$ such that

$$d_0^t\overline{W} = {}_0^t\bar{S}_{ij}\, d_0^t\epsilon_{ij} \tag{6.129}$$

and hence

$${}_0^t\bar{S}_{ij} = \frac{\partial_0^t\overline{W}}{\partial_0^t\epsilon_{ij}} \tag{6.130}$$

where the overbar in $d_0^t\overline{W}$ and on the second Piola-Kirchhoff stress (and other quantities in the following discussion) denotes that the quantity is computed only from the displacement fields. Since we shall interpolate the displacements and the pressure independently, the actual stress ${}_0^tS_{ij}$ will also contain the interpolated pressure.

We note that such incremental potential is given for elastic materials and also for inelastic materials provided the normality rule holds. A consequence of (6.129) is that the tensor

$$ {}_0\bar{C}_{ijrs} = \frac{\partial {}^t_0\bar{S}_{ij}}{\partial {}^t_0\epsilon_{rs}} = \frac{\partial^2 {}^t_0\overline{W}}{\partial {}^t_0\epsilon_{rs}\, \partial {}^t_0\epsilon_{ij}} \tag{6.131} $$

has the symmetry property $ {}_0\bar{C}_{ijrs} = {}_0\bar{C}_{rsij} $

and the pure displacement and displacement/pressure formulations produce symmetric coefficient matrices.

Using (6.130), the principle of virtual displacements at time t in total Lagrangian form with displacements as the only variables can be written as

$$ \begin{aligned} \int_{{}_0V} \frac{\partial {}^t_0\overline{W}}{\partial {}^t_0\epsilon_{ij}} \delta {}^t_0\epsilon_{ij}\, d^0V &= \int_{{}_0V} \delta {}^t_0\overline{W}\, d^0V \\ &= \delta\left(\int_{{}_0V} {}^t_0\overline{W}\, d^0V \right) = {}^t\mathcal{R} \end{aligned} \tag{6.132} $$

The linearization and finite element discretization of (6.132) was presented in Section 6.3. We now use (6.132) as the starting equation to develop the displacement/pressure formulation for large deformations.

The basic element interpolations that we shall use are

$$ {}^tu_i = \sum_{k=1}^{N} h_k\, {}^tu_i^k; \qquad {}^t\tilde{p} = \sum_{i=1}^{q} g_i\, {}^t\hat{p}_i \tag{6.133} $$

where the h_k are the displacement interpolation functions and the g_i are the pressure interpolation functions, with ${}^t\tilde{p}$ as the *total* element pressure at time t. Note that the interpolation of the pressure may correspond to the u/p or to the u/p-c formulation (see Section 5.3.5).

The key step in the construction of the displacement/pressure formulation is to properly modify the potential to include the effect of the interpolated pressure. For this purpose we add to the potential ${}^t_0\overline{W}$ a properly chosen potential ${}^t_0Q$, which is a function of the displacements and the separately interpolated pressure ${}^t\tilde{p}$ (see T. Sussman and K. J. Bathe [B]). The principle of virtual work is then given by

$$ \delta\left(\int_{{}_0V} {}^t_0W\, d^0V \right) = {}^t\mathcal{R} \tag{6.134} $$

where

$$ {}^t_0W = {}^t_0\overline{W} + {}^t_0Q \tag{6.135} $$

and we now consider the variation with respect to the interpolated displacements and the interpolated pressure.

The modified potential ${}^t_0W$ must fulfill the requirements that use of (6.134) gives ${}^t\tilde{p}$ as the actual solution for the pressure and also yields a physically reasonable constraint between the interpolated pressure and the pressure computed only from the displacements.

A potential that fulfills these requirements for the isotropic materials considered later is given by

$$ {}^t_0W = {}^t_0\overline{W} - \frac{1}{2\kappa}({}^t\bar{p} - {}^t\tilde{p})^2 \tag{6.136} $$

where κ is the constant bulk modulus of the material. Using (6.136), the governing finite element equations can be derived with the approach for linearization presented in Section 6.3.1. Hence, we obtain for a typical element,

$$\begin{pmatrix} {}^t\mathbf{KUU} & {}^t\mathbf{KUP} \\ {}^t\mathbf{KPU} & {}^t\mathbf{KPP} \end{pmatrix} \begin{pmatrix} \hat{\mathbf{u}} \\ \hat{\mathbf{p}} \end{pmatrix} = \begin{pmatrix} {}^{t+\Delta t}\mathbf{R} \\ \mathbf{0} \end{pmatrix} - \begin{pmatrix} {}^t\mathbf{FU} \\ {}^t\mathbf{FP} \end{pmatrix} \tag{6.137}$$

where $\hat{\mathbf{u}}$ and $\hat{\mathbf{p}}$ are vectors of the increments in the nodal point displacements ${}^t\hat{u}_i$ and nodal point or element internal pressure variables ${}^t\hat{p}_i$ [note that here ${}^t\hat{u}_i$ is any one of the components ${}^tu_i^k$ in (6.122), (6.128), and (6.133)]. The vectors ${}^t\mathbf{FU}$ and ${}^t\mathbf{FP}$ contain the entries

$$\begin{aligned} {}^tFU_i &= \frac{\partial}{\partial {}^t\hat{u}_i}\left(\int_{{}^0V} {}^t_0W \, d^0V\right) \\ {}^tFP_i &= \frac{\partial}{\partial {}^t\hat{p}_i}\left(\int_{{}^0V} {}^t_0W \, d^0V\right) \end{aligned} \tag{6.138}$$

and the matrices ${}^t\mathbf{KUU}$, ${}^t\mathbf{KUP}$, ${}^t\mathbf{KPU}$, and ${}^t\mathbf{KPP}$ contain the elements

$$\begin{aligned} {}^tKUU_{ij} &= \frac{\partial {}^tFU_i}{\partial {}^t\hat{u}_j} \\ {}^tKUP_{ij} &= \frac{\partial {}^tFU_i}{\partial {}^t\hat{p}_j} = \frac{\partial {}^tFP_j}{\partial {}^t\hat{u}_i} = {}^tKPU_{ji} \\ {}^tKPP_{ij} &= \frac{\partial {}^tFP_i}{\partial {}^t\hat{p}_j} \end{aligned} \tag{6.139}$$

Using chain differentiation, we obtain

$$\begin{aligned} {}^tFU_i &= \int_{{}^0V} {}^t_0S_{kl} \frac{\partial {}^t_0\epsilon_{kl}}{\partial {}^t\hat{u}_i} \, d^0V \\ {}^tFP_i &= \int_{{}^0V} \frac{1}{\kappa}({}^t\bar{p} - {}^t\tilde{p}) \frac{\partial {}^t\tilde{p}}{\partial {}^t\hat{p}_i} \, d^0V \\ {}^tKUU_{ij} &= \int_{{}^0V} {}_0CUU_{klrs} \frac{\partial {}^t_0\epsilon_{kl}}{\partial {}^t\hat{u}_i} \frac{\partial {}^t_0\epsilon_{rs}}{\partial {}^t\hat{u}_j} \, d^0V + \int_{{}^0V} {}^t_0S_{kl} \frac{\partial^2 {}^t_0\epsilon_{kl}}{\partial {}^t\hat{u}_i \, \partial {}^t\hat{u}_j} \, d^0V \\ {}^tKUP_{ij} &= \int_{{}^0V} {}_0CUP_{kl} \frac{\partial {}^t_0\epsilon_{kl}}{\partial {}^t\hat{u}_i} \frac{\partial {}^t\tilde{p}}{\partial {}^t\hat{p}_j} \, d^0V \\ {}^tKPP_{ij} &= \int_{{}^0V} -\frac{1}{\kappa} \frac{\partial {}^t\tilde{p}}{\partial {}^t\hat{p}_i} \frac{\partial {}^t\tilde{p}}{\partial {}^t\hat{p}_j} \, d^0V \end{aligned} \tag{6.140}$$

where

$$\begin{aligned} {}^t_0S_{kl} &= {}^t_0\bar{S}_{kl} - \frac{1}{\kappa}({}^t\bar{p} - {}^t\tilde{p}) \frac{\partial {}^t\bar{p}}{\partial {}^t_0\epsilon_{kl}} \\ {}_0CUU_{klrs} &= {}_0\bar{C}_{klrs} - \frac{1}{\kappa} \frac{\partial {}^t\bar{p}}{\partial {}^t_0\epsilon_{kl}} \frac{\partial {}^t\bar{p}}{\partial {}^t_0\epsilon_{rs}} - \frac{1}{\kappa}({}^t\bar{p} - {}^t\tilde{p}) \frac{\partial^2 {}^t\bar{p}}{\partial {}^t_0\epsilon_{kl} \, \partial {}^t_0\epsilon_{rs}} \\ {}_0CUP_{kl} &= \frac{1}{\kappa} \frac{\partial {}^t\bar{p}}{\partial {}^t_0\epsilon_{kl}} \end{aligned} \tag{6.141}$$

Note that in (6.141) we have

$$
\begin{aligned}
{}^t_0\bar{S}_{kl} &= \frac{1}{2}\left(\frac{\partial {}^t_0\overline{W}}{\partial {}^t_0\epsilon_{kl}} + \frac{\partial {}^t_0\overline{W}}{\partial {}^t_0\epsilon_{lk}}\right) \\
{}^t_0\bar{C}_{klrs} &= \frac{1}{2}\left(\frac{\partial {}^t_0\bar{S}_{kl}}{\partial {}^t_0\epsilon_{rs}} + \frac{\partial {}^t_0\bar{S}_{kl}}{\partial {}^t_0\epsilon_{sr}}\right)
\end{aligned}
\tag{6.142}
$$

Furthermore, we note that with the interpolations of (6.133) we have

$$
\frac{\partial {}^t\tilde{p}}{\partial {}^t\hat{p}_i} = g_i \tag{6.143}
$$

and (see Exercise 6.42)

$$
\frac{\partial {}^t_0\epsilon_{kl}}{\partial {}^tu^L_n} = \frac{1}{2}({}^t_0x_{n,k}\,{}_0h_{L,l} + {}^t_0x_{n,l}\,{}_0h_{L,k}) \tag{6.144}
$$

$$
\frac{\partial^2 {}^t_0\epsilon_{kl}}{\partial {}^tu^L_n\,\partial {}^tu^M_m} = \frac{1}{2}({}_0h_{L,k}\,{}_0h_{M,l} + {}_0h_{L,l}\,{}_0h_{M,k})\delta_{nm} \tag{6.145}
$$

where a typical nodal point displacement is denoted as ${}^tu^L_n$ (with the appropriate indices n and L). These strain derivatives give the same contributions as do the quantities ${}_0e_{ij}$ and ${}_0\eta_{ij}$ used in Table 6.2.

A study of the above relations shows that if the pressure interpolation is not included, the equations reduce to the total Lagrangian formulation already presented in Section 6.2.3 (see Exercise 6.43).

The displacement/pressure formulation is effective for the analysis of rubberlike materials in large strains. In this case, the Mooney-Rivlin or Ogden material laws may be used, for which the strain energy density per unit volume ${}^t_0\overline{W}$ is explicity defined (see Section 6.6.2).

Let us demonstrate that this formulation, when used in small strain elastic analysis, reduces to the formulation already discussed in Section 5.3.5.

EXAMPLE 6.19: Show how the displacement/pressure formulation discussed above reduces to the formulation presented in Section 5.3.5 when isotropic linear elasticity with small displacements and small strains is considered.

Considering the general equations (6.137) to (6.145), we note that in this case:

The second Piola-Kirchhoff stress ${}^t_0S_{kl}$ reduces to the engineering stress measure ${}^t\sigma_{kl}$.

The Green-Lagrange strains ${}^t_0\epsilon_{kl}$ reduce to the infinitesimally small engineering strains ${}^te_{kl}$.

The nonlinear strain stiffness matrix in (6.140) is neglected.

The integration is over the volume V (which is equal to ${}^0V$) and the subscript 0 on the constitutive tensors is also not needed.

In this case we have

$$
\bar{C}_{klrs} = \lambda\delta_{kl}\delta_{rs} + \mu(\delta_{kr}\delta_{ls} + \delta_{ks}\delta_{lr})
$$

where λ and μ are the Lamé constants,

$$
\lambda = \frac{E\nu}{(1+\nu)(1-2\nu)}; \qquad \mu = \frac{E}{2(1+\nu)}
$$

with E and ν the Young's modulus and the Poisson's ratio. The bulk modulus κ is

$$\kappa = \frac{E}{3(1-2\nu)}$$

We have

$$^t\bar{p} = -\kappa\, {}^te_{mm}$$

$$\frac{\partial {}^t\bar{p}}{\partial {}^te_{ki}} = -\kappa\, \delta_{ki}$$

$$\frac{\partial^2 {}^t\bar{p}}{\partial {}^te_{ki}\, \partial {}^te_{rs}} = 0$$

so that

$$^t\sigma_{ki} = {}^tS_{ki} - {}^t\bar{p}\, \delta_{ki}$$

$$CUU_{kirs} = \bar{C}_{kirs} - \kappa\, \delta_{ki}\, \delta_{rs}$$

$$CUP_{ki} = -\delta_{ki}$$

On substituting these quantities into (6.137), we note that the general formulation reduces, in this case, to the formulation already presented in Sections 4.4.3 and 5.3.5.

6.4.2 Updated Lagrangian Formulation

As we discussed in Section 6.2.3, the updated Lagrangian formulation is conceptually identical to the total Lagrangian formulation but uses the configuration at time t as reference configuration. In this case ${}^t_tS_{ij} = {}^t\tau_{ij}$ and $d{}^t_te_{ij} = d_te_{ij}$, with the subscript T denoting the configuration[8] that is fixed and used as reference, and

$$d_te_{ij} = \frac{1}{2}\left(\frac{\partial du_i}{\partial {}^tx_j} + \frac{\partial du_j}{\partial {}^tx_i}\right) \tag{6.146}$$

Following the presentation of the previous section, we thus obtain

$$d{}^t_t\overline{W} = {}^t\bar{\tau}_{ij}\, d_te_{ij} \tag{6.147}$$

and note that

$${}^t_t\overline{W}\, d^TV = {}^t_0\overline{W}\, d^0V \tag{6.148}$$

If in addition we use

$${}^t_tQ\, d^TV = {}^t_0Q\, d^0V; \qquad \frac{d^TV}{d^0V} = \det {}^T_0\mathbf{X} \tag{6.149}$$

we can write the principle of virtual work (6.134) as

$$\delta \int_{^tV} ({}^t_t\overline{W} + {}^t_tQ)\, d^TV = {}^t\mathcal{R} \tag{6.150}$$

Note that if we use the modification to the total potential ${}^t_0\overline{W}$ in the previous section,

$${}^t_0Q = -\frac{1}{2\kappa}({}^t\bar{p} - {}^t\tilde{p})^2 \tag{6.151}$$

[8] We use the capital letter T to denote the reference configuration considered fixed at time t, so that when differentiations are performed, it is realized that no variation of this configuration is allowed.

then
$$ {}^{t}_{t}Q = -\frac{1}{2\kappa^*}({}^{t}\bar{p} - {}^{t}\tilde{p})^2 \tag{6.152} $$

with
$$ \kappa^* = \kappa \det {}^{t}_{0}\mathbf{X} \tag{6.153} $$

The governing finite element equations can now be derived by chain differentiation, and provided the same physical material descriptions are used, the same finite element equations are obtained as in the total Lagrangian formulation. The details of the derivation are given by T. Sussman and K. J. Bathe [B].

6.4.3 Exercises

6.41. Show that using (6.136), the actual solution for the pressure is given by the independently interpolated value ${}^{t}\tilde{p}$.

6.42. Let ${}^{t}u_n = \Sigma_L h_L {}^{t}u_n^L$ and prove that (6.144) and (6.145) hold. Here you may want to recall that

$$ \frac{\partial(A_{M,i}\,{}^{t}u_i^M)}{\partial {}^{t}u_k^L} = A_{M,i}\delta_{ik}\delta_{ML} = A_{L,k} $$

where δ_{ik} is the Kronecker delta.

6.43. Show explicitly that the pressure/displacement mixed formulation reduces to the pure displacement-based formulation if the pressure interpolation is not included.

6.44. Prove the relations in (6.140) and (6.141).

6.45. Consider the 4/1 plane strain element shown. Develop in detail all expressions for the calculation of the matrices in (6.137) assuming large strain analysis but do not perform any integrations. (*Hint:* See Example 4.32.)

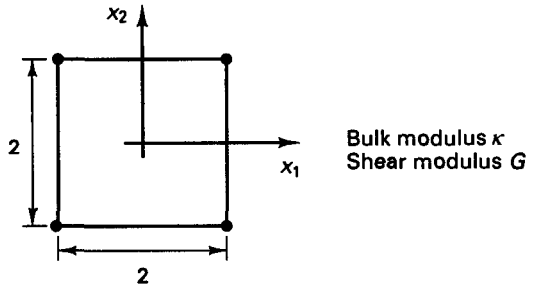

6.46. Consider the 4/1 element in Exercise 6.45 and develop in detail all expressions for the calculation of the matrices in (6.137) but corresponding to the updated Lagrangian formulation. However, do not perform any integrations.

6.47. You want to obtain some insight into whether the computer program you use employs the tangent stiffness matrix in plane strain analysis. Consider a single nine-node element in the deformed state shown. Assuming that the calculation of the stresses and the force vector ${}^{t}\mathbf{F}$ is correct, design a test to determine whether the stiffness matrix calculation for node 1 is probably also correct. For this analysis case the u/p formulation (9/3 element) would be efficient. (*Hint:* Note that ${}^{t}\mathbf{K} = \partial {}^{t}\mathbf{F}/\partial {}^{t}\mathbf{U}$.)

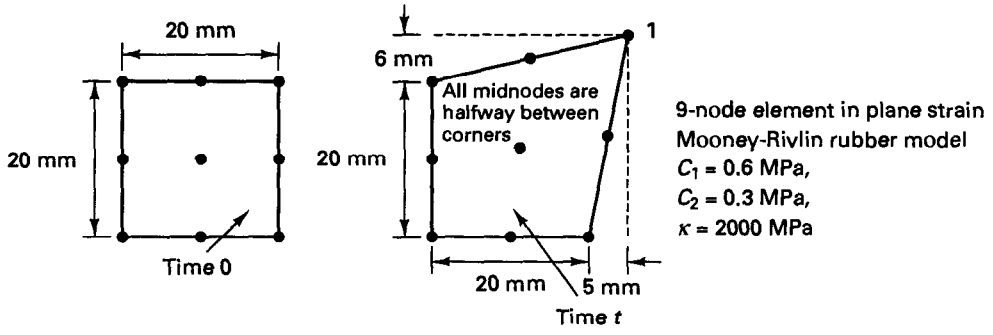

6.48. Perform the numerical experiment in Exercise 6.47 for the case of the axisymmetric element shown.

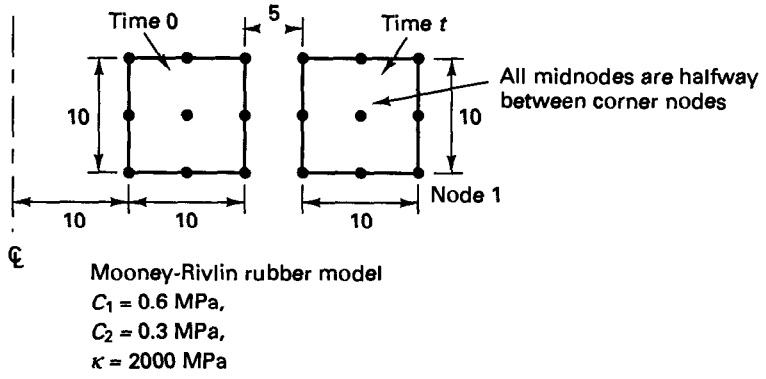

6.49. Use a computer program to analyze the thick disk shown. The applied pressure increases uniformly, and the analysis is required up to a maximum displacement of 3 in.

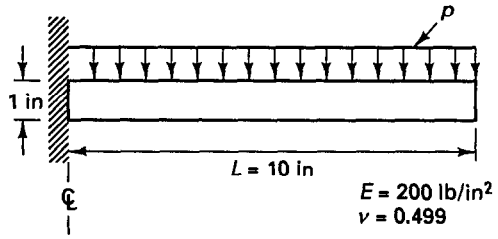

6.50. Use a computer program to analyze the plate with a hole shown on the following page. The plate is stretched by imposing a uniform horizontal displacement at the right end.

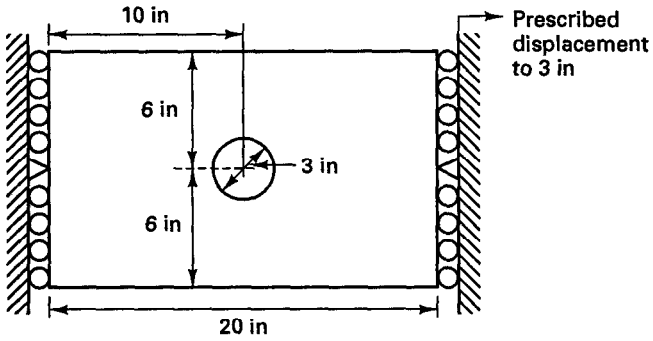

6.5 STRUCTURAL ELEMENTS

A large number of beam, plate, and shell elements have been proposed for nonlinear analysis (see, for example, A. K. Noor [A]). Our objective here is not to survey the various formulations proposed in the literature but to present briefly those elements that we already have discussed for linear analysis in Section 5.4. These beam, plate, and shell elements have evolved from the isoparametric formulation and are particularly attractive because of the consistent formulation, the generality of the elements, and the computational efficiency.

In the following discussion, we first consider beam and axisymmetric shell elements and then discuss plate and general shell elements.

6.5.1 Beam and Axisymmetric Shell Elements

In this section we consider the one-dimensional bending elements that we discussed in Section 5.4.1 for linear analysis; there we considered the plane stress and plane strain planar beam elements, an axisymmetric shell element, and a general three-dimensional beam element. We observed that the planar beam and the axisymmetric shell element formulations are actually cases easily derivable from the general three-dimensional beam element formulation. Hence, we consider here the calculation of the element matrices pertaining to the large displacement–large rotation behavior of a general beam of rectangular cross-sectional area. The relations given can be directly used to also obtain the matrices corresponding to the planar beam elements and axisymmetric shell elements (see Examples 6.20 and 6.21).

Figure 6.5 shows a typical element in the original configuration and the position at time t. To describe the element behavior we use the same assumptions that we employed in linear analysis (namely, that plane sections initially normal to the neutral axis remain plane and that only the longitudinal stress and two shear stresses are nonzero), but the displacements and rotations of the element can now be arbitrarily large. The element strains are still

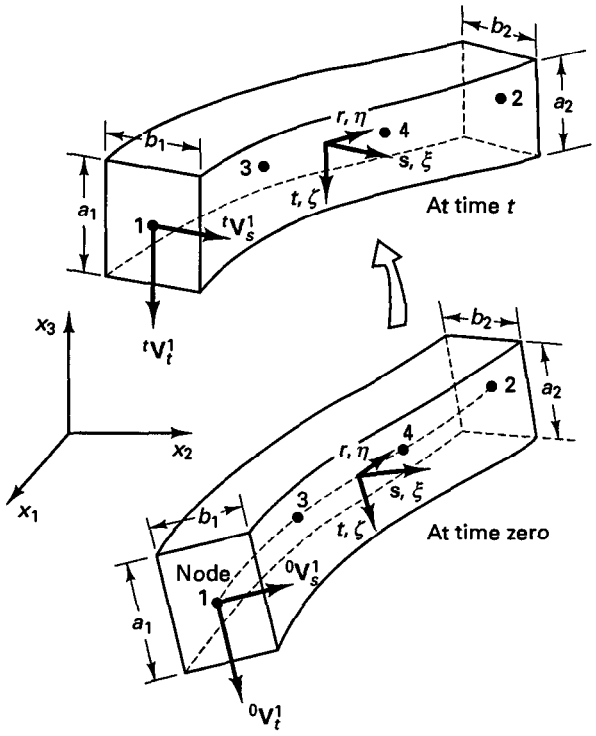

Figure 6.5 Beam element undergoing large displacements and rotations

assumed to be small, which means that the cross-sectional area does not change.[9] This is an appropriate assumption for most geometrically nonlinear analyses of beam-type structures.

Using the general continuum mechanics equations for nonlinear analysis presented in Section 6.2, the beam element matrices for nonlinear analysis are evaluated by a direct extension of the formulation given in Section 5.4.1. The calculations are performed as in the evaluation of the matrices of the finite elements with displacement degrees of freedom only (see Sections 5.4.1 and 6.3).

With the same notation as in Section 5.4.1, the geometry of the beam element at time t is given by

$$^tx_i = \sum_{k=1}^{q} h_k\, {}^tx_i^k + \frac{t}{2}\sum_{k=1}^{q} a_k h_k\, {}^tV_{ti}^k + \frac{s}{2}\sum_{k=1}^{q} b_k h_k\, {}^tV_{si}^k \qquad i = 1, 2, 3 \tag{6.154}$$

where the coordinates of a typical point in the beam are $^tx_1$, $^tx_2$, $^tx_3$. Considering the

[9] To have the element formulation applicable to large strains, the changes in thickness and width varying along the length of the element would need to be calculated. These changes depend on the stress-strain material relationship of the element.

configurations at times 0, t, and $t + \Delta t$, the displacement components are

$$ {}^{t}u_i = {}^{t}x_i - {}^{0}x_i \tag{6.155} $$

and

$$ u_i = {}^{t+\Delta t}x_i - {}^{t}x_i \tag{6.156} $$

Substituting (6.154) into (6.155) and (6.156), we obtain expressions for the displacement components in terms of the nodal point displacements and changes in the direction cosines of the nodal point director vectors; i.e.,

$$ {}^{t}u_i = \sum_{k=1}^{q} h_k\, {}^{t}u_i^k + \frac{t}{2}\sum_{k=1}^{q} a_k h_k({}^{t}V_{ti}^k - {}^{0}V_{ti}^k) + \frac{s}{2}\sum_{k=1}^{q} b_k h_k({}^{t}V_{si}^k - {}^{0}V_{si}^k) \tag{6.157} $$

and

$$ u_i = \sum_{k=1}^{q} h_k u_i^k + \frac{t}{2}\sum_{k=1}^{q} a_k h_k V_{ti}^k + \frac{s}{2}\sum_{k=1}^{q} b_k h_k V_{si}^k \tag{6.158} $$

where

$$ V_{ti}^k = {}^{t+\Delta t}V_{ti}^k - {}^{t}V_{ti}^k \tag{6.159} $$

$$ V_{si}^k = {}^{t+\Delta t}V_{si}^k - {}^{t}V_{si}^k \tag{6.160} $$

The relation in (6.157) is directly employed to evaluate the total displacements and total strains (hence also total stresses) for both the UL and TL formulations and holds for any magnitude of displacement components.

We use the relation in (6.158) in the linearization of the principle of virtual work and need to express the components V_{ti}^k and V_{si}^k of the vectors $\mathbf{V}_t^k$, $\mathbf{V}_s^k$ in terms of nodal rotational degrees of freedom. Depending on the size of the incremental step, the actual rotation corresponding to the vectors $\mathbf{V}_t^k$ and $\mathbf{V}_s^k$ may be a large rotation, and therefore cannot be represented by vector component rotations about the Cartesian axes. However, we recall that our objective is to express the continuum linear and nonlinear strain increments in Tables 6.2 and 6.3 by finite element degrees of freedom and corresponding interpolations so as to achieve a full linearization of the principle of virtual work (see Section 6.3.1). For this purpose we define the vector of nodal rotational degrees of freedom $\boldsymbol{\theta}_k$ with components measured about the Cartesian axes and use the second-order approximations (see Exercise 6.56),

$$ \mathbf{V}_t^k = \boldsymbol{\theta}_k \times {}^{t}\mathbf{V}_t^k + \frac{1}{2}\boldsymbol{\theta}_k \times (\boldsymbol{\theta}_k \times {}^{t}\mathbf{V}_t^k) \tag{6.161} $$

$$ \mathbf{V}_s^k = \boldsymbol{\theta}_k \times {}^{t}\mathbf{V}_s^k + \frac{1}{2}\boldsymbol{\theta}_k \times (\boldsymbol{\theta}_k \times {}^{t}\mathbf{V}_s^k) \tag{6.162} $$

The only purpose of using $\boldsymbol{\theta}_k$ is to evaluate (approximations to) the new director vectors, and $\boldsymbol{\theta}_k$ is discarded thereafter.

Substituting from (6.161) and (6.162) into (6.158) we obtain the expression for u_i to evaluate the continuum linear and nonlinear incremental strain tensors in Tables 6.2 and 6.3. Since the relations in (6.161) and (6.162) involve quadratic expressions, we neglect all higher-order terms in the solution variables to obtain the fully linearized form of the principle of virtual work equation—linearized about the state at time t with respect to the solution variables (the nodal point displacements and rotations). With this process, the exact tangent stiffness matrix is arrived at and employed in the incremental finite element

solution. However, we should note that the continuum *linear* strain increments in Tables 6.2 and 6.3 now include *quadratic* terms in rotations, and hence the right-hand-side terms

$$\int_{{}^0V} {}_0^t S_{ij}\, \delta_0 e_{ij}\, d^0V \qquad \text{and} \qquad \int_{{}^tV} {}^t\tau_{ij}\, \delta_t e_{ij}\, d^tV$$

in (6.74) and (6.75) contribute, in this case, to the tangent stiffness matrices of the TL and UL formulations. The same incremental equations are of course also obtained if we use the procedure in Section 6.3.1 to develop these equations.

A kinematic assumption in this interpolation is that "plane sections remain plane," and hence warping is not included. However, warping displacement behavior can be added to the assumed deformations as discussed in Section 5.4.1.

The linear and nonlinear strain displacement matrices of the beam element corresponding to the UL formulation can now be evaluated using the approach employed in linear analysis. That is, using (6.158), the strain components are calculated corresponding to the global axes and are then transformed to obtain the strain components corresponding to the local beam axes, η, ξ, ζ. Since the element stiffness matrix is evaluated using numerical integration, the transformation from global to local strain components must be performed during the numerical integration at each integration point.

Considering the TL formulation, we recognize that, first, derivatives analogous to those used in the UL formulation are required, but the derivatives are taken with respect to the coordinates at time 0. In addition, however, in order to include the initial displacement effect, the derivatives of the displacements at time t with respect to the original coordinates are needed. These derivatives are evaluated using (6.157).

The above interpolations lead to the displacement-based finite element formulation which, as discussed in Section 5.4.1, yields a very slowly converging discretization. In order to obtain an effective scheme a mixed interpolation should be used which, for the beam formulation, is equivalent to employing an appropriate Gauss integration order for the r-direction integration: namely one-point integration for the two-node element, two-point integration for the three-node element, and three-point integration for the four-node element.

The finite element equations thus arrived at are

$${}^t\mathbf{K} \begin{bmatrix} \vdots \\ \mathbf{u}_k \\ \boldsymbol{\theta}_k \\ \vdots \end{bmatrix} = {}^{t+\Delta t}\mathbf{R} - {}^t\mathbf{F} \tag{6.163}$$

Having solved (6.163) for $\mathbf{u}_k$ and $\boldsymbol{\theta}_k$, we obtain approximations for the nodal point displacements and director vectors at time $t + \Delta t$ using

$${}^{t+\Delta t}\mathbf{u}_k = {}^t\mathbf{u}_k + \mathbf{u}_k \tag{6.164}$$

and

$${}^{t+\Delta t}\mathbf{V}_t^k = {}^t\mathbf{V}_t^k + \int_{\boldsymbol{\theta}_k} d\boldsymbol{\theta}_k \times {}^\tau\mathbf{V}_t^k \tag{6.165}$$

$${}^{t+\Delta t}\mathbf{V}_s^k = {}^t\mathbf{V}_s^k + \int_{\boldsymbol{\theta}_k} d\boldsymbol{\theta}_k \times {}^\tau\mathbf{V}_s^k \tag{6.166}$$

The integrations in (6.165) and (6.166) can be performed in one step using an orthogonal matrix for finite rotations (see, for example, J. H. Argyris [B] and Exercise 6.55) or in a number of steps using a simple Euler forward method (see Section 9.6). Of course, $\boldsymbol{\theta}_k$ (and $\mathbf{u}_k$) are approximations to the actual required increments (because of the linearization of the principle of virtual work), but with the integrations in (6.165) and (6.166) we intend to arrive at a more accurate evaluation of the new director vectors than by simply substituting into (6.161) and (6.162).

The above presentation corresponds of course to the first iteration of the usual Newton-Raphson iterative solution process or to a typical iteration when the last calculated values of coordinates and director vectors are used.

It should be noted that this beam element formulation admits very large displacements and rotations and has an important advantage when compared with the formulation of a straight beam element based on Hermitian displacement interpolations: all individual displacement components are expressed using the same functions because the displacement expressions are derived from the geometry interpolation. Thus there is no directionality in the displacement interpolations, and the change in the geometry of the beam structure with increasing deformations is modeled more accurately than by using straight beam elements based on Hermitian functions, as for example presented by K. J. Bathe and S. Bolourchi [A].

We mentioned earlier that this general beam formulation can be used to derive the matrices pertaining to the formulations of planar beam elements for plane stress or plane strain conditions or axisymmetric shell elements. We demonstrate such derivations in the following examples.

EXAMPLE 6.20: Consider the two-node beam element shown in Fig. E6.20. Evaluate the coordinate and displacement interpolations and derivatives that are required for the calculation of the strain-displacement matrices of the UL and TL formulations.

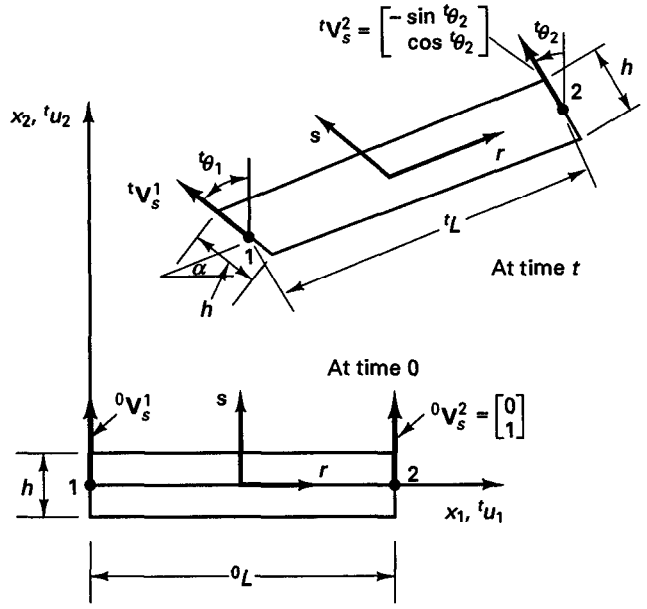

Figure E6.20 Two-node beam element in large displacements and rotations

Using the variables in Fig. E6.20, we have corresponding to (6.154),

$$
\begin{aligned}
{}^{t}x_1 &= \left(\frac{1-r}{2}\right){}^{t}x_1^1 + \left(\frac{1+r}{2}\right){}^{t}x_1^2 - \frac{sh}{2}\left(\frac{1-r}{2}\right)\sin{}^{t}\theta_1 - \frac{sh}{2}\left(\frac{1+r}{2}\right)\sin{}^{t}\theta_2 \\
{}^{t}x_2 &= \left(\frac{1-r}{2}\right){}^{t}x_2^1 + \left(\frac{1+r}{2}\right){}^{t}x_2^2 + \frac{sh}{2}\left(\frac{1-r}{2}\right)\cos{}^{t}\theta_1 + \frac{sh}{2}\left(\frac{1+r}{2}\right)\cos{}^{t}\theta_2 \\
{}^{0}x_1 &= \left(\frac{1+r}{2}\right){}^{0}L \\
{}^{0}x_2 &= \frac{sh}{2}
\end{aligned}
$$

Hence, the displacement components are at any point at time t,

$$
\begin{aligned}
{}^{t}u_1 &= \left(\frac{{}^{t}x_1^1 + {}^{t}x_1^2 - {}^{0}L}{2}\right) + \left(\frac{{}^{t}x_1^2 - {}^{t}x_1^1 - {}^{0}L}{2}\right)r - \frac{sh}{2}\left[\left(\frac{1-r}{2}\right)\sin{}^{t}\theta_1 + \left(\frac{1+r}{2}\right)\sin{}^{t}\theta_2\right] \\
{}^{t}u_2 &= \left(\frac{{}^{t}x_2^1 + {}^{t}x_2^2}{2}\right) + \left(\frac{{}^{t}x_2^2 - {}^{t}x_2^1}{2}\right)r + \frac{sh}{2}\left[\left(\frac{1-r}{2}\right)\cos{}^{t}\theta_1 + \left(\frac{1+r}{2}\right)\cos{}^{t}\theta_2 - 1\right]
\end{aligned}
$$

The incremental displacements are given by (6.158); hence,

$$
\begin{aligned}
u_1 = {} & \frac{1-r}{2}u_1^1 + \frac{1+r}{2}u_1^2 + \frac{sh}{2}\left(\frac{1-r}{2}\right)\left[(-\cos{}^{t}\theta_1)\theta_1 + \underline{\underline{\frac{1}{2}\sin{}^{t}\theta_1(\theta_1)^2}}\right] \\
& + \frac{sh}{2}\left(\frac{1+r}{2}\right)\left[(-\cos{}^{t}\theta_2)\theta_2 + \underline{\underline{\frac{1}{2}\sin{}^{t}\theta_2(\theta_2)^2}}\right] \qquad \text{(a)} \\
u_2 = {} & \frac{1-r}{2}u_2^1 + \frac{1+r}{2}u_2^2 + \frac{sh}{2}\left(\frac{1-r}{2}\right)\left[(-\sin{}^{t}\theta_1)\theta_1 - \underline{\underline{\frac{1}{2}\cos{}^{t}\theta_1(\theta_1)^2}}\right] \\
& + \frac{sh}{2}\left(\frac{1+r}{2}\right)\left[(-\sin{}^{t}\theta_2)\theta_2 - \underline{\underline{\frac{1}{2}\cos{}^{t}\theta_2(\theta_2)^2}}\right] \qquad \text{(b)}
\end{aligned}
$$

We note the quadratic terms in nodal rotations, which are underlined with a dashed line. Using (a) and (b) to evaluate the continuum incremental strain terms ${}_0e_{ij}$, ${}_te_{ij}$, ${}_0\eta_{ij}$, and ${}_t\eta_{ij}$ in Tables 6.2 and 6.3, we recognize that the fully linearized finite element equations are obtained by including the underlined terms in the evaluation of $\int_{{}_0V} {}_0^t S_{ij}\,\delta_0 e_{ij}\,d^0V$ and $\int_{{}_tV} {}^t\tau_{ij}\,\delta_t e_{ij}\,d^tV$. These terms add for the structural elements a contribution to the nonlinear strain stiffness matrices. However, these quadratic terms in rotation do not contribute in the linearized form of the other integrals because they result in those integrals in higher-order terms that are neglected in the linearization.

In considering the UL formulation, the required derivatives for the Jacobian are

$$
\begin{aligned}
\frac{\partial {}^{t}x_1}{\partial r} &= \frac{L\cos\alpha}{2} - \frac{sh}{4}(\sin{}^{t}\theta_2 - \sin{}^{t}\theta_1) \\
\frac{\partial {}^{t}x_1}{\partial s} &= \left(-\frac{h}{2}\right)\left[\left(\frac{1-r}{2}\right)\sin{}^{t}\theta_1 + \left(\frac{1+r}{2}\right)\sin{}^{t}\theta_2\right] \\
\frac{\partial {}^{t}x_2}{\partial r} &= \frac{L\sin\alpha}{2} + \frac{sh}{4}(\cos{}^{t}\theta_2 - \cos{}^{t}\theta_1)
\end{aligned}
$$

$$\frac{\partial {}^{t}x_2}{\partial s} = \frac{h}{2}\left[\left(\frac{1-r}{2}\right)\cos {}^{t}\theta_1 + \left(\frac{1+r}{2}\right)\cos {}^{t}\theta_2\right]$$

where we assumed ${}^{t}L = {}^{0}L = L$.

Next we consider the TL formulation. Here we use

$${}^{0}\mathbf{J} = \begin{bmatrix} \frac{{}^{0}L}{2} & 0 \\ 0 & \frac{h}{2} \end{bmatrix}$$

Also, the initial displacement effect is taken into account using the derivatives

$${}^{t}_{0}u_{1,1} = (\cos\alpha - 1) - \frac{sh}{2L}(\sin {}^{t}\theta_2 - \sin {}^{t}\theta_1)$$

$${}^{t}_{0}u_{1,2} = -\left(\frac{1-r}{2}\right)\sin {}^{t}\theta_1 - \left(\frac{1+r}{2}\right)\sin {}^{t}\theta_2$$

$${}^{t}_{0}u_{2,1} = \sin\alpha + \frac{sh}{2L}(\cos {}^{t}\theta_2 - \cos {}^{t}\theta_1)$$

$${}^{t}_{0}u_{2,2} = \left(\frac{1-r}{2}\right)\cos {}^{t}\theta_1 + \left(\frac{1+r}{2}\right)\cos {}^{t}\theta_2 - 1$$

where we again assumed ${}^{t}L = {}^{0}L = L$.

In each case, we note that these expressions lead to the strain terms corresponding to the global stationary coordinate system. These terms must be transformed to the local η, ξ axes for construction of the strain-displacement matrix of the element.

Finally, we should note that the element can be employed in plane stress or plane strain conditions, depending on the stress-strain relation used (see Section 4.2.3). In plane stress analysis the thickness of the element (normal to the x_1, x_2 plane) must of course be given (this thickness is assumed to be unity in plane strain analysis).

EXAMPLE 6.21: The two-node element in Example 6.20 is to be used as a shell element in axisymmetric conditions. Discuss what terms in addition to those given in Example 6.20 need to be included in the construction of the strain-displacement matrices for the TL formulation.

In axisymmetric analysis the integration is performed over 1 radian and the hoop strain effect must be included (see Example 5.9). Table 6.5 gives the incremental hoop strain ${}_{0}\epsilon_{33}$, which must be evaluated using the interpolations stated in Example 6.20 to give a third row in the strain-displacement matrices ${}^{t}_{0}\mathbf{B}_{L0}$ and ${}^{t}_{0}\mathbf{B}_{L1}$. The third row of the matrix ${}^{t}_{0}\mathbf{B}_{L0}$ corresponds to the term $u_1/{}^{0}x_1$, hence,

$${}^{t}_{0}\mathbf{B}_{L0} = \left[\begin{array}{c|c|c|c|c|c} \cdots & \cdots & \cdots & \cdots & \cdots & \cdots \\ \cdots & \cdots & \cdots & \cdots & \cdots & \cdots \\ \dfrac{1-r}{2\,{}^{0}x_1} & 0 & \dfrac{-sh}{2}\left(\dfrac{1-r}{2}\right)\dfrac{\cos {}^{t}\theta_1}{{}^{0}x_1} & \dfrac{1+r}{2\,{}^{0}x_1} & 0 & \dfrac{-sh}{2}\left(\dfrac{1+r}{2}\right)\dfrac{\cos {}^{t}\theta_2}{{}^{0}x_1} \end{array}\right]$$

where we have used the following ordering of nodal variables in the solution vector

$$\hat{\mathbf{u}}^T = [u_1^1 \quad u_2^1 \quad \theta_1 \quad u_1^2 \quad u_2^2 \quad \theta_2]$$

and ${}^{0}x_1 = [(1+r)/2]L$. The third row of the matrix ${}^{t}_{0}\mathbf{B}_{L1}$ corresponds to the strain term ${}^{t}u_1 u_1/({}^{0}x_1)^2$ and for its evaluation the interpolations of ${}^{t}u_1$, ${}^{0}x_1$, and u_1 are similarly used.

The terms in the nonlinear strain stiffness matrix corresponding to ${}^t_0S_{33}$ are evaluated from the expression

$$
\begin{aligned}
{}^t_0S_{33}\Bigg\{ & \delta\theta_1\left[\frac{sh}{2}\left(\frac{1-r}{2}\right)\frac{\sin {}^t\theta_1}{{}^0x_1}\left(1+\frac{{}^tu_1}{{}^0x_1}\right)\right]\theta_1+\delta\theta_2\left[\frac{sh}{2}\left(\frac{1+r}{2}\right)\frac{\sin {}^t\theta_2}{{}^0x_1}\left(1+\frac{{}^tu_1}{{}^0x_1}\right)\right]\theta_2 \\
& +\left(\frac{1-r}{2\,{}^0x_1}\,\delta u_1^1-\left[\frac{sh}{2}\left(\frac{1-r}{2}\right)\frac{\cos {}^t\theta_1}{{}^0x_1}\right]\delta\theta_1+\frac{1+r}{2\,{}^0x_1}\,\delta u_1^2-\left[\frac{sh}{2}\left(\frac{1+r}{2}\right)\frac{\cos {}^t\theta_2}{{}^0x_1}\right]\delta\theta_2\right) \\
& \times\left(\frac{1-r}{2\,{}^0x_1}\,u_1^1-\left[\frac{sh}{2}\left(\frac{1-r}{2}\right)\frac{\cos {}^t\theta_1}{{}^0x_1}\right]\theta_1+\frac{1+r}{2\,{}^0x_1}\,u_1^2-\left[\frac{sh}{2}\left(\frac{1+r}{2}\right)\frac{\cos {}^t\theta_2}{{}^0x_1}\right]\theta_2\right)\Bigg\}
\end{aligned}
$$

This expression is of the form $\delta\hat{\mathbf{u}}^T({}^t_0\mathbf{K}^*_{NL})\hat{\mathbf{u}}$, where $\mathbf{K}^*_{NL}$ represents a contribution to the element nonlinear strain stiffness matrix.

6.5.2 Plate and General Shell Elements

Many plate and shell elements have been proposed for the nonlinear analysis of plates, specific shells, and general shell structures. However, as with the beam element discussed in the previous section, the isoparametric formulations of plate and shell elements for nonlinear analysis are very attractive because these formulations are both consistent and general, and the elements can be employed in an effective manner for the analysis of a variety of plates and shells. As in linear analysis, in essence a very general shell theory is employed in the formulation so that the shell elements are applicable, in principle, to the analysis of any plate and shell structure.

Considering a plate undergoing large deflections, we recognize that as soon as the plate has deflected significantly, the action of the structure is really that of a shell; i.e., the structure is now curved, and both membrane and bending stresses are significant. Therefore, in the discussion below we consider only general shell elements, where we imply that if a specific element is initially flat, it represents a plate.

In the following presentation we consider the nonlinear formulation of the MITC shell elements discussed for linear analysis in Section 5.4.2. Figure 6.6 shows a typical nine-node

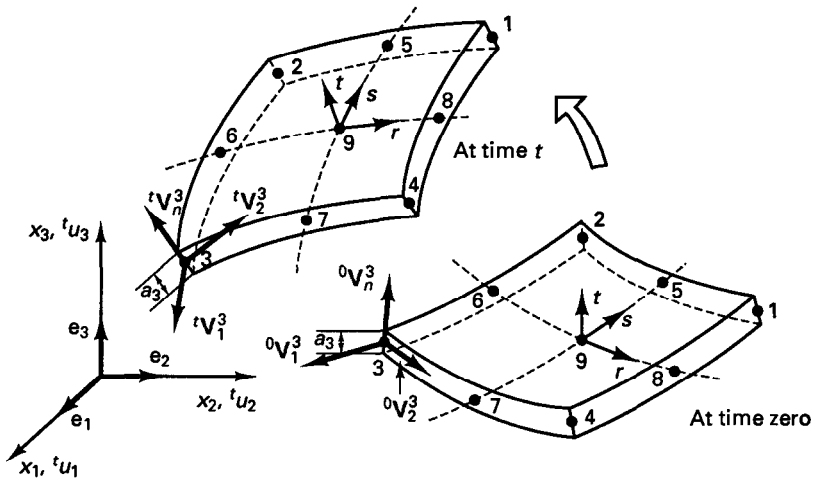

Figure 6.6 Shell element undergoing large displacements and rotations

element in its original position and its configuration at time t. The element behavior is based on the same assumptions that are employed in linear analysis, namely, that straight lines defined by the nodal director vectors (which, usually, give lines that in the original configuration are close to normal to the midsurface of the shell) remain straight during the element deformations and that no transverse normal stress is developed in the directions of the director vectors. However, the nonlinear formulation given here does admit arbitrarily large displacements and rotations of the shell element.[10]

The UL and TL formulations of the shell element are based on the general continuum mechanics equations presented in Section 6.2.3 and are a direct extension of the formulation for linear analysis. Also, the calculation of the element matrices follows closely the calculations used for the beam elements (see Section 6.5.1).

Using the same notation as in Section 5.4.2, the coordinates of a generic point in the shell element now undergoing very large displacements and rotations are (see K. J. Bathe and S. Bolourchi [B])

$$ {}^{t}x_i = \sum_{k=1}^{q} h_k\, {}^{t}x_i^k + \frac{t}{2} \sum_{k=1}^{q} a_k h_k\, {}^{t}V_{ni}^k \tag{6.167} $$

Using (6.167) at times 0, t, and $t + \Delta t$, we thus have

$$ {}^{t}u_i = {}^{t}x_i - {}^{0}x_i \tag{6.168} $$

and

$$ u_i = {}^{t+\Delta t}x_i - {}^{t}x_i \tag{6.169} $$

Substituting from (6.167) into (6.168) and (6.169), we obtain

$$ {}^{t}u_i = \sum_{k=1}^{q} h_k\, {}^{t}u_i^k + \frac{t}{2} \sum_{k=1}^{q} a_k h_k\, ({}^{t}V_{ni}^k - {}^{0}V_{ni}^k) \tag{6.170} $$

and

$$ u_i = \sum_{k=1}^{q} h_k u_i^k + \frac{t}{2} \sum_{k=1}^{q} a_k h_k V_{ni}^k \tag{6.171} $$

where

$$ V_{ni}^k = {}^{t+\Delta t}V_{ni}^k - {}^{t}V_{ni}^k \tag{6.172} $$

The relation in (6.170) is employed to evaluate the total displacements and total strains (hence also total stresses for both the UL and TL formulations) of the particles in the element. To apply (6.171) the same thoughts as in the beam element formulation for use of (6.158), (6.161), and (6.162) are applicable. Now we express the vector components V_{ni}^k in terms of rotations about two vectors that are orthogonal to ${}^{t}\mathbf{V}_n^k$. These two vectors ${}^{t}\mathbf{V}_1^k$ and ${}^{t}\mathbf{V}_2^k$ are defined at time 0 (as in linear analysis) using

$$ {}^{0}\mathbf{V}_1^k = \frac{\mathbf{e}_2 \times {}^{0}\mathbf{V}_n^k}{\| \mathbf{e}_2 \times {}^{0}\mathbf{V}_n^k \|_2} \tag{6.173} $$

$$ {}^{0}\mathbf{V}_2^k = {}^{0}\mathbf{V}_n^k \times {}^{0}\mathbf{V}_1^k \tag{6.174} $$

where we set ${}^{0}\mathbf{V}_1^k$ equal to $\mathbf{e}_3$ if ${}^{0}\mathbf{V}_n^k$ is parallel to $\mathbf{e}_2$. The vectors for time t are then obtained by an integration process briefly described for the director vector in (6.177).

[10] As in the beam formulation in Section 6.5.1, to have the element formulation applicable to large strains, the change in thickness varying over the surface of the element would need to be calculated. The change in thickness depends on the material stress-strain relationship of the element.

Let α_k and β_k be the rotations of the director vector ${}^t\mathbf{V}_n^k$ about the vectors ${}^t\mathbf{V}_1^k$ and ${}^t\mathbf{V}_2^k$ in the configuration at time t. Then we have approximately for small angles α_k and β_k, but including second-order rotation effects (see Exercise 6.57),

$$\mathbf{V}_n^k = -{}^t\mathbf{V}_2^k\,\alpha_k + {}^t\mathbf{V}_1^k\,\beta_k - \tfrac{1}{2}(\alpha_k^2 + \beta_k^2)\,{}^t\mathbf{V}_n^k \tag{6.175}$$

We include the quadratic terms in rotations because we want to arrive at the consistent tangent stiffness matrix, and these terms contribute to the nonlinear strain stiffness effects. Namely, substituting from (6.175) into (6.171), we obtain

$$u_i = \sum_{k=1}^{q} h_k u_i^k + \frac{t}{2}\sum_{k=1}^{q} a_k h_k\left[-{}^tV_{2i}^k\,\alpha_k + {}^tV_{1i}^k\,\beta_k - \frac{1}{2}(\alpha_k^2 + \beta_k^2)\,{}^tV_{ni}^k\right] \tag{6.176}$$

Using this expression to evaluate the continuum terms in Tables 6.2 and 6.3, we notice that the terms $\int_{{}^tV} {}^t\tau_{ij}\,\delta_t e_{ij}\,d^tV$ and $\int_{{}^0V} {}_0^tS_{ij}\,\delta_0 e_{ij}\,d^0V$ result in a stiffness contribution due to the quadratic terms in (6.176) that we naturally add to the other terms of the nonlinear strain stiffness matrix.

We arrived at a similar result in the formulation of the isoparametric beam elements discussed in the previous section [see (6.161) and (6.162) and the ensuing discussion].

The finite element solution will yield the nodal point variables u_i^k, α_k, and β_k, which can then be employed to evaluate ${}^{t+\Delta t}\mathbf{V}_n^k$,

$${}^{t+\Delta t}\mathbf{V}_n^k = {}^t\mathbf{V}_n^k + \int_{\alpha_k,\beta_k} -{}^\tau\mathbf{V}_2^k\,d\alpha_k + {}^\tau\mathbf{V}_1^k\,d\beta_k \tag{6.177}$$

This integration can be performed in one step using an orthogonal matrix for finite rotations (see, for example, J. H. Argyris [B] and Exercise 6.57) or using the Euler forward method and a number of steps (see Section 9.6).

The relations in (6.167) to (6.176) can be directly employed to establish the strain-displacement matrices of displacement-based shell elements. However, as discussed in Section 5.4.2, these elements are not efficient because of the phenomena of shear and membrane locking. In Section 5.4.2, we introduced the mixed interpolated elements for linear analysis, and an important feature of these elements is that they can be directly extended to nonlinear analysis. (In fact, the elements were formulated originally for nonlinear analysis, and the linear analysis elements are obtained simply by neglecting all nonlinear terms.)

The starting point of the formulation is the principle of virtual work written in terms of covariant strain components and contravariant stress components. In the total Lagrangian formulation we use

$$\int_{{}^0V} {}_0^{t+\Delta t}\tilde{S}^{ij}\,\delta\,{}_0^{t+\Delta t}\tilde{\epsilon}_{ij}\,d^0V = {}^{t+\Delta t}\mathcal{R} \tag{6.178}$$

and in the updated Lagrangian formulation we use

$$\int_{{}^tV} {}_t^{t+\Delta t}\tilde{S}^{ij}\,\delta\,{}_t^{t+\Delta t}\tilde{\epsilon}_{ij}\,d^tV = {}^{t+\Delta t}\mathcal{R} \tag{6.179}$$

The incremental forms are of course given in Tables 6.2 and 6.3, but here covariant strain and contravariant stress components are employed.

As discussed in Section 5.4.2, the basic step in the MITC shell element formulation is to assume strain interpolations and to tie these to the strains obtained from the displacement interpolations.

The strain interpolations are as detailed in Section 5.4.2, but of course the interpolations are now used for the Green-Lagrange strain components ${}^{t+\Delta t}_{0}\tilde{\epsilon}_{ij}^{AS}$ and ${}^{t+\Delta t}_{t}\tilde{\epsilon}_{ij}^{AS}$, where the superscript *AS* denotes *a*ssumed *s*train. These assumed strain components are tied to the strain components ${}^{t+\Delta t}_{0}\tilde{\epsilon}_{ij}^{DI}$ and ${}^{t+\Delta t}_{t}\tilde{\epsilon}_{ij}^{DI}$, obtained from the displacement interpolations (6.170) and (6.171).

The covariant strain components ${}^{t+\Delta t}_{0}\tilde{\epsilon}_{ij}^{DI}$ and ${}^{t+\Delta t}_{t}\tilde{\epsilon}_{ij}^{DI}$ are calculated from the fundamental expressions using base vectors,

$$ {}^{t+\Delta t}_{0}\tilde{\epsilon}_{ij}^{DI} = \tfrac{1}{2}({}^{t+\Delta t}\mathbf{g}_i \cdot {}^{t+\Delta t}\mathbf{g}_j - {}^{0}\mathbf{g}_i \cdot {}^{0}\mathbf{g}_j) \tag{6.180} $$

and

$$ {}^{t+\Delta t}_{t}\tilde{\epsilon}_{ij}^{DI} = \tfrac{1}{2}({}^{t+\Delta t}\mathbf{g}_i \cdot {}^{t+\Delta t}\mathbf{g}_j - {}^{t}\mathbf{g}_i \cdot {}^{t}\mathbf{g}_j) \tag{6.181} $$

where

$$ {}^{t+\Delta t}\mathbf{g}_i = \frac{\partial {}^{t+\Delta t}\mathbf{x}}{\partial r_i}; \qquad {}^{t}\mathbf{g}_i = \frac{\partial {}^{t}\mathbf{x}}{\partial r_i}; \qquad {}^{0}\mathbf{g}_i = \frac{\partial {}^{0}\mathbf{x}}{\partial r_i} \tag{6.182} $$

and we use $r_1 \equiv r$, $r_2 \equiv s$, $r_3 \equiv t$, and of course,

$$ {}^{t+\Delta t}\mathbf{x} = {}^{0}\mathbf{x} + {}^{t+\Delta t}\mathbf{u}; \qquad {}^{t}\mathbf{x} = {}^{0}\mathbf{x} + {}^{t}\mathbf{u} \tag{6.183} $$

Using the interpolations discussed in Section 5.4.2, with the above strain components, the MITC shell elements already presented for linear analysis in Section 5.4.2 are now obtained, including large displacement and large rotation effects. These elements satisfy the criteria of reliability and effectiveness that we enumerated in Section 5.4.2.

It may be noted once more that the shell elements discussed above are general elements since no specific shell theory has been employed in their formulation. In fact, the use of the general incremental virtual work equation with only the two basic shell assumptions—that lines originally normal to the shell midsurface remain straight and that the transverse normal stress remains zero (more accurately, actually the directions of the director vectors are used)—is equivalent to using a general nonlinear shell theory. This generality in the formulation is preserved by employing the above interpolations of the shell geometry, displacements, and strains. An important feature is the use of the director vector of the shell midsurface which makes it possible for the elements to undergo arbitrary large displacements and rotations.

6.5.3 Exercises

6.51. Consider the two-node beam element shown.

(a) Plot the displacements of the material particles corresponding to ${}^{t}u_1^2$, ${}^{t}u_2^2$, and ${}^{t}\theta_2$, and evaluate the Green-Lagrange strain components corresponding to these displacements at $r = s = 0$.

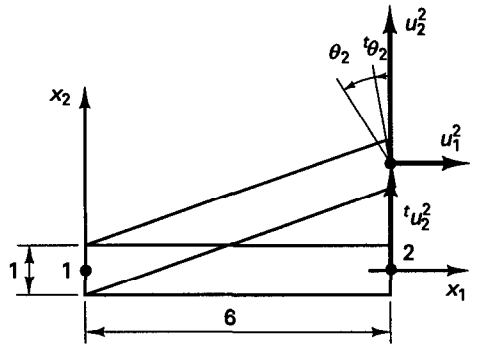

(b) Establish the derivatives ${}_0u_{i,j}$ (i.e., $\partial u_i/\partial {}^0x_j$), $i = 1, 2; j = 1, 2$, corresponding to the nodal incremental displacement and rotation variables u_1^2, u_2^2, and θ_2.
At node 1 displacements and rotations are zero; at node 2 ${}'u_1^2 = 0$, ${}'u_2^2 = 2$, ${}'\theta_2 = 10°$.

6.52. Consider the two-node beam element shown. Calculate for the degrees of freedom u_1^2, u_2^2, and θ_2 the stiffness matrix ${}'\mathbf{K}$ and nodal force vector ${}'\mathbf{F}$ using the total Lagrangian formulation.
(a) Use the displacement method and analytical integration.
(b) Use one-point Gauss integration for the r direction.

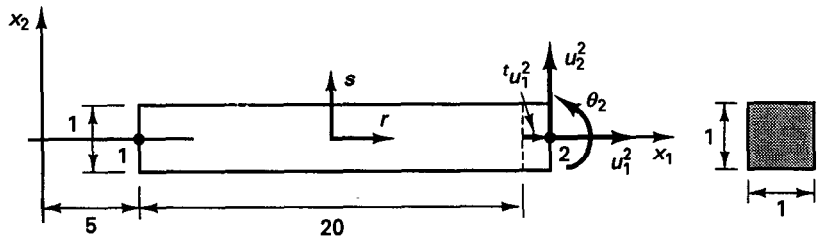

All nodal point displacements and rotations are zero at time t, except ${}^tu_1^2 = 0.1$

Young's modulus E
Shear modulus G

6.53. Perform the same calculations as in Exercise 6.52 but now assume that the element is an axisymmetric shell element, with the x_2 axis the axis of revolution.

6.54. Consider the beam element in Exercise 6.52. Calculate the stiffness matrix ${}'\mathbf{K}$ and force vector ${}'\mathbf{F}$ for the degrees of freedom at node 2 using the mixed interpolation of linear displacements and rotations and constant transverse shear strain (see Section 5.4.1).

6.55. Consider the four-node shell element shown. Evaluate the displacements of the particles in the element for the given nodal point displacements and director vectors at time t. Draw these displacements over the original geometry of the element.

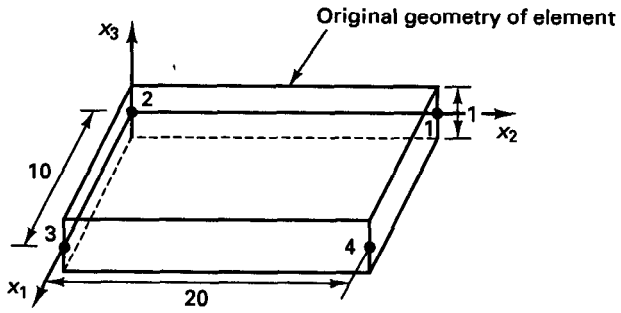

$${}^tu_i^k = 0 \qquad \text{for } i = 1, 2, 3; \qquad k = 1, 2, 3$$

$${}^t\mathbf{V}_n^k = \begin{bmatrix} 0 \\ 0 \\ 1 \end{bmatrix}; \qquad k = 1, 2, 3$$

$${}^tu_1^4 = 0.1; \qquad {}^tu_2^4 = 0.1; \qquad {}^tu_3^4 = 1$$

$${}^t\mathbf{V}_n^4 = \frac{1}{2}\begin{bmatrix} 0 \\ -1 \\ \sqrt{3} \end{bmatrix}$$

6.56. Show that the expressions in (6.161) and (6.162) contain all second-order terms in $\boldsymbol{\theta}_k$ to obtain the increments in the director vectors. Obtain the result by a simple geometric argument and by the fact that the rotation can be expressed through the rotation matrix $\mathbf{Q}$, see, for example, J. H. Argyris [B], where

$$\mathbf{Q} = \mathbf{I} + \frac{\sin \gamma_k}{\gamma_k}\mathbf{S}_k + \frac{1}{2}\left(\frac{\sin \frac{\gamma_k}{2}}{\frac{\gamma_k}{2}}\right)^2 \mathbf{S}_k^2; \qquad \gamma_k = (\theta_{k1}^2 + \theta_{k2}^2 + \theta_{k3}^2)^{\frac{1}{2}}$$

and

$$\mathbf{S}_k = \begin{bmatrix} 0 & -\theta_{k3} & \theta_{k2} \\ \theta_{k3} & 0 & -\theta_{k1} \\ -\theta_{k2} & \theta_{k1} & 0 \end{bmatrix}$$

6.57. Show that the expression in (6.175) includes all second-order terms in α_k and β_k to obtain the increment in the director vector ${}^t\mathbf{V}_n^k$. Obtain the result by a simple geometric argument and by use of the matrix $\mathbf{Q}$ of Exercise 6.56 but with

$$\gamma_k = (\alpha_k^2 + \beta_k^2)^{\frac{1}{2}} \qquad \mathbf{S}_k = \begin{bmatrix} 0 & 0 & \beta_k \\ 0 & 0 & -\alpha_k \\ -\beta_k & \alpha_k & 0 \end{bmatrix}$$

6.58. Calculate the covariant strain terms ${}_0\tilde{\epsilon}_{ij}^{DI}$ for the element and its deformation given in Exercise 6.56.

6.59. Use a computer program to solve for the large displacement response of the cantilever shown. Analyze the structure for a tip rotation of π (180 degrees) and compare your displacement and stress results with the analytical solution. (*Hint*: The four-node isoparametric mixed interpolated beam element performs particularly well in this analysis.)

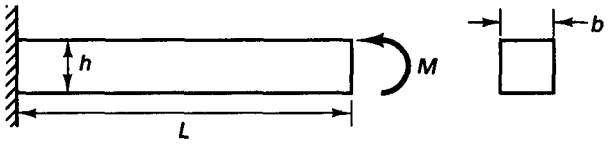

$E = 200{,}000$
$\nu = 0.30$
$h = 1$
$L = 100$
$b = 1$

6.60. Use a computer program to solve for the response of the spherical shell structure shown. Calculate the displacements and stresses accurately. (The solution of this structure has been extensively used in the evaluation of shell elements; see, for example, E. N. Dvorkin and K. J. Bathe [A]).

All edges of shell are hinged

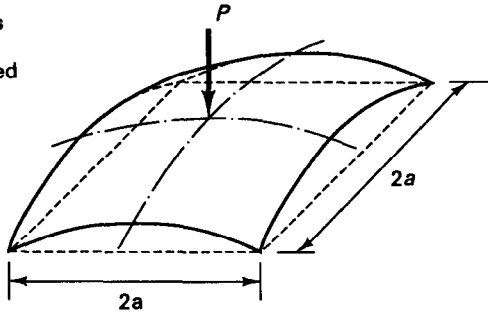

Radius = 2540
Thickness = 99.45
a = 784.90
$E = 68.95$
$\nu = 0.30$

6.6 USE OF CONSTITUTIVE RELATIONS

In Sections 6.3 to 6.5 we discussed the evaluation of the displacement and strain-displacement relations for various elements. We pointed out that these kinematic relations yield an accurate representation of large deformations (including large strains in the case of two- and three-dimensional continuum elements).

The kinematic descriptions in the element formulations are therefore very general. However, it must be noted that in order for a formulation of an element to be applicable to a specific response prediction, *it is also necessary to use appropriate constitutive descriptions.* Clearly, the finite element equilibrium equations contain the displacement and strain-displacement matrices plus the constitutive matrix of the material (see Table 6.4). Therefore, *in order for a formulation to be applicable to a certain response prediction, it is imperative that both the kinematic and the constitutive descriptions be appropriate.* For example, assume that the TL formulation is employed to describe the kinematic behavior of a two-dimensional element and a material law is used which is formulated only for small strain conditions. In this case the analysis can model only small strains although the TL kinematic formulation does admit large strains.

The objective in this section is to present some fundamental observations pertaining to the use of material laws in nonlinear finite element analysis. Many different material laws are employed in practice, and we shall not attempt to survey and summarize these models. Instead, our only objectives are to discuss the stress and strain tensors that are used effectively with certain classes of material models and to present some important general observations pertaining to material models, their implementations, and their use.

The three classes of models that we consider in the following sections are those with which we are widely concerned in practice, namely, elastic, elastoplastic, and creep material models. Some basic properties of these material descriptions are given in Table 6.7, which provides a very brief overview of the major classes of material behavior.

In our discussion of the use of the material models, we need to keep in mind how the complete nonlinear analysis is performed incrementally. Referring to the previous sections, and specifically to relations (6.11), (6.78), and (6.79) and Section 6.2.3, we can summarize the complete process as given in Table 6.8.

This table shows that the material relationships are used at two points of the solution process: the evaluation of the stresses and the evaluation of the tangent stress-strain matrices. The stresses are used in the calculation of the nodal point force vectors and the nonlinear strain stiffness matrices, and the tangent stress-strain matrices are used in the calculation of the linear strain stiffness matrices. As we pointed out earlier (see Section 6.1), it is imperative that the stresses be evaluated with high accuracy since otherwise the solution result is not correct, and it is important that the stiffness matrices be truly tangent matrices since otherwise, in general, more iterations to convergence are needed than necessary.

Table 6.8 shows that the basic task in the evaluation of the stresses and the tangent stress-strain matrix is the following:

Given all stress components ${}^t\boldsymbol{\sigma}$ and strain components ${}^t\mathbf{e}$ and any internal material variables that we call here ${}^t\kappa_i$, all corresponding to time t,

$$\{{}^t\boldsymbol{\sigma}, {}^t\mathbf{e}, {}^t\kappa_1, {}^t\kappa_2, \ldots\}$$

TABLE 6.7 *Overview of some material descriptions*

Material model	Characteristics	Examples
Elastic, linear or nonlinear	Stress is a function of strain only; same stress path on unloading as on loading. $^{t}\sigma_{ij} = {}^{t}C_{ijrs}\,{}^{t}e_{rs}$ linear elastic: $^{t}C_{ijrs}$ is constant nonlinear elastic: $^{t}C_{ijrs}$ varies as a function of strain	Almost all materials provided the stresses are small enough: steels, cast iron, glass, rock, wood, and so on, before yielding or fracture
Hyperelastic	Stress is calculated from a strain energy functional W, $^{t}_{0}S_{ij} = \frac{\partial W}{\partial\, {}^{t}_{0}\epsilon_{ij}}$	Rubberlike materials, e.g., Mooney-Rivlin and Ogden models
Hypoelastic	Stress increments are calculated from strain increments $d\sigma_{ij} = C_{ijrs}\,de_{rs}$ The material moduli C_{ijrs} are defined as functions of stress, strain, fracture criteria, loading and unloading parameters, maximum strains reached, and so on.	Concrete models (see, for example, K. J. Bathe, J. Walczak, A. Welch, and N. Mistry [A])
Elastoplastic	Linear elastic behavior until yield, use of yield condition, flow rule, and hardening rule to calculate stress and plastic strain increments; plastic strain increments are instantaneous.	Metals, soils, rocks, when subjected to high stresses
Creep	Time effect of increasing strains under constant load, or decreasing stress under constant deformations; creep strain increments are noninstantaneous.	Metals at high temperatures
Viscoplasticity	Time-dependent inelastic strains; rate effects are included.	Polymers, metals

and also given all strain components corresponding to time $t + \Delta t$ and end of iteration $(i - 1)$, denoted as $^{t+\Delta t}\mathbf{e}^{(i-1)}$

Calculate all stress components, internal material variables, and the tangent stress-strain matrix, corresponding to $^{t+\Delta t}\mathbf{e}^{(i-1)}$,

$$\{{}^{t+\Delta t}\boldsymbol{\sigma}^{(i-1)},\ \mathbf{C}^{(i-1)},\ {}^{t+\Delta t}\kappa_1^{(i-1)},\ {}^{t+\Delta t}\kappa_2^{(i-1)},\ \ldots\}$$

Hence we shall assume in the following discussion that the strains are known corresponding to the state for which the stresses and the stress-strain tangent relationship are required. For ease of writing, we shall frequently also not include the superscript $(i - 1)$ but simply denote the current strain state as $^{t+\Delta t}\mathbf{e}$. This convention shall not imply that no equilibrium iterations are performed. However, since the solution process for the stresses

TABLE 6.8 *Solution process in incremental nonlinear finite element analysis*

Accepted and known solution at time t: stresses ${}^t\boldsymbol{\sigma}$
strains ${}^t\mathbf{e}$
internal material parameters ${}^t\kappa_1, {}^t\kappa_2, \ldots$

1. *Known*: nodal point variables ${}^{t+\Delta t}\mathbf{U}^{(i-1)}$ and hence element strains ${}^{t+\Delta t}\mathbf{e}^{(i-1)}$
2. *Calculate*: stresses ${}^{t+\Delta t}\boldsymbol{\sigma}^{(i-1)}$
   tangent stress-strain matrix corresponding to ${}^{t+\Delta t}\boldsymbol{\sigma}^{(i-1)}$, denoted as $\mathbf{C}^{(i-1)}$
   internal material parameters ${}^{t+\Delta t}\kappa_1^{(i-1)}, {}^{t+\Delta t}\kappa_2^{(i-1)}, \ldots$
   a. In elastic analysis: the strains ${}^{t+\Delta t}\mathbf{e}^{(i-1)}$ directly give the stresses ${}^{t+\Delta t}\boldsymbol{\sigma}^{(i-1)}$ and the stress-strain matrix $\mathbf{C}^{(i-1)}$
   b. In inelastic analysis: an integration process is performed for the stresses

$$ {}^{t+\Delta t}\boldsymbol{\sigma}^{(i-1)} = {}^t\boldsymbol{\sigma} + \int_t^{t+\Delta t^{(i-1)}} d\boldsymbol{\sigma} $$

   and the tangent stress-strain matrix $\mathbf{C}^{(i-1)}$ corresponding to the state $t + \Delta t$, end of iteration $(i - 1)$, is evaluated *consistent* with this integration process.

   In isoparametric finite element analysis these stress and strain computations are performed at all integration points of the mesh in order to establish the equations used in step 3.
3. *Calculate*: nodal point variables $\Delta\mathbf{U}^{(i)}$ using ${}^{t+\Delta t}\mathbf{K}^{(i-1)}\,\Delta\mathbf{U}^{(i)} = {}^{t+\Delta t}\mathbf{R} - {}^{t+\Delta t}\mathbf{F}^{(i-1)}$, and then ${}^{t+\Delta t}\mathbf{U}^{(i)} = {}^{t+\Delta t}\mathbf{U}^{(i-1)} + \Delta\mathbf{U}^{(i)}$

Repeat Steps 1 to 3 until convergence.

and the tangent stress-strain matrix is identical whether or not equilibrium iterations are used, we need not show the iteration superscript. All that matters is that the conditions are completely known at time t and a new strain state has been calculated for which the new stresses, internal material parameters, and the new tangent stress-strain matrix shall be evaluated.

We should note that the evaluation of the stresses and the tangent stress-strain matrix is, in our numerical evaluation of the element stiffness matrix and force vector, performed at each element integration point. Hence, it is imperative that these computations be performed as efficiently as possible.

In inelastic analysis, an integration process is needed from the state at time t to the current strain state, but in elastic analysis no integration of the stresses is required (as we employ a total strain formulation and not a rate-type formulation; see Example 6.24). In elastic analysis, the stresses and the tangent stress-strain matrix can be directly evaluated for a given strain state. Hence, in the following discussion when considering elastic conditions (Sections 6.6.1 and 6.6.2), we shall also, for further ease of writing, simply consider the strain state at time t and evaluate the corresponding stresses and tangent stress-strain matrix at that time [the same procedure is used for any time, including time $t + \Delta t$].

6.6.1 Elastic Material Behavior—Generalization of Hooke's Law

A simple and widely used elastic material description for large deformation analysis is obtained by generalizing the linear elastic relations summarized in Chapter 4 (see Table 4.3) to the TL formulation:

$$ {}^t_0S_{ij} = {}^t_0C_{ijrs}\,{}^t_0\epsilon_{rs} \tag{6.184} $$

where the ${}^t_0S_{ij}$ and ${}^t_0\epsilon_{rs}$ are the components of the second Piola-Kirchhoff stress and Green-Lagrange strain tensors and the ${}^t_0C_{ijrs}$ are the components of the constant elasticity tensor. Considering three-dimensional stress conditions, we have

$$ {}^t_0C_{ijrs} = \lambda\delta_{ij}\delta_{rs} + \mu(\delta_{ir}\delta_{js} + \delta_{is}\delta_{jr}) \tag{6.185} $$

where λ and μ are the Lamé constants and δ_{ij} is the Kronecker delta,

$$ \lambda = \frac{E\nu}{(1+\nu)(1-2\nu)}; \qquad \mu = \frac{E}{2(1+\nu)} $$

$$ \delta_{ij} = \begin{cases} 0; & i \neq j \\ 1; & i = j \end{cases} $$

The components of the elasticity tensor given in (6.185) are identical to the values given in Table 4.3 (see Exercise 2.10).

Considering this material description we can make a number of important observations. We recognize that in infinitesimal displacement analysis, the relation in (6.184) reduces to the description used in linear elastic analysis because under these conditions the stress and strain variables reduce to the engineering stress and strain measures. However, an important observation is that *in large displacement and large rotation but small strain analysis*, the relation in (6.184) provides a natural material description because the components of the second Piola-Kirchhoff stress and Green-Lagrange strain tensors do not change under rigid body rotations (see Section 6.2.2 and Examples 6.12 to 6.15). Thus, only the actual straining of material will yield an increase in the components of the stress tensor, and as long as this material straining (accompanied by large rotations and displacements) is small, the use of the relation (6.184) is completely equivalent to using Hooke's law in infinitesimal displacement conditions.

The fundamental observation that "the second Piola-Kirchhoff stress and Green-Lagrange strain components do not change measured in a fixed coordinate system when the material is subjected to rigid body motions" is important not only for elastic analysis. Indeed, this observation implies that any material description which has been developed for infinitesimal displacement analysis using engineering stress and strain measures can directly be employed in large displacement and large rotation but small strain analysis, provided second Piola-Kirchhoff stresses and Green-Lagrange strains are used. Figure 6.7 illustrates this fundamental fact. A practical consequence is, for example, that elastoplastic and creep material models (see Section 6.6.3) can be directly employed for large displacement, large rotation, and small strain analysis by simply substituting second Piola-Kirchhoff stresses and Green-Lagrange strains for the engineering stress and strain measures.

The preceding observations are of special importance because, in practice, Hooke's law is applicable only to small strains and because there are many engineering problems in which large displacements, large rotations, but only small strain conditions are encountered. This is, for example, frequently the case in the elastic or elastoplastic buckling or collapse analysis of slender (beam or shell) structures.

The stress-strain description given in (6.184) implicitly assumes that a TL formulation is used to analyze the physical problem. Let us now assume that we want to employ a UL formulation but that we are given the constitutive relationship in (6.184). In this case we can write, substituting (6.184) into (6.72),

$$ \int_{{}^0V} {}^t_0C_{ijrs}\, {}^t_0\epsilon_{rs}\, \delta {}^t_0\epsilon_{ij}\, d^0V = {}^t\mathcal{R} \tag{6.186} $$

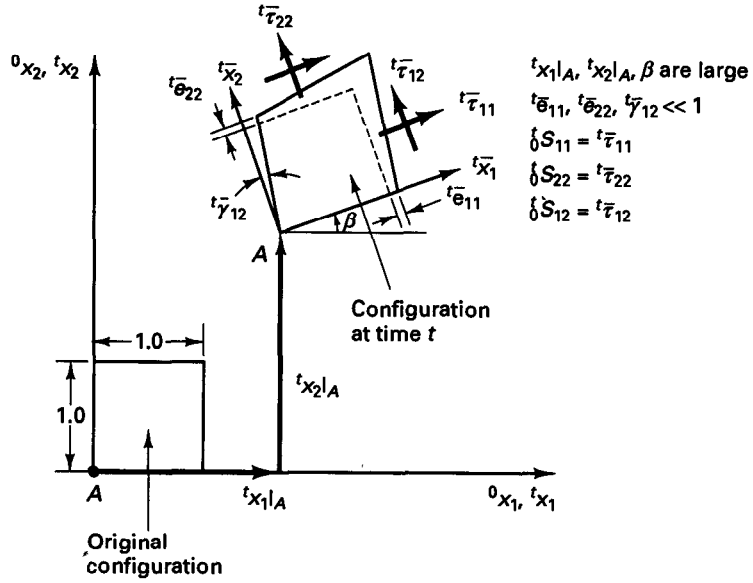

Figure 6.7 Large displacement/large rotation but small strain conditions

Thus, if we define a new constitutive tensor,

$$ {}^{t}C_{mnpq} = \frac{{}^{t}\rho}{{}^{0}\rho} {}^{t}_{0}x_{m,i} {}^{t}_{0}x_{n,j} {}^{t}_{0}C_{ijrs} {}^{t}_{0}x_{p,r} {}^{t}_{0}x_{q,s} \tag{6.187} $$

meaning that

$$ {}^{t}_{0}C_{ijrs} = \frac{{}^{0}\rho}{{}^{t}\rho} {}^{0}_{t}x_{i,m} {}^{0}_{t}x_{j,n} {}^{t}C_{mnpq} {}^{0}_{t}x_{r,p} {}^{0}_{t}x_{s,q} \tag{6.188} $$

and if we use (see Example 6.10)

$$ \delta_t e_{mn} = {}^{0}_{t}x_{i,m} {}^{0}_{t}x_{j,n} \, \delta {}^{t}_{0}\epsilon_{ij} \tag{6.189} $$

we recognize that (6.186) can be written as

$$ \int_{{}^{t}V} {}^{t}C_{mnpq} \, {}^{t}\epsilon^{A}_{pq} \, \delta_t e_{mn} \, d^{t}V = {}^{t}\mathcal{R} \tag{6.190} $$

where

$$ {}^{t}\tau_{mn} = {}^{t}C_{mnpq} \, {}^{t}\epsilon^{A}_{pq} \tag{6.191} $$

and the ${}^{t}\epsilon^{A}_{pq}$ are the components of the *Almansi strain tensor,*

$$ {}^{t}\epsilon^{A}_{pq} = {}^{0}_{t}x_{r,p} \, {}^{0}_{t}x_{s,q} \, {}^{t}_{0}\epsilon_{rs} \tag{6.192} $$

Like the Green-Lagrange strain tensor, the Almansi strain tensor can also be defined in a number of different but completely equivalent ways,[11] namely,

$$ {}^{t}\epsilon^{A}_{ij} = \tfrac{1}{2}({}^{t}u_{i,j} + {}^{t}u_{j,i} - {}^{t}u_{k,i} \, {}^{t}u_{k,j}) \tag{6.193} $$

and we have

$$ {}^{t}\epsilon^{A}_{ij} \, d^{t}x_i \, d^{t}x_j = \tfrac{1}{2}\{(d^{t}s)^2 - (d^{0}s)^2\} \tag{6.194} $$

[11] However, in contrast,to the Green-Lagrange strain tensor, the components of the Almansi strain tensor are not invariant under a rigid body rotation of the material.

EXAMPLE 6.22: Prove that the definitions of the Almansi strain tensor given in (6.192) to (6.194) are all equivalent.

The relation in (6.192) can be written in matrix form as

$$ {}^{t}_{t}\boldsymbol{\epsilon}^{A} = {}^{0}_{t}\mathbf{X}^{T}\, {}^{t}_{0}\boldsymbol{\epsilon}\, {}^{0}_{t}\mathbf{X} \tag{a} $$

But using (6.54) to substitute for ${}^{t}_{0}\boldsymbol{\epsilon}$ in (a) and recognizing that

$$ {}^{0}_{t}\mathbf{X}\, {}^{t}_{0}\mathbf{X} = \mathbf{I} $$

we obtain

$$ {}^{t}_{t}\boldsymbol{\epsilon}^{A} = \tfrac{1}{2}(\mathbf{I} - {}^{0}_{t}\mathbf{X}^{T}\, {}^{0}_{t}\mathbf{X}) \tag{b} $$

However, we have

$$ {}^{0}_{t}\mathbf{X} = [{}_{t}\nabla\, {}^{0}\mathbf{x}^{T}]^{T} $$

where, in accordance with (6.21),

$$ {}_{t}\nabla = \begin{bmatrix} \dfrac{\partial}{\partial {}^{t}x_1} \\ \dfrac{\partial}{\partial {}^{t}x_2} \\ \dfrac{\partial}{\partial {}^{t}x_3} \end{bmatrix}; \qquad {}^{0}\mathbf{x}^{T} = [{}^{0}x_1 \quad {}^{0}x_2 \quad {}^{0}x_3] $$

Substituting into (b), we obtain

$$ {}^{t}_{t}\boldsymbol{\epsilon}^{A} = \tfrac{1}{2}\{\mathbf{I} - [{}_{t}\nabla({}^{t}\mathbf{x}^{T} - {}^{t}\mathbf{u}^{T})][{}_{t}\nabla({}^{t}\mathbf{x}^{T} - {}^{t}\mathbf{u}^{T})]^{T}\} $$

Since

$$ {}_{t}\nabla\, {}^{t}\mathbf{x}^{T} = \mathbf{I} $$

we thus obtain

$$ {}^{t}_{t}\boldsymbol{\epsilon}^{A} = \tfrac{1}{2}[\mathbf{I} - (\mathbf{I} - {}_{t}\nabla\, {}^{t}\mathbf{u}^{T})(\mathbf{I} - {}_{t}\nabla\, {}^{t}\mathbf{u}^{T})^{T}] $$

or

$$ {}^{t}_{t}\boldsymbol{\epsilon}^{A} = \tfrac{1}{2}[{}_{t}\nabla\, {}^{t}\mathbf{u}^{T} + ({}_{t}\nabla\, {}^{t}\mathbf{u}^{T})^{T} - ({}_{t}\nabla\, {}^{t}\mathbf{u}^{T})({}_{t}\nabla\, {}^{t}\mathbf{u}^{T})^{T}] \tag{c} $$

and the components of ${}^{t}_{t}\boldsymbol{\epsilon}^{A}$ in (c) are the relations in (6.193).

To show that (6.194) also holds, we use the relation in (b) to obtain

$$ d{}^{t}\mathbf{x}^{T}\, {}^{t}_{t}\boldsymbol{\epsilon}^{A}\, d{}^{t}\mathbf{x} = \tfrac{1}{2}(d{}^{t}\mathbf{x}^{T}\, d{}^{t}\mathbf{x} - d{}^{0}\mathbf{x}^{T}\, d{}^{0}\mathbf{x}) \tag{d} $$

because

$$ d{}^{0}\mathbf{x} = {}^{0}_{t}\mathbf{X}\, d{}^{t}\mathbf{x} $$

But (d) can also be written as

$$ d{}^{t}\mathbf{x}^{T}\, {}^{t}_{t}\boldsymbol{\epsilon}^{A}\, d{}^{t}\mathbf{x} = \tfrac{1}{2}[(d{}^{t}s)^{2} - (d{}^{0}s)^{2}] \tag{e} $$

because

$$ d{}^{t}\mathbf{x}^{T}\, d{}^{t}\mathbf{x} = (d{}^{t}s)^{2}; \qquad d{}^{0}\mathbf{x}^{T}\, d{}^{0}\mathbf{x} = (d{}^{0}s)^{2} $$

and (e) is equivalent to (6.194).

Of course, using (6.190) with the Almansi strain and the constitutive tensor ${}^{t}_{t}C_{mnpq}$ is quite equivalent to transforming the second Piola-Kirchhoff stress ${}^{t}_{0}S_{ij}$ (obtained using ${}^{t}_{0}S_{ij} = {}^{t}_{0}C_{ijrs}\, {}^{t}_{0}\epsilon_{rs}$) to the Cauchy stress and then using (6.13) to evaluate ${}^{t}\mathcal{R}$. Indeed, if ${}^{t}_{0}C_{ijrs}$ is known, this procedure is computationally more efficient, and the definition and use of the Almansi strain with (6.190) may be regarded as only of theoretical interest.

However, in the following example we prove an important result, which can be stated in summary as follows.

Consider the TL and UL formulations in Tables 6.2 and 6.3,

$$ \int_{{}^{0}V} {}_{0}C_{ijrs}\, {}_{0}e_{rs}\, \delta_{0}e_{ij}\, d{}^{0}V + \int_{{}^{0}V} {}^{t}_{0}S_{ij}\, \delta_{0}\eta_{ij}\, d{}^{0}V = {}^{t+\Delta t}\mathcal{R} - \int_{{}^{0}V} {}^{t}_{0}S_{ij}\, \delta_{0}e_{ij}\, d{}^{0}V \tag{6.195} $$

$$\int_{{}^tV} {}_tC_{ijrs}\, {}_te_{rs}\, \delta_t e_{ij}\, d^tV + \int_{{}^tV} {}^t\tau_{ij}\, \delta_t \eta_{ij}\, d^tV = {}^{t+\Delta t}\mathcal{R} - \int_{{}^tV} {}^t\tau_{ij}\, \delta_t e_{ij}\, d^tV \tag{6.196}$$

The corresponding integral terms in the formulations are identical provided the transformations for the stresses given in (6.69) and for the constitutive tensors given in (6.187) are used. Hence, whether we choose the TL or the UL continuum formulation is decided merely by considerations of numerical efficiency.

EXAMPLE 6.23: Consider the total and updated Lagrangian formulations in incremental form (see Tables 6.2 and 6.3).

(a) Derive the relationship that should be satisfied between the tensors ${}_0C_{ijrs}$ and ${}_tC_{ijrs}$ so that the incremental relations

$${}_0S_{ij} = {}_0C_{ijrs}\, {}_0\epsilon_{rs} \tag{a}$$

and

$${}_tS_{ij} = {}_tC_{ijrs}\, {}_t\epsilon_{rs} \tag{b}$$

refer to the *same* physical material response.

(b) Show that when the relationship derived in part (a) is satisfied, each integral term in the linearized TL formulation is identical to its corresponding term in the UL formulation.

A constitutive law relates a stress measure to a strain measure. Since there are different stress and corresponding strain measures, the constitutive law for a given material may take different forms, but these forms are related by the fact that they all describe the same given material. Hence, if equations (a) and (b) describe the same material, ${}_0C_{ijrs}$ and ${}_tC_{ijrs}$ must be related by purely kinematic transformations.

To derive the kinematic transformations we express ${}_tS_{ij}$ in terms of ${}_0S_{ij}$, and ${}_t\epsilon_{rs}$ in terms of ${}_0\epsilon_{rs}$.

We have

$${}_tS_{ij} = {}^{t+\Delta t}_{t}S_{ij} - {}^t\tau_{ij} \tag{c}$$

Using

$${}^t\tau_{ij} = \frac{{}^t\rho}{{}_0\rho}\, {}^t_0x_{i,r}\, {}^t_0S_{rs}\, {}^t_0x_{j,s} \tag{d}$$

and

$${}^{t+\Delta t}_{t}S_{ij} = \frac{{}^t\rho}{{}_0\rho}\, {}^t_0x_{i,r}\, {}^{t+\Delta t}_{0}S_{rs}\, {}^t_0x_{j,s}$$

and (c), we obtain

$${}_tS_{ij} = \frac{{}^t\rho}{{}_0\rho}\, {}^t_0x_{i,r}\, {}^t_0x_{j,s}\, {}_0S_{rs} \tag{e}$$

We also have for the strain terms

$${}_0\epsilon_{ij} = {}^{t+\Delta t}_{0}\epsilon_{ij} - {}^t_0\epsilon_{ij}$$

and

$${}_t\epsilon_{ij} = {}^{t+\Delta t}_{t}\epsilon_{ij}$$

Hence,

$${}_0\epsilon_{ij} = \tfrac{1}{2}({}^{t+\Delta t}_{0}x_{k,i}\, {}^{t+\Delta t}_{0}x_{k,j} - {}^t_0x_{k,i}\, {}^t_0x_{k,j}) \tag{f}$$

and

$${}_t\epsilon_{ij} = \tfrac{1}{2}({}^{t+\Delta t}_{t}x_{k,i}\, {}^{t+\Delta t}_{t}x_{k,j} - \delta_{ij}) \tag{g}$$

We should note here that ${}_t\epsilon_{ij}$ is the Green-Lagrange strain based on the displacements from time t to time $t + \Delta t$, with the reference configuration at time t.[12]

[12] For example, ${}^t_t\epsilon_{ij} = 0$, and this strain measure should not be confused with the Almansi strain ${}^t_t\epsilon^A_{ij}$ defined in (6.192).